The role of residential photovoltaic-coupled battery storages in the energy system from a regional perspective

A spatiotemporal assessment of residential photovoltaic and battery storage systems and their effects on the energy flows

Dissertation zur Erlangung des Doktorgrades

an der Fakultät für Geowissenschaften

der Ludwig-Maximilians-Universität München

vorgelegt von

Andrea Reimuth

München, 12.08.2020

Erstgutachter:	Prof. Dr. Wolfram Mauser
Zweitgutachter:	Prof. Dr. Ralf Ludwig
Tag der mündlichen Prüfung:	27.11.2020

For my grandparents.

Summary

The electric energy systems face a fundamental transformation triggered by the tackling of climate change, the long-term depletion of fossil fuels and the cost-decrease of renewable technologies. Especially photovoltaic (PV) energy installed on rooftops has become a major driver of the current energy transition. Residential buildings are often additionally equipped with battery storages raising the self-consumption of PV energy by the balancing of load and production. The increasing decentralization of the energy generation systems represents a challenge for the grid infrastructure, which has not been dimensioned for the feed-in on low voltage level in the past.

This dissertation assesses the impact of residential PV-coupled battery storages on the energy systems from a regional perspective under consideration of the great multitude and heterogeneity of the systems. The divergence arises from the differences in equipment, PV sizes, battery capacities, efficiencies and consumption loads, but also from locally varying meteorological conditions. For reproducing this spatial variance, the raster-based land surface processes model Processes of radiation, mass and energy transfer (PROMET) is extended by a residential consumption, a PV and a battery storage component. This allows a physically based simulation of the energy flows considering the individual parameterization of the residential buildings and their spatiotemporal dependencies.

The application of this model approach shows that the choice of the battery charging has a crucial influence on the regional integration of rooftop PV but also on the increase of PV self-consumption. The utilization of daily, dynamic feed-in limitations yields the highest reduction of residual loads while also maximizing self-consumption. The application of this charging strategy should be supported especially for larger PV and battery storage systems in order to reduce grid impacts.

Apart from the battery management, the PV and battery expansion plays an essential role for their grid integration on regional scale. The diversity of residential energy systems offers further balancing potential due to the spatial variance in their residual loads. The highest regional grid-balancing is obtained when 30% of the buildings is equipped with PV systems. In this case, the additional utilization of battery storages reduces this effect to the benefit of higher self-consumption rates and therefore does not contribute to the reduction of grid excesses. This is different for high PV installation rates, as grid balancing diminishes. For this reason, financial support for batteries should be adjusted to the regional PV installation rates.

Apart from the management strategies and expansion rates, the climatological and consumption-related boundary conditions have crucial impact on residential batteries and their potentials for increasing self-consumption and grid-relief. Both factors will undergo significant changes in the future. Scenarios until 2040 project that climate change affects the battery utilization in winter,

whereas the effects of efficiency enhancement of domestic appliances dominates in the summer. The resulting increase in PV excesses could rise grid stresses further. In order to reduce potential losses, these developments should be considered in the dimensioning of batteries.

The results show that the spatial variance between residential energy systems has a crucial impact on PV-coupled battery storages on regional scale. The developed approach, which is based on the extended utilization of a land surface processes model, offers the possibility to simulate the interactions between the residential energy flows for a multitude of buildings and to map regionally adjusted strategies for the integration of PV systems.

Zusammenfassung

Die elektrischen Energiesysteme stehen vor einem grundlegenden Wandel, der durch den Kampf gegen den Klimawandel, die langfristige Erschöpfung fossiler Brennstoffe und fallende Kosten für regenerative Technologien eingeleitet wird. Insbesondere die gebäudegebundene Photovoltaik (PV) Technologie hat sich zu einem der Haupttreiber der Energiewende entwickelt. Häufig werden in Wohngebäuden neben PV Systemen zusätzliche Batteriespeicher zum Schwankungsausgleich von Produktion und Verbrauch installiert, um den Eigenverbrauch der selbsterzeugten PV Energie zu erhöhen. Die steigende Dezentralisierung der Energieproduktion stellt jedoch eine Herausforderung für die Netzinfrastruktur dar, die nicht für die Einspeisung auf Niederspannungsebene ausgelegt ist.

Diese Dissertation untersucht die Auswirkungen von PV-gekoppelten Batteriespeichern von Wohngebäuden aus einer regionalen Perspektive. Hierbei muss die Vielzahl der Anlagen mit unterschiedlichen Ausprägungen der einzelnen Systeme berücksichtigt werden. Diese entstehen durch unterschiedliche Ausstattungen, Anlagengrößen, Batteriespeicherkapazitäten, Wirkungsgrade und Verbrauchsraten sowie den standortabhängigen, klimatologischen Bedingungen. Um diese räumliche Varianz abzubilden wurde das raster-basierte Landoberflächenprozessmodell PROMET um ein Wohngebäudemodell mit Verbrauchs-, PV- und Batteriekomponente erweitert. Auf diese Weise können die Energieflüsse simuliert werden bei individueller Parametrisierung der Gebäudeenergiesysteme und ihrer raumzeitlichen Einflüsse.

Mithilfe dieses Modells wurde festgestellt, dass die Wahl der Batterieladestrategie einen wesentlichen Einfluss auf die regionale Integration von PV Dachanlagen und die Erhöhung des Eigenverbrauchs hat. Variable PV-Einspeiselimits auf täglicher Basis führen hierbei zur höchsten Netzlast-Reduzierung bei gleichzeitiger Maximierung des Eigenverbrauchs. Die Nutzung dieser Ladestrategie sollte insbesondere für große Anlagen unterstützt werden, um die Netzauswirkungen zu reduzieren.

Auch die PV und Batterieausbaurate spielt auf regionaler Ebene eine wesentliche Rolle für deren Integration, denn die Diversität der Gebäudeenergiesysteme bietet ein zusätzliches Ausgleichspotential der Überschüsse aufgrund der räumlichen Varianz der Residuallasten. Der höchste Netzausgleich der Residuallasten von Wohngebäuden ergibt sich, wenn 30% eine PV Anlage besitzen. Bei dieser Ausbaurate tragen Batteriespeicher kaum zu einer Abnahme von Netzüberschüssen bei, da sie den räumlichen Ausgleich zugunsten höherer Eigenverbrauchsraten verringern. Bei hohen PV-Ausbauraten jedoch spielt der Netzausgleich keine Rolle mehr, sodass der Einsatz von Batterien einen wichtigen Anteil zur Integration von PV-Anlagen übernimmt. Aus diesem Grund

empfiehlt es sich, die Förderstrukturen für Batteriespeicher an die regionalen PV Ausbauraten anzupassen.

Neben Ladestrategien und Ausbaugraden wirken sich auch die klimatologischen und verbrauchsbezogenen Rahmenbedingungen auf die Batteriespeicher aus, die sich in den nächsten Jahrzehnten stark verändern werden. Szenarien bis 2040 sagen vorher, dass sich der Klimawandel im Winter und Effizienzsteigerungen von Haushaltsgeräten im Sommer auf die Nutzung der Batterien auswirken. Steigende PV Überschüsse könnten die Netze in den Sommermonaten zukünftig verstärkt belasten. Diese Entwicklungen sollten auch bei der Dimensionierung der Batteriespeicherkapazitäten berücksichtigt werden, um potenzielle Verluste zu mindern.

Die Ergebnisse zeigen, dass die kleinräumige Varianz der Gebäudeenergiesysteme auf regionaler Ebene einen großen Einfluss auf PV-gekoppelten Batteriespeichern haben. Der in dieser Arbeit entwickelte Ansatz, der auf der erweiterten Anwendung eines Landoberflächenprozessmodells basiert, bietet die Möglichkeit, auch die raumzeitlichen Wechselwirkungen zwischen den Energieflüssen für eine Vielzahl von Wohngebäuden zu erfassen und damit Strategien für die Integration von PV Systemen an regionale Gegebenheiten anzupassen.

Acknowlegdement

During the four years at the Department of Geography at LMU Munich, I have had the pleasure to meet very inspiring people I now want to acknowledge for their support.
First of all, I would like to express my gratitude to my supervising professor Wolfram Mauser for giving me the opportunity of pursuing a doctorate. His openness for interdisciplinary research and his willingness to give his time for topics beyond the traditional fields of geographic applications have made this dissertation possible. He supported me during the whole time with his experience and the trust in going my way. His door was always open for fruitful discussions and feedback.
I want to thank my second reviewer Prof. Ralf Ludwig for his profound interest and time for the review. I also express my thank you to Prof. Wolfgang Mayer from Hochschule Kempten, who reviews my thesis as external member of the doctoral commission.
I acknowledge with gratitude the Federal Ministry for research and education of Germany, and the European Centre for Medium-Range Weather Forecasts (ECMWF) for financial support in the projects INOLA and C3S-511.
I want to express my gratitude to Dr. Monika Prasch and Dr. Martin Danner for their assistance and support during the last years. Both created a positive, and warm atmosphere, so that work was a pleasure for me. A special thanks goes to my office roommate Veronika Locherer for having always an open ear for all my thoughts. It was a great fun, motivation, and pleasure to spend the working days with her.
My gratitude goes to the whole team from the INOLA-project for many inspiring discussions, successful workshops, and the close interdisciplinary collaboration. I acknowledge Energiewende Oberland, Hochschule Kempten, and Stadtwerke Bad Tölz for data provision. I further want to thank Ben Müller for giving me the possibility of getting in touch with the world of satellite data as he introduced me into this field of research during the PhD.
My gratitude goes to Prof. Eckart Priesack and his former PhDs Christian, Flo, Christian and Christoph from the working unit Modelling Plant-Soil Systems at the Helmholtz Center Munich. In this group, I experienced the fascination of science and I enjoyed the creativity and freedom of this work for the first time.
I also want to thank my colleagues from LMU, who welcomed me warmly and openly. I will always remember our intense discussions about all the important topics of real-life during the lunch and coffee breaks, dinners in Frida, beer evenings, which filled the days with happiness, motivation, and fun. I thank to my virtual office mates Flo, Ben and Raul; with them I didn't spend the days of Corona restrictions lonesome.

A big thank you also goes to all my friends who ensured that I relax from demanding days. Especially Mischan, Marcus, Martina, Eric, Beatriz, and Nicolas, they reminded me that there is a lot of more in life than just work. I thank them for the all the fun we had and for your patience in times of doubts.
Finally, I want to thank my parents and my sister with her family, who have always believed in me and supported me in developing my abilities and following my dreams.

Table of Contents

Summary I

Zusammenfassung III

Acknowlegdement V

Table of Contents VII

List of Figures XI

List of Tables XIV

Abbreviations XV

1 Introduction 1

1.1 Motivation of the thesis 2

1.1.1 The transition of the electrical energy systems 2

1.1.2 The role of residential energy systems with PV-coupled batteries 3

1.1.3 Challenges of integrating rooftop PV into the grid systems and potentials of residential batteries 4

1.2 Modeling of residential energy systems with PV system and battery storage 5

1.2.1 Fundamentals of photovoltaic energy generation 5

1.2.2 Operation principles of battery storage systems 7

1.2.3 Integration of PV and battery systems into residential power networks 8

1.2.4 State of the art in the modelling of residential PV-coupled battery storage systems 11

1.2.5 Research objectives 13

1.2.6 Scientific publications 14

1.2.7 Framing of the publications 15

2 Influence of different battery charging strategies on residual grid power flows and self-consumption rates at regional scale 18

Abstract 18

2.1 Introduction 19

2.2 Materials and methods 20

2.2.1 The domestic energy model environment 21

2.2.2 The production model 22

2.2.3 The consumption model 23
2.2.4 The battery model 23
2.2.5 The charging strategies 24
2.3 Evaluation parameters 25
2.4 The study area 26
2.5 Input data 27
2.5.1 Meteorology 27
2.5.2 Input of the domestic energy model 27
2.6 Results 28
2.6.1 The grid power flows and curtailment losses without battery storages 28
2.6.2 Influence of the charging strategies on the grid flows 29
2.6.3 The influence of the charging strategies on the domestic energy systems 31
2.7 Discussion 32
2.7.1 Assessment of the charging strategies 32
2.7.2 Evaluation of the raster-based approach for modeling domestic energy systems with battery storages 34
2.8 Conclusion 35
Acknowledgement 36
Supplementary materials 37
3 How does the rate of photovoltaic installations and coupled batteries affect regional energy balancing and self-consumption of residential buildings? ____ 38
Abstract 38
3.1 Introduction 39
3.2 Materials and methods 41
3.2.1 Model environment 41
3.2.2 Description of the study area 43
3.2.3 Input data 44
3.2.4 Temporal and spatial downscaling of the consumption rates 44
3.2.5 Dimensioning of the PV systems and batteries 46
3.3 Results 48

3.3.1 Regional balancing and self-sufficiency ... 48
3.3.2 Self-consumption and energy surplusses ... 49
3.3.3 Residual loads and regional balancing flows ... 50
3.4 Discussion ... 53
3.4.1 Relation between regional balancing, energy surplusses and self-consumption ... 53
3.4.2 Applicability of the results to other municipalities ... 54
3.4.3 Policy implications ... 56
3.5 Conclusions ... 56
Appendix ... 58
4 How do changes in climate and consumption loads affect residential PV coupled battery energy systems? ... 59
Abstract ... 59
4.1 Introduction ... 60
4.2 Materials and methods ... 61
4.2.1 Model environment ... 61
4.2.2 Generation of the meteorological scenarios ... 64
4.3 Case study ... 65
4.3.1 Description of the study area ... 65
4.3.2 Basic input for the domestic energy model ... 65
4.3.3 Input required for the climate generator ... 66
4.3.4 Scenario generation ... 67
4.4 Results ... 68
4.4.1 Temporal course of the energy flows ... 68
4.4.2 Variance of the energy flows ... 70
4.4.3 Development of the residual loads ... 71
4.4.4 Self-consumption and self-supply ... 72
4.5 Discussion ... 73
4.5.1 Battery utilization ... 73
4.5.2 Residual loads ... 74
4.5.3 Limitations of the study ... 75

4.5.4 Implications for the battery dimensioning 76
4.6 Conclusion 76
Acknowledgement 77
Supplementary materials 78
5 Synthesis 84
Bibliography 86
Curriculum Vitae ..... Fehler! Textmarke nicht definiert.

List of Figures

Fig. 1-1: Increase in the energy production of different renewable technologies since 2007 (left) and distribution of the rooftop PV applications (right) 4

Fig. 1-2: Structure and energy generation of a PV cell (left) and electron transfer from valence band to conduction band (right) 6

Fig. 1-3: The discharging of a galvanic cell means a flow of electrons and anions from a anode to cathode (left). The flows of electrons and anions are reversed when charging (right) a battery 7

Fig. 1-4: Options for coupling the battery to the residential network 9

Fig. 1-5: Top row: Energy balance in a residential building with PV generation and battery storage at a sunny day (left) and distribution of the resulting residual loads between public grid and residential energy system (right). Bottom row: Schematic self-consumption of the PV production (left) and self-supply of the consumption rate (right) in a residential building 10

Fig. 1-6: Keywords in the research of residential PV-coupled battery storage systems (left) and model scales in their assessment (right) 11

Fig. 1-7: Overview of the publications addressing Research Questions I to V 16

Fig. 2-1: Structure of the domestic energy module containing the energy production of the PV-panels, the battery with its environment and the grid power flows. 21

Fig. 2-2: Study region with a total area of 2,944 km², 356,122 inhabitants, and the distribution of 4,906 PV-systems selected in this study 26

Fig. 2-3: Hourly power excesses (purple) and deficits (light green) of 4906 domestic energy systems without the influence of battery storages and the obtained regional balancing effect of the residential residual loads RL (dark green line) (left) and hourly curtailment losses CTL at average (red) and cumulated (grey line) (right) 28

Fig. 2-4: Spatial distribution of the grid flows from the domestic energy systems at the hour with the highest regional balancing effect 29

Fig. 2-5: Residual loads including curtailment losses (left) and curtailment losses (right) using the charging strategies maximization of the self-consumption rate (MSC), fixed feed-in limit (FFL), and daily dynamic feed-in limit (DFL) when compared to no battery storage systems 29

Fig. 2-6: Average, range of minimum, maximum and range of 5% / 95% quantile of the domestic residual loads at daytime with maximum negative delta in 2016 with (a) no battery storage, (b) charging strategy Maximization of self-consumption (MSC), (c) charging strategy Fixed feed-in limit (FFL) and (d) charging strategy Daily dynamic feed-in limit (DFL) 31

Fig. 3-1: Location of the study area and distribution of residential buildings 43

Fig. 3-2: (a) Distribution of floor numbers used for the estimation of the living areas; (b) distribution of the average consumption rates per building 46

Fig. 3-3: (a) Distribution of the nominal PV power dimensioned according to the current German distribution considering the technical constraints of the buildings; (b) distribution of the ratios between nominal PV power and annual demand (right side) 48

Fig. 3-4: (a) Regional balancing and (b) self-sufficiency for different PV installation and battery-coupling rates as percentage of consumption (with the PV installation rate of 32% in dashed grey) 48

Fig. 3-5: (a) Self-consumption and (b) energy excesses for different PV installation and battery-coupling rates as percentage of consumption (with the PV installation rate of 32% in dashed grey) 50

Fig. 3-6: Duration curves of (a) residual loads of the residential buildings and (b) balancing flows between the buildings for different PV installation rates without the utilization of battery storage systems. The residual load and distribution of the balancing flows for PV installation rate leading to the highest regional balancing are marked in black 50

Fig. 3-7: Duration curves of (a) residual loads and (b) balancing flows for different battery-coupling rates at a PV installation rate of 32% 51

Fig. 3-8: Duration curves of (a) residual loads and (b) balancing flows for different battery-coupling rates at a PV installation rate of 99% 52

Fig. 4-1: Structure of the domestic energy module including the energy production of the PV panels, the battery with its environment and the grid power flows (left) and selected charging and discharging strategy (right). RSL denotes the residual loads, DFL the dynamic feed-in limit 62

Fig. 4-2: Location of the study area (left) and distribution of the 4906 selected households (right) 65

Fig. 4-3: Cumulated energy flows of consumption, production, battery and grid flows for an average domestic energy system (left), and cumulated differences between the future energy flows of Scenario A, B, and C and the baseline scenario (right) 69

Fig. 4-4: Quantiles of the domestic annual energy flows for consumption, production, battery, and grid per kWp-PV power for Scenario 0, A, B, and C 70

Fig. 4-5: Distribution of the hourly residual loads of 2505 selected domestic energy systems with the minimum and maximum extrema enclosing the average flows for the battery systems having capacities of less than 8 kWh, 8–10.99 kWh, 11–14.99 kWh, and larger than 14 kWh 71

Fig. 4-6: Degree of Self-Consumption (DSC), Degree of Self-Supply (DSS), Degree of Autarky (DA), and Number of Cycles (NoC) in dependency of the battery capacity. The lines represent the fitted curves, which are in logarithmic form for DSC and DA, and exponential form for DSS and NoC 72

Appendix:

Fig. A. 2-1: Load profiles of a household with an average annual electrical energy demand of 5119.35 kWh 37

Fig. A. 3-1: The load factors for three different daily profiles and the seasons (a) winter, (b) spring, and (c) summer represent the hourly percentage of the annual consumption in 1.000kWh/a of a residential building 58

Fig. A. 4-1: Load profiles of an average household with an annual electrical energy demand of 5119.35 kWh 82

Fig. A. 4-2: Fitted temperature trends to decadal ensemble of the projected temperature increases since 01.01.1970 82

Fig. A. 4-3: Relative changes of the weekly temperatures and precipitation sums from the ensemble means of 2021 to 2050 compared to 1961 to 1990 82

Fig. A. 4-4: Annual mean production rates, battery flows and grid flows with the selected marked in black year representing average meteorological conditions in scenario A 83

Fig. A. 4-5: Selected year representing average meteorological conditions in scenario B 83

Fig. A. 4-6: Selected year representing average meteorological conditions in scenario C 83

List of Tables

Tab. 1-1: Overview of publications 15

Tab. 2-1: Average number of battery cycles, degree of self-consumption, self-supply and autarky without storages and with batteries applying strategy Maximization of the self-consumption, Fixed feed-in limit of 70% kWp power and Daily dynamic feed-in limit 32

Tab. 3-1: Specification of the input parameters of the PV and battery model 44

Tab. 4-1: Boundary conditions for three future scenarios concerning the IPCC emission scenarios and the progresses in energy efficiency 68

Appendix:

Tab. A. 2-1: Technical input parameters for the domestic energy model 37

Tab. A. 4-1: Technical input parameters for the domestic energy model 79

Tab. A. 4-2: Parameters for adjusted curves for fitted temperature trend of type $y = a \cdot x3 + b \cdot x2 + c \cdot x + d$ with x as the days since 01.01.1970 [d] 80

Tab. A. 4-3: Annual average and 5 % / 95 % confidence intervals (CI) for the production, battery and grid flows normalized per kWp PV-power in [kWh/kWp PV] 80

Tab. A. 4-4: Parameters for adjusted curves for degree of self-consumption and degree of autarky of type $y = expa + b \cdot x$ with x as the theoretical battery capacity [kWh] 81

Tab. A. 4-5: Parameters for adjusted curves for degree of self-supply and cycles numbers of type $y = a + b \cdot logx$ with x as the theoretical battery capacity [kWh] 81

Abbreviations

AC	Alternative Current
BMS	Battery Management System
CI	Confidence Interval
CTL	Curtailment Losses
DA	Degree of Autarky
DFL	Dynamic daily Feed-in Limit
DSC	Degree of Self-Consumption
DSS	Degree of Self-Supply
DWD	Deutscher Wetterdienst (German weather service)
ECWMF	European Center for Medium-Range Weather Forecasts
EEG	Erneuerbare Energien Gesetz (Renewable Resources Act)
EWO	Bürgerstiftung Energiewende Oberland (Civic foundation Energiewende Oberland)
FFL	Fixed Feed-in Limit
GIS	Geographic Information System
IEA	International Energy Agency
IPCC	Intergovernmental Panel on Climate Change
LfL	Landesanstalt für Landwirtschaft (Research Center for Agriculture)
MPP	Maximum-Power-Point
MSC	Maximization of Self-Consumption
NoC	Number of Cycles
OECD	Organisation for Economic Co-operation and Development
PROMET	Processes of Radiation, Mass and Energy Transfer
PV	Photovoltaic
RCP	Representative Concentration Pathway
RQ	Research Question
VDI	Verein Deutscher Ingenieure (Association of German Engineers)

ZAMG	Zentralanstalt für Meteorologie und Geodynamik (Central Institution for Meteorology and Geodynamics)

1 Introduction

Since the electrification of industrial processes and residential life, electricity has been playing a crucial role in modern societies. In the end-use energy consumption of OECD nations, electrical power ranks on the second place behind oil-based fuels (IEA 2019a). The access, reliability, and affordability to electrical energy are key indicators for the degree of development of a country. In China and India, the growth in economy and prosperity of the last twenty years was accompanied by a rise in the electrical energy demand of factor ten (IEA 2019a). At present, three quarter of the total produced electrical power is consumed by the OECD nations, China, and India (IEA 2019a).

Electrical energy systems of industrialized nations are normally optimized for providing cheap and reliable power of high quality (Bhattacharyya 2019). The energy production is based on large-scale thermal power plants managed by profit-oriented energy groups or state companies (Lin et al. 2017). On central sites, electrical power is produced by electromechanical generators with capacities of several GWh that are driven by steam turbines. The necessary heat is usually generated by firing natural gas, coal, and oil or by the decay of radioactive substances. Currently, these types of fuels account for three quarters of the production rate in the OECD (IEA 2019a).

The production rates are adjusted to consumption via the price, as electrical energy is traded on stock exchanges (Cramton 2017). The energy price is driven by many further factors like country specific tax dues, or the costs for fuels, maintenance, grid infrastructure, and demand. Energy-intensive industries, for instance, often bid on real-time markets taking advantage of short-term price fluctuations. Residential consumers in contrast are usually bonded to fixed electricity tariffs that are sporadically adjusted.

In the last century, the electrical energy systems have always been subject to changes arising from political decisions, economic developments, or societal changes (Smil 2010). After the oil crisis in the 70ies for instance, the utilization of alternative energy sources increasingly replaced oil-based power plants in order to reduce the dependency on oil imports (Bhattacharyya 2019).

However, today the energy systems face a fundamental transformation, which concerns all components and exceeds previous adjustments of recent decades (Bruckner et al. 2014). The utilization of fossil fuels for generating electricity accounts for 25% of the rise in greenhouse gas concentrations in the atmosphere. The transition to zero-emitting energy resources is an essential contribution to reduce the future risks and hazards of climate change. For this reason, regulative measures and state subsidies for the rollout of efficiency enhancement measures and regenerative technologies have already been fixed in multiple governmental action plans.

Moreover, the economic development induces changes in non-regenerative energy systems. Rising scarcity, instability, and efforts in the extraction of fossil fuels face decreasing costs for renewable production technologies (Chow et al. 2003). In the long term, the depletion of fossil fuels will make a transition to inexhaustible energy resources inevitable (Shafiee et al. 2009). Local, and renewable energy production can imply independency and energy security, which is especially attractive for nations without own oil, coal and gas resources (Bhattacharyya 2019). This development also contributes to the initialization of a new energy age additionally to governmental intervention.

1.1 Motivation of the thesis

The transition of the electrical energy systems is an already ongoing, longer lasting technological and societal process, and the optimal strategy towards sustainability is not yet clear (Bolwig et al. 2019). Several possibilities have been investigated in recent years, which can contribute to the decarbonization of the energy systems.

1.1.1 The transition of the electrical energy systems

One leverage factor in the transition to higher sustainability in the electrical energy systems is the reduction of consumption. This can be achieved by energy savings due to active changes in behavior and by the increase in energy efficiency of the electrical appliances (IEA 2019b). A lower electrical energy demand entails less production capacities and resources that have to be provided for a secure supply (Sims et al. 2011).

Additionally, conventional fuels as coal, oil or gas must be substituted by zero-emitting based technologies. In contrast to the fossil fuels, heir resources for energy production are based on natural phenomena that are replenished immediately (Ellabban et al. 2014). Technologically mature options for renewable energy generation currently include hydropower plants, wind energy plants, photovoltaic systems, biogas plants, geothermal power plants, concentrated solar power and ocean plants (IEA 2019c).

Although technical solutions have already become marketable, their optimal integration into existing structures presents a challenge when preserving supply security, affordability and quality on current levels (IEA 2020). One reason is that renewable production systems are substantially different in their spatial availability (Rogner et al. 2012). In contrast to conventional power plants, they provide lower energy densities and depend on the physical conditions of the sites, like solar irradiation or hydrological discharge. Economically feasible plants may be located far from existing infrastructures and energy consumers like offshore wind farms, which makes the extensions of the power networks necessary.

The production rate of the renewable systems does not only vary by location but also by time (Sims et al. 2011). Especially in the temperate zones, solar and wind power plants are subject to high fluctuations from seasonal scale down to milliseconds. This is reasoned in strongly varying weather conditions leading to instabilities in the energy production. This constitutes a major problem for traditional energy systems as a secure and high-quality power supply is based on a continuous balance of the energy flows (Sims et al. 2011). Currently, our energy systems have only limited capacities for balancing production and consumption rates in the grids, as fuel-based plants are fully operated according to demand. For this reason, balancing mechanisms need to be much more established, when renewables dominate the production (IRENA 2020). A multitude of methods is already proposed for various types of energy storages, demand-side management or the coupling of the heat, traffic and electricity sector.

The infrastructural changes arising with the expansion of the renewables fundamentally transform the energy markets. Because of declining investment costs, zero-emitting production systems become affordable for smaller market participants (IRENA 2017a). New business models are created as civil cooperatives for instance, aiming at a full, decentral self-supply of single communities (Lowitzsch et al. 2019; van der Schoor et al. 2015). This reduces the dominance of the large energy companies on the energy markets. Due to increasing economic benefits even house owners are increasingly turning to energy producers by installing PV systems on their rooftops (IEA PVPS 2019).

1.1.2 The role of residential energy systems with PV-coupled batteries

The PV technology is considered a key driver of the energy transition regarding its strong expansion in recent years. As shown in Fig. 1-1 left, PV records the highest annual growth of renewable electrical energy production rates up 60% increase since 2007 (IEA 2019c). The installation of PV systems on rooftops offers a large potential, which is usually free of fundamental conflicts. Other renewables have higher production capacities but often compete with other forms of land-uses as settlement or food production (Rogner et al. 2012; Huber et al. 2017). Rooftop PV systems are widely considered as a green technology with low visibility, which prevents a disruption of the landscape (Sütterlin et al. 2017). Therefore, PV belongs to the most popular renewable technologies for electrical energy generation (Schumacher et al. 2019).

In the last years, PV systems have become more and more affordable for rooftop applications due to high governmental subsidies and declining prices for PV systems at the purchase (Frankfurt School-UNEP Centre/BNEF 2019). Currently, 8% of the global, renewable energy production capacities is obtained by small-scale rooftop photovoltaic systems (IEA 2019c). With 55 GW in total, residential installations account for 28% of the growth in rooftop PV systems since 2007 (see Fig. 1-1 right). The International Energy Agency projects a further annual rise to 140 GW in the next

years, which accounts for 7% of the projected increase of the total renewable electrical energy capacity (IEA 2019c).

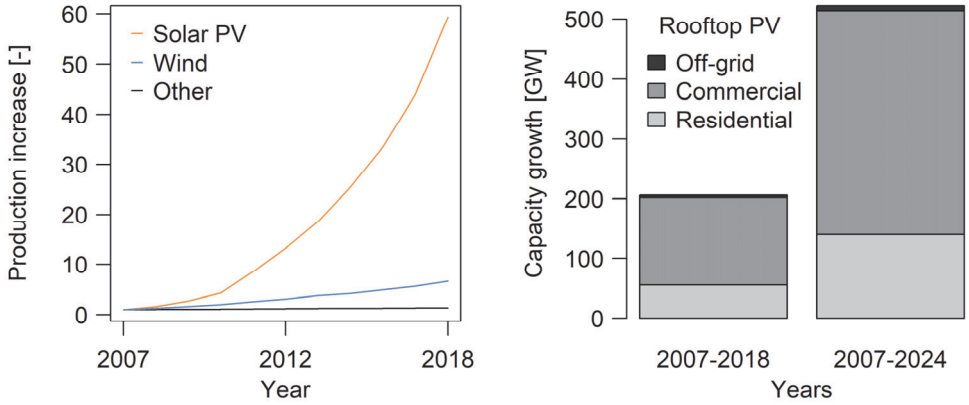

Fig. 1-1: Increase in the energy production of different renewable technologies since 2007 (left) and distribution of the rooftop PV applications (right). (Data source: IEA (2019c))

However, the PV production rates, which are constrained by the irradiation conditions, coincide with the load profiles of residential buildings only partly during daytime. For this reason, residential battery storage systems have become similarly attractive as PV systems, as they offer the possibility of increasing the consumption of PV energy (Klingler 2017). Apart from increasing the independency from grid supply, cost savings further motivate PV owners for the purchase (Agnew et al. 2017). Especially the price decline in lithium-ion technology has created new markets for this type of small-scale storages, which meet the specific demands of households for raising self-consumption in a cost-efficient way. In Germany for instance, every second newly installed PV system was coupled to a residential battery in the recent years (Figgener et al. 2018). Despite the usually small size of residential batteries, they have become a relevant factor in the storage sector. In Australia, the capacity of residential storages accounts for a total of 1 GWh (Clean Energy Council 2020). It is expected that this trend is amplified in the future due to a further decline in the battery production costs (Tsiropoulos et al. 2018). Scenarios project an increase of the global capacities up to 93 GWh until 2030 so that the impact of residential battery storages on the electrical energy systems is expected to rise further in the future (IRENA 2017b).

1.1.3 Challenges of integrating rooftop PV into the grid systems and potentials of residential batteries

The strong rise of rooftop PV implies a strong decentralization of the power sector. This has some challenging impacts for the grid suppliers, as the power systems have not been designed for a distributed energy production. Usually, the infrastructure for the transmission from production site to consumption of the energy flows is structured according to the used voltage. As the large-scale power plants constructed in recent decades are often located far from consumers, electrical energy is transported via high voltage grid networks, which can be operated over long distances

at low loss rates. Due to safety reasons, the voltage is then reduced to lower levels for the final transmission to the end-users. Residential PV systems counter this hierarchical order, as the power excesses are fed into the low-voltage distribution grids. In times of low consumption and high solar irradiation, the PV energy excesses can reverse the direction of the power flows in the grids, which may even damage the infrastructure (Agnew et al. 2015).

Another issue is the large number of residential systems with low rated capacities, to which grid suppliers often do not have access for actively curtailing the PV feed-in (Alboaouh et al. 2020). For this reason, cost-intensive measures must be undertaken, which stabilize the electrical energy systems like the strengthening of the infrastructure or the installation of central storages.

Residential battery systems offer potential for mitigating these problems (Zahedi 2011). The temporal decoupling of production and consumption increases PV self-consumption, as the generated energy can be delivered according to demand. Due to this balancing of PV production and consumption, batteries can contribute to the levelling of residual loads and the damping of PV excesses. However, many questions are still open concerning the effects of the small-scale storages on the residential and the public grid systems. How to combine the goals of owners for PV self-consumption with the requests of grid suppliers for peak-shaving have not yet been finally discussed. But also, the quantities to which residential batteries can contribute to the integration of rooftop PV systems into the grids are not yet fully assessed.

1.2 Modeling of residential energy systems with PV system and battery storage

1.2.1 Fundamentals of photovoltaic energy generation

Principally, the energy production from PV systems is based on the photoelectric effect, which transforms solar irradiation into electrical energy. A variety of structures is suitable to absorb sunlight and generate electrical energy (Green 2002). However, the established technology for rooftop PV systems is based on non-organic, semi conductive materials. A solar cell consists of contact plates, a protecting glass layer and the semiconductor with an n-type and a p-type layer, which is suitable to produce photocurrent (see Fig. 1-2 left).

Silicon is the mainly used semiconductor material (IRENA 2019) due to high conversion efficiencies, low costs, and high availability (Parida et al. 2011). Silicon belongs to the group of metalloids, which form a crystalline structure with a periodic arrangement of the atomic nuclei (Hersch et al. 1982).

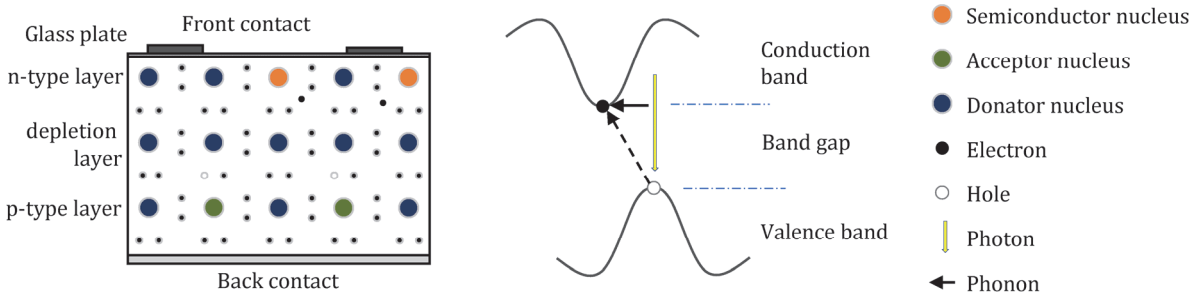

Fig. 1-2: Structure and energy generation of a PV cell (left) and electron transfer from valence band to conduction band (right).

In pure form and under ambient temperature, silicon is generally characterized by a low electrical conductivity. For this reason, impurities are added systematically in order to increase the electrical productivity of the solar cell as shown in Fig. 1-2 left (Hersch et al. 1982). The top layer of the cell called n-type is doped with electron donators creating the excess of electrons. The bottom side of the solar cell (p-type) is doped with electron acceptors, which leads to a deficit of electrons in the layer. For silicon solar cells, phosphorus is commonly used as donator so that one additional electron is available per each phosphorus atom. The acceptors consist of boron atoms creating one additional hole per atom.

In order to obtain neutrality, the electrons and holes diffuse through the p-type to the n-type layer and create an electric field, which corresponds to the built-in voltage of the solar cell (Luque et al. 1989). The formation of an electrical field inhibits the full balancing and charges the depletion zone electrically. This region is relevant for the creation of electrical energy, as the electrons and holes form dynamic bands, on which they can move relatively free from their nuclei (see Fig. 1-2 right for a simplified model). The valence band allows the movement of holes to the back of the solar cell, whereas the conduction band can transport the electrons to the front contact. The gap between the bands cannot be occupied by electrons. Generally, the distributions of the bands are dependent on the periodic energy potential of the semiconductor material. In Silicon solar cells form indirect band gaps, as the maxima of the bands are shifted.

As soon as a photon with an energy level exceeding the band gap hits the valence band, an electron is excited and moves to the conduction band (Luque et al. 1989). This leads to the creation of an additional hole in the valence band, as the charges are separated. For indirect band gap semiconductor materials like silicon, phonons bridge the lateral offset between the maxima of valence and conduction band (see Fig. 1-2 right). These particles arise from lattice vibrations in the semiconductor.

The excited electron moves to the conduction band and is finally transported to the front contact of the solar cell. As soon as leaving the solar cell, the electron is transported in the external electric circuit. After doing work, it returns to the solar cell and fills the generated hole in the p-type layer again (Hersch et al. 1982).

The energy production of the solar cell depends on the temperature of the cell and the amount and energy content of the photons (Luque et al. 1989). These parameters are driven by the installation as the angle between PV panel and sun and site-specific meteorological conditions. As climatic conditions largely vary over the globe, the location of the PV systems is indirectly an important factor for its productivity. For this reason, the potential for PV production is also subject to spatial variation apart from technical aspects (Arvizu et al. 2011).

The nominal power of a PV system is defined as the amount of electrical energy produced under a light intensity of 1000 W/m² at 25° C and a normed solar spectrum (Luque et al. 1989). In this way, the PV systems can be easily compared. The nominal power does not represent the maximum possible energy production, since better irradiation and temperature conditions can occur on Earth.

1.2.2 Operation principles of battery storage systems

The storage effect of a battery is based on the transformation of electrical and chemical energy, which is determined by the electrochemical properties of the applied materials (Gür 2018). Suitable materials are basically characterized by high reactivity and a strong tendency of losing respectively accepting electrons in their valence shells. Whereas lead and lead-dioxide were mostly used for residential PV storage applications in the past, Lithium-based accumulators dominate the markets today (Tsiropoulos et al. 2018).

A battery storage consists of interconnected galvanic cells, which produce electrical energy from the transfer of electrons in a redox reaction (Linden 1995). In a galvanic cell, oxidation and reduction reactions take place within two half cells, which are spatially separated by a membrane insulating against electrons (see Fig. 1-3). The half-cells contain an anode and a cathode, which are connected via an external electrical conductor.

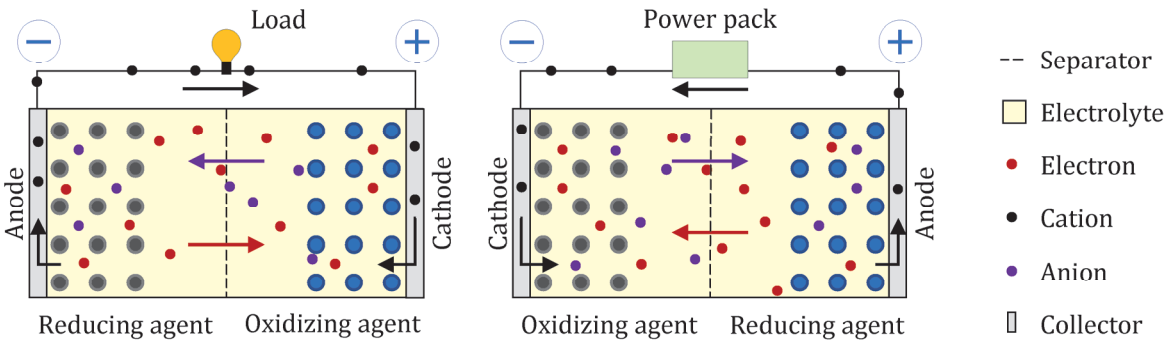

Fig. 1-3: The discharging of a galvanic cell means a flow of electrons and anions from a anode to cathode (left). The flows of electrons and anions are reversed when charging (right) a battery.

The battery cell is discharged, and electrical energy is generated, when closing the circuit between minus and plus pole as shown in Fig. 1-3 left (Linden 1995). The reducing agent oxidizes the anode

so that electrons are released to the external circuit. Since they cannot pass the electronically insulated separator, the electrons flow to the cathode via an external conductor. They are gained by the positively charged cathode, which is reduced in this way. The rising charges within the half-cells are balanced via the electrolyte, as the anions and cations flow to the anode respectively cathode by passing the separator. The battery cell is completely discharged, as soon as the materials available in the half-cells are fully oxidized respectively reduced.

Accumulators, which have to be used for balancing PV power, have the ability of reversing this process (Linden 1995). When connecting the battery cell to a power pack, the electrons flow from the positive to the negative pole of the battery (see Fig. 1-3 right). The oxidation takes place at the positively charged anode and the reduction at the negative cathode so that the ions pass the separator in opposite direction. With the inversion of the redox reaction, the battery is recharged.

The maximum voltage, that can be theoretically delivered by a battery cell, is determined by the electrode potential between oxidizing and reducing agent and is therefore dependent on the material (Linden 1995). If connecting multiple battery cells in series, the voltage can be increased to the desired magnitude. Usually, the battery cells are additionally connected in parallel forming battery stacks in order to obtain the desired storage capacity.

The theoretical capacity of a rechargeable battery cell is determined by its amount of electrolytic, reducing and oxidizing materials (Linden 1995). However, the useable capacity for charging and discharging is lower due to multiple factors like imbalanced proportions between the materials, material aging of the separator and electrodes, or temperature effects. Voltage drops and polarization effects that arise during discharging lead to the production of waste heat, so that the amount of available energy is further reduced. Additionally, the materials in the cells are subject to side-reactions, which discharges the battery independently of its active utilization.

Battery storage systems, which are based on highly inflammable materials like Lithium, require a careful monitoring of current and temperature in order to preserve the battery from exploding (Pistoia 2013). For this reason, battery energy management systems (BMS) are usually integrated into the cell stacks in order to prevent a thermal runaway. A BMS usually includes a thermal and an energy management system keeping the temperature and current flows within a safe and smooth operation mode to ensure a secure and stable operation of the accumulator.

1.2.3 Integration of PV and battery systems into residential power networks

Traditionally, the provision of energy for households in low voltage grids is based on alternating current circuits at frequencies of 50 or 60 Hz (IEC 2020). However, solar cells and battery storage systems produce direct current electricity. This makes additional equipment necessary to integrate rooftop PV and battery systems into the households' power network.

PV systems are connected to the household grid by solar inverters, which transform the energy produced by the solar cells from direct into alternating current. Additionally, maximum-power-point (MPP) Trackers optimize the power output of the solar cells under the changing irradiation and temperature conditions.

Two common ways of integrating the battery storage system into the residential energy system exist (Weniger et al. 2014). The battery storage system can be coupled to the home network separately from the PV system using an additional inverter (see Fig. 1-4 left). This configuration has the advantage that the battery can also be subsequently integrated into the residential grid network.

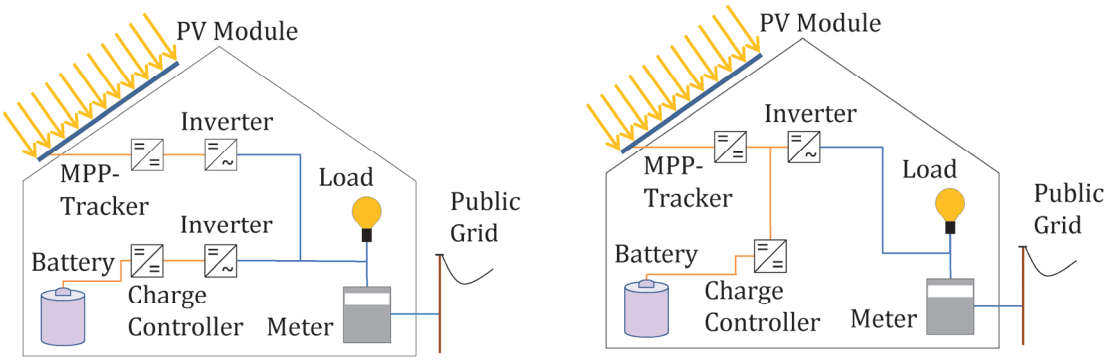

Fig. 1-4: Options for coupling the battery to the residential network.

The monetary more efficient form of integrating the production and storage system into the networks is the direct coupling of PV system and battery storage using a battery converter and a hybrid inverter (see Fig. 1-4 right). Since PV production and the battery operation are both working on direct current, additional costs and losses of a second inverter are eliminated.

Usually, intelligent meters are used in buildings with PV systems, which monitor the energy flows at the connection to the public grid in real-time. In this way, the management of the residential energy system can be optimized and revenues for PV energy excesses can be precisely determined.

Fig. 1-5 (top left) shows the energy balance of a residential energy system when equipped with a PV system and a battery storage at a day with PV energy excesses. The battery is utilized to temporally shift the supply with self-produced PV energy into times of deficit so that the imbalances between energy consumption and energy production rate are levelled to a higher degree.

The residuals of the residential energy production, consumption and the battery flows are balanced by the public grid (see Fig. 1-5 top right). The term residual load is defined as the flows between the public power grid and the residential energy system. This includes the supply of electrical energy via grid in times of deficit and the feed in of PV excesses, which are neither directly consumed nor stored in the battery.

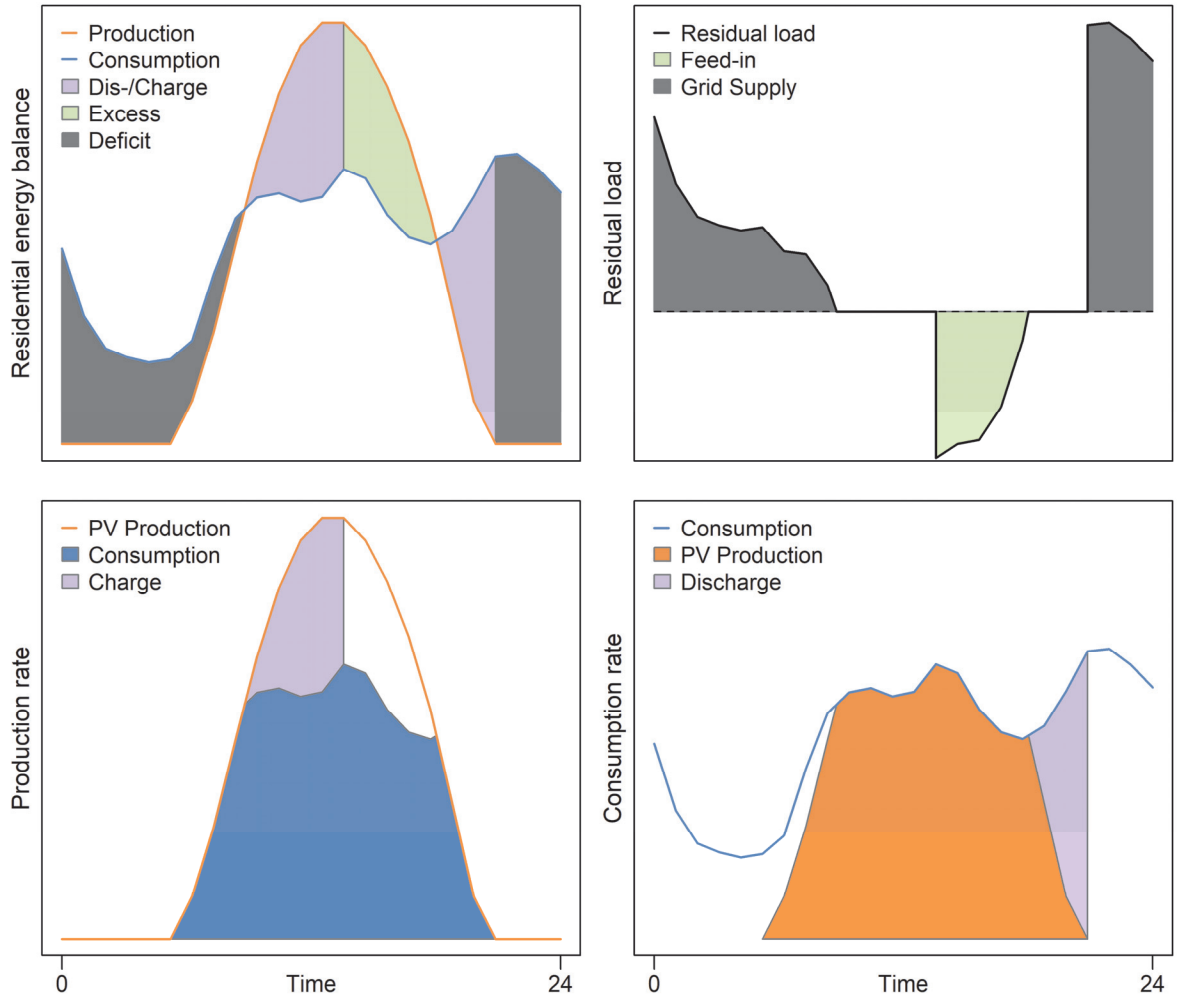

Fig. 1-5: Top row: Energy balance in a residential building with PV generation and battery storage at a sunny day (left) and distribution of the resulting residual loads between public grid and residential energy system (right). Bottom row: Schematic self-consumption of the PV production (left) and self-supply of the consumption rate (right) in a residential building.

One important parameter in the assessment of PV systems is the degree of PV self-consumption shown in Fig. 1-5 (bottom left). It is defined as the amount of PV energy of the total production that is directly consumed by the households or used for charging the battery. The degree of self-supply describes, how much of the consumption can be supplied by the PV system and the storage (see Fig. 1-5 bottom right).

The degree of self-consumption and self-supply can strongly vary between the residential energy systems, since they depend on multiple building-specific factors. These include not only the residential energy demand or the dimensions and properties of the PV and battery systems but also the spatially varying physical conditions, which constrain the productivity of the PV systems to different degrees.

1.2.4 State of the art in the modelling of residential PV-coupled battery storage systems

With the rising deployment of residential energy storages, the research activity in the assessment of PV-coupled battery systems has strongly increased focusing on the benefits of residential owners and the potentials for grid integration. Fig. 1-6 shows the main investigated thematic areas of recent years.

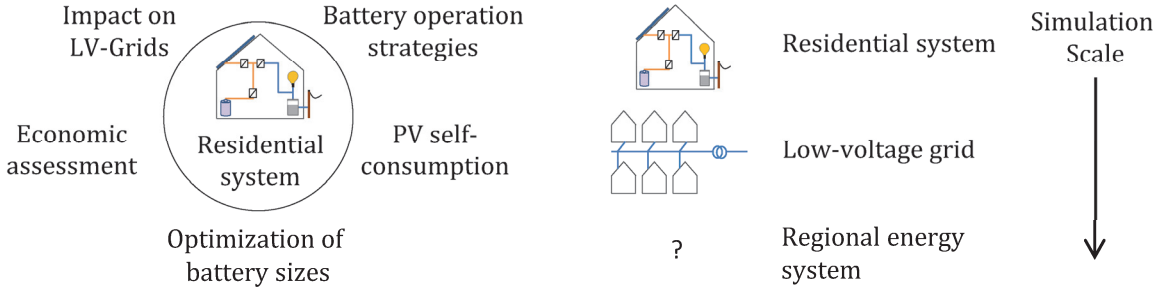

Fig. 1-6: Keywords in the research of residential PV-coupled battery storage systems (left) and model scales in their assessment (right).

One major research area, which has developed alongside the rising deployment of PV-coupled batteries, investigates the quantification of the effects of residential batteries on residual loads due to the balancing of PV production and consumption. This mainly includes the evaluation of utilizing residential batteries for grid relief. Behind-the-meter storages offer the potential for peak-shaving in two ways: They can reduce grid loads arising from consumption peaks by up to 50% (Schram et al. 2019). But they can also dampen critical backflows from PV surpluses and integrate residential PV energy into the grids at low loss rates (Moshövel et al. 2015).

Thereby, grid relief effects are closely connected to the battery management. Meanwhile, battery operation strategies are often based on dynamic algorithms, which forecast PV-production and consumption rate in order to predict the optimal periods of battery charging. The controlled operation of the charging and discharging periods and quantities is one decisive factor decreasing critical voltage fluctuations and grid backflows (von Appen et al. 2014). Grid relief can also be achieved when maximizing self-consumption (Luthander et al. 2016). Research in the battery management also addresses the development of strategies focusing on the benefits for the PV-battery owners. Luthander et al. (2015) could show that residential batteries raise the degree of PV self-consumption between 13% and 24% depending on the storage capacities, meteorological conditions, consumption loads and PV sizes. Further optimization goals include the enhancement of battery lifetime (Angenendt et al. 2018) or the maximization of the system profitability (Sani Hassan et al. 2017).

Apart from an adjusted management, the choice of the battery size also determines about the economic performance of the residential storages. From an economic perspective, the optimal battery

size maximizes the levelized costs of storage and therefore the returns for their owner. The profitability of a system is driven by several factors as the magnitude of investment costs, the potential of reducing electricity purchase due to increased self-consumption or the battery type, which have to be considered in the battery sizing (Hesse et al. 2017). But also the tariff-models for the purchase of electricity have to be taken into account for a robust battery design (Dufo-López 2015). Furthermore, Schopfer et al. (2018) underline that the optimal battery capacity also depends on the load profiles, which largely vary between the residential energy systems. Consequently, the economic performance of the batteries and their optimal dimensions are also subject to variance due to the high diversity of the residential systems.

In the assessment of residential PV-coupled batteries, several model scales have been established depending on the scopes as presented in Fig. 1-6 right. Most studies simulate the residential energy system by combining a PV production, battery storage and consumption model, when analyzing the energy flows and monetary consequences on detail. This methodology allows an easy evaluation of results and their robustness via sensitivity analyses. However, it is of limited applicability concerning the evaluation of the impacts of residential PV on the grid flows on a larger spatial scale.

When evaluating the interactions between residential energy systems and grids, vector-based model approaches are often applied, since they enable the modeling of residential energy flows in combination with grid constraints. On this model scale, whole segments of the low voltage grids with a higher number of buildings can be simulated. In this way, potential bottlenecks can be identified and the costs for grid enhancement are derived. Due to computational and data constraints, these models are often restricted to single segments of the low-voltage grid.

So far, only little research activity has been conducted in the assessment of residential battery storages from a regional perspective. The effects of residential PV systems on the energy systems and mitigation potentials of batteries have been assessed only to very limited extent on a larger spatial scale. It is well known that residual loads and self-consumption rates underly a large variance due to the heterogeneity of the residential buildings. However, the effects on a regional energy system where multiple buildings are equipped with PV systems and battery storages, have not yet been investigated comprehensively. It is yet unclear, how the high diversity of the residential buildings, their spatial peculiarities and the small-scale variance in the meteorological conditions change the regional energy flows. For these analyses, new approaches need to be developed which integrate the classical small-scale methods into geographic modelling approaches forming a novel hybrid method of a regional assessment of the energy production and storage system.

1.2.5 Research objectives

For a deeper understanding of the impacts of residential PV-coupled storages on the energy systems in a regional energy system, it is necessary to consider the physical peculiarities of a region additionally to the modeling of the techno-economic parameters. This especially includes the small-scale, spatial variations and the temporal volatility of the weather patterns in a region, to which the energy production is subject. It further concerns the PV potential, which can largely vary between the buildings due to different rooftop orientations, inclination angles, and available areas. These aspects constrain the available production capacity of the PV systems and therefore indirectly also drive the utilization of residential batteries. Apart from this, the residential energy systems themselves underly a high variance due to different equipment, PV sizes, battery capacities, efficiencies, or consumption loads, for instance. The first research question (RQ) investigates in which way the physical and technical boundary conditions can be parameterized individually for a multitude of buildings and how they are integrated into a regional energy system.

Research Question I: How can the impact of residential energy systems with PV-coupled battery storages be assessed on regional scale under consideration of the differences in the equipment, and consumption loads taking the spatial and temporal patterns in residential energy systems into account?

This physically based model approach forms the basis for following research questions, analyzing the effects of residential batteries on the energy flows in a regional energy system from different perspectives. One research focus is set on the optimization of the battery management depending on the targets as the grid integration of PV and maximization of PV self-consumption. As already largely investigated for the example of single system set-ups, the battery charging strategy has a significant impact on grid flows and self-consumption of a building and consequently also on the potential of batteries for PV integration. Research question II addresses the effects of different operation strategies on the energy system on larger scale when applied by a multitude of buildings with different PV sizes, battery capacities, consumption profiles, and meteorological conditions.

Research Question II: How are PV self-consumption and grid relief influenced by the charging strategy of residential batteries from a regional perspective?

Apart from the load balancing option within the residential energy system, the residual loads are also additionally balanced in the grids. This balancing effect is obtained by the spatial differences in the grid flows, which result from the varying PV sizes, consumption loads, battery capacities and meteorological conditions. Previous research has already shown that high PV installation rates lead to a low grid balancing effect but cause large energy surpluses in the low voltage grids. However, it is not well known, how far the rate of buildings equipped with PV systems affects

residual loads and grid surpluses. This poses the question, how the degree of spatial balancing via the grids and self-consumption depend on the regional PV installation rate.

Research Question III: How are self-consumption, grid balancing, and PV excesses correlated in a local energy system under different PV installation rates?

The PV installation rate also influences the potential of batteries for reducing grid excesses. The effects of the storages on the regional energy system are not well understood for a small share of residential buildings equipped with storages. The question arises how far the additional utilization shifts the correlations between self-consumption, PV surpluses and grid balancing under different PV installation rates investigated in RQ III.

Research Question IV: What are the regional effects of residential battery storages on grid balancing, energy surpluses and self-consumption, when the buildings are only partially equipped with PV systems and storages?

The third option driving the integration potential of residential storages is the battery capacity, which constraints the amounts of electrically stored energy. Depending on the optimization goals, the development of robust dimensioning approaches often includes projections for the techno-economic developments. However, future changes in the meteorological conditions and the consumption loads arising from climate change and efficiency enhancement of domestic appliances have not yet been evaluated. This thesis inquires in Research Question V how PV, battery and grid flows are influenced by the variation of these two boundary conditions for dimensioning approaches.

Research Question V: How do changes in climate and consumption loads affect residential PV coupled battery energy systems on regional scale?

1.2.6 Scientific publications

The dissertation addresses the five research questions in the following three scientific publications:

Publication I: Andrea Reimuth, Monika Prasch, Veronika Locherer, Martin Danner, and Wolfram Mauser. 2019. "Influence of different battery charging strategies on residual grid power flows and self-consumption rates at regional scale." *Applied Energy* 238: 572-581.

Publication II: Andrea Reimuth, Veronika Locherer, Martin Danner, and Wolfram Mauser. 2020. "How Does the Rate of Photovoltaic Installations and Coupled Batteries Affect Regional Energy Balancing and Self-Consumption of Residential Buildings?" *Energies* 13 (11): 2738.

Publication III: Andrea Reimuth, Veronika Locherer, Martin Danner, and Wolfram Mauser. 2020. "How do changes in climate and consumption loads affect residential PV coupled battery energy systems?" *Energy* 198: 117339.

Publication I, which was published in the Elsevier Applied Energy Journal in 2019, addresses research question I and II. The second publication investigating research question III and IV was published in 2020 in the special issue "Assessment of Photovoltaic-Battery systems" of the MDPI Energies journal. Research question V is assessed in Publication III published in 2020 in the Elsevier Energy journal (see Tab. 1-1). The findings were investigated during the project *INOLA – Innovationen für ein nachhaltiges Land- und Energiemanagement auf regionaler Ebene* funded by the Federal Ministry of Education and Research of Germany (grant code: 033L155AN, project period: 01.10.3014 – 31.12.2019).

Tab. 1-1: Overview of publications (Impact factor according to Clarivate Analytics (2020))

	Publication I	Publication II	Publication III
Research Questions	RQ I and RQ II	RQ III and IV	RQ V
Publication Year	2019	2020	2020
Journal	Applied Energy	Energies*	Energy
Energy and Fuels	8/103	56/103	15/103
5Year Impact Factor	8.558	2.990	5.747

**Published in the special issue "Assessment of Photovoltaic-Battery systems"*

1.2.7 Framing of the publications

Fig. 1-7 gives an overview of the objectives of this thesis and the publications addressing the according research questions.

Publication I presents the basic approach developed to assess the regional influence of residential PV-coupled battery storage systems. It contains the description of the residential energy systems component consisting of a PV-production unit, the consumption unit and the battery storage model and the integration into the land surface processes model PROMET. This GIS-based model approach allows the evaluation of the small-scale batteries and their potential from a regional perspective under consideration of the spatial peculiarities. In this way, constraints in the number of simulated systems are overcome and deeper insights into the interrelations between the residential energy systems can be obtained.

Regional assessment of residential PV-coupled battery storage systems **RQ1**: Conception of the model approach **Publication I**		
Residential action level **RQ 2**: Evaluation of different battery charging strategies **Publication I**	Regional action level **RQ 3, RQ 4**: Assessment of the PV and battery installation rate **Publication II**	Boundary conditions **RQ 5**: Influence of climate change and consumption loads **Publication III**

Fig. 1-7: Overview of the publications addressing Research Questions I to V.

This paper further adds to the discussion of the possibilities of the battery owners for integrating rooftop PV. Answering RQ II, Publication I focusses on regional effects of different battery management strategies. Based on the regional model approach, three different charging strategies are evaluated for a multitude of residential buildings located within a study area with individually parameterized PV systems, consumption loads, and battery storages in order to gain insight into their effects on the regional energy system. The selected charging strategies, which aim at the goal of (1) maximizing self-consumption, (2) minimizing curtailment losses and (3) maximizing grid relief in terms of rising self-consumption, have already been largely investigated at the example of single systems or small parts of the low voltage grids. Publication I gives insight into the variation between the individual buildings within a region in terms of the potential of batteries for rising self-consumption, decreasing energy surpluses, and reducing curtailment losses. Based on the obtained results several implications for policy measures as feed-in restrictions are derived for motivating the owners of PV-coupled battery systems to use grid-friendly charging strategies.

Publication II builds upon the developed model environment and results introduced in the first paper. As shown in Publication I, the residual loads of residential buildings underly a strong spatial variation due to varying system configurations and meteorological conditions, which could be partly balanced via the grids. After the assessment of the PV integration potential on building level in RQ II, the potential of residential batteries for grid integration is now analyzed on this superordinate, regional scale. Publication II first addresses RQ III and presents the correlations between the degree of self-consumption, energy surpluses and regional grid balancing in a regional energy system. The degree of residential buildings in a municipality equipped with PV plays an important role, how far the energy flows can be balanced in the grids between the buildings. Especially, at high installation rates, the residual loads could be critical and mitigation measures become necessary for the grid integration of PV.

After assessing the spatial balancing potential for different PV installation rates, Publication II further evaluates the temporal balancing effect of the energy flows behind-the-meter introduced by residential batteries. Residential batteries can contribute to the reduction of grid surpluses only

to limited degree at low and medium PV installation rates, whereas the excesses can be significantly reduced at a high degree of buildings with PV systems. The potential of batteries for the PV integration in a regional energy system does not only depend on the charging strategy but also on the PV installation rate.

Apart from these two factors, the boundary conditions have a crucial impact on how residential PV systems and batteries affect the regional electrical energy systems. Publication I and II address Research question II to IV under the current climatic and consumption conditions. However, these factors will undergo significant changes due to climate change and its mitigation measures as it was formulated in Research question V. Publication III assesses how far these changes in the boundary conditions affect residential battery storages. The paper includes three scenarios for the near-term future, which project different developments of the climate and efficiency enhancement of domestic appliances. It is evaluated how far the production rates of residential PV systems are changed by the varied meteorological conditions and in which way, consumption will decrease due to the lower energy demand. The paper analyzes the influence on battery and grid flows to obtain a comprehensive picture, how the self-consumption rates on the one hand, but also the potential for grid stresses on the other hand will develop in the future.

The analyses in Publication I and III were carried out for three administrative districts with 362,000 inhabitants located in the south of Germany (Bayerisches Landesamt für Statistik 2020). Publication II focuses on a single municipality in this study area with representative physical conditions. The investigated region is characterized by a pre-Alpine and Alpine landscape with an average solar irradiation of 1167 kWh/m² (DWD CDC 2016). Currently, 8% of the residential buildings are equipped with rooftop PV (Bayerisches Landesamt für Statistik 2017; Bayerisches Landesamt für Digitalisierung 2015a). The residential sector accounts for 21.6% of the electrical energy demand with an average consumption of 5127 kWh per building (Lechwerke 2017; Bayernwerk 2017; Elektrizitätswerke Tegernsee 2017; Gemeindewerke Holzkirchen 2017; Gemeindewerke Peißenberg 2017; Stadtwerke Bad Tölz 2017; Elektrizitätswerke Böbing e.G. 2017). In order to derive building-specific consumptions loads, top-down approaches have been applied, which scale annual consumption data from municipal to building level. In Publication I and III the simulated PV sizes are based on georeferenced data sets, whereas in Publication II they are determined from the available technical potential and statistical data. The battery storage capacities were derived using an already established dimensioning approach and assuming state-of-the art battery technology.

2 Influence of different battery charging strategies on residual grid power flows and self-consumption rates at regional scale

This chapter was published in the Elsevier journal *Applied Energy*:

Reimuth, Andrea, Monika Prasch, Veronika Locherer, Martin Danner, and Wolfram Mauser. 2019. "Influence of different battery charging strategies on residual grid power flows and self-consumption rates at regional scale." *Applied Energy* 238: 572-581.

Abstract

Battery storage systems can help to integrate excess Photovoltaic (PV) energy into the local energy systems but also increase the request for higher self-consumption rates of the households. This study uses a spatially resolved approach with hourly time steps to analyze the influence of batteries on the domestic residual loads on a regional scale. A domestic energy component is developed consisting of a PV-system model, the demand component, and a battery storage device. The study area is located in the south of Bavaria and 4906 households with PV-systems between 3 and 10 kWp power were selected assuming a battery capacity of 6.2 kWh in average. Three charging strategies for domestic battery storage systems are assessed: (1) Maximization of self-consumption, (2) Fixed feed-in limit of 70% of the PV-peak power, and (3) Daily dynamic feed-in limit based on ideal forecasts. The best result is obtained through the third strategy with a self-consumption of 78.5% on average a

nd the highest reduction of the grid flows by 20% by damping grid excesses. The influence of the charging strategy rises with increasing size of PV- and battery storage systems and therefore residual loads. Regional variations are further caused by the meteorological conditions, different PV- and battery sizes and parameters and demand profiles on municipal scale. Consequently, a sufficient sample size with different set-ups is recommended for a full evaluation of battery charging strategies.

- Raster-based model of regionally distributed domestic energy systems.
- Assessment of three charging strategies for PV-coupled battery systems.
- Optimum of self-consumption and grid relief with daily dynamic feed-in limits.
- High spatial variation due to meteorology, plant parameters and consumption rates.

2.1 Introduction

Solar power belongs to the category of renewable energy technologies with the highest acceptance among the population in Germany and it yields a high potential for the energy system transformation (Institut für Demoskopie 2015). After the millennium break, the German government started to raise the request for small-scale rooftop PV-panels offering lucrative funding opportunities with fixed feed-in tariffs. For instance, 120,000 solar panels with a total peak power of 700 MW were installed in private households in 2011 (Bundesministerium für Wirtschaft und Energie 2015). With the stepwise reduction of financial support and the beginning expirations of the funding periods the incentives for high grid feed-in rates are vanishing. For this reason, the owners have given more and more priority to the domestic use of the generated energy to reduce their electricity costs. However, the PV-production profiles match to the domestic loads only partially, which encourages the development of adaption strategies. Battery storage systems belong to the marketable and affordable products to increase the self-consumption rates and therefore the economic efficiency of the PV-plants. In 2050 between 25% and 67% of the German households are estimated to operate battery storage systems for domestic use (Agora Energiewende 2014).

From the grid suppliers' perspective, the high penetration of residential PV-plants combined with low consumption rates has increased the amount of bottlenecks occurring at the low-voltage grids especially during the summer months. The increasing costs of grid adjustment can be damped by feed-in restrictions of the PV-systems to decrease harmful peaks in the local grids (Moshövel et al. 2015). In Germany for instance, the maximum feed-in power must be capped to 70% of the nominal power of small scale PV-plants by the owners according to §9(2) German Renewable Energy Sources Act (2017) (Bundesministerium für Wirtschaft und Energie 2017). Using intelligent management approaches, domestic battery storage systems can also help to reduce curtailment losses and the costs for grid adjustment.

Substantial research has been done in the development of optimal strategies for increasing the self-consumption rates (Luthander et al. 2015). It could be further shown that batteries which are dimensioned with the sole objective of maximizing the self-consumption have the potential of reducing negative feed-in peaks (Schram et al. 2018). A number of studies has been carried out which focus on the development of charging strategies optimal for the requests of households as well as grid suppliers (Angenendt et al. 2018). A recent study compared the impact of different charging strategies on the consumption rates, voltage reductions, and losses (Resch et al. 2015). The best result was obtained for a daily dynamic feed-in limit based on forecast data for grid suppliers and battery owners. An easily applicable, dynamic management approach was developed, which reduces the high backflows even better than the fixed feed-in limit of 70%. However, a feed-

in limitation is still recommended to damp peaks occurring from forecast errors (Moshövel et al. 2015).

Several case studies have analyzed the influence of different battery numbers, sizes, and positions on the power flows in the low-voltage distribution grid. They emphasized that the full potential of roof mounted PV-systems can only be utilized with local energy storage systems due to the limitations in the grid capacities (Lödl et al. 2011). It could also be shown that domestic battery storages significantly relieve the distribution grid using a charging strategy adjusted to grid-balancing incentives (Faessler et al. 2017). These studies are case studies limited to the small scale of the selected local distribution grids with a few households, PV-systems, and batteries.

Another approach for the evaluation of battery storage systems has been developed in the field of assessing the regional PV-energy potentials on rooftops. This approach seeks to improve the generation of solar cadasters using geo information systems (GIS). For instance, a method of estimating the sizes of the battery storages from time series data of one year has been developed for a better integration of the PV-systems into the grid (Ramirez Camargo et al. 2015). A case study in Germany and the Czech Republic analyzes the spatial influence on the PV-sizes and storages capacities for a self-sufficient supply from weather measurements and demand data (Ramirez Camargo et al. 2018). Another study presents an approach of assessing the limited influence of randomly distributed batteries on the overvoltage problems in low distribution grids, when maximizing the self-consumption (Crossland et al. 2018). This opens the question of the influence of different storage management strategies on regional scale assessing the batteries under technical constraints.

In this study, we aim at analyzing the impacts of an increased use of battery storage systems on regional scale to obtain a better quantification of the consequences on the domestic energy balances. We assess three charging strategies including local variations in the residential energy demand, the meteorological conditions, as well as different PV and battery parameters. We also examine the influence on the grid power feeds of the households as the reduction of negative peaks but also the benefits to the owners.

We developed a domestic energy model consisting of three components: the energy demand, the PV-production, and the battery energy storage. This approach is embedded into a raster based land surface model, which has already been validated for different scales (Mauser et al. 2009).

2.2 Materials and methods

The domestic energy model applied in this study is integrated into the physically based land surface model Processes of Radiation, Mass and Energy Transfer (PROMET) (Mauser et al. 2009). This model was originally developed for hydrological analyses of watersheds and has already been

successfully tested for a variety of study areas and extents. It strictly follows the conservation of mass and energy, and therefore does not need to be calibrated.

PROMET is fully spatially distributed and raster based, which means that each location in the study area is represented within a grid structure. For this purpose, the land surface is segmented into a matrix of equally distributed grid elements of adjustable size. The energy systems, which are simulated in the domestic energy component, are referenced to the grid points of the raster according to their spatial distribution. The electrical energy balances are calculated individually under the meteorological conditions of their associated pixels. If more than one energy system is located on a grid element, the results are aggregated to pixel resolution, as the output is formatted according to the defined raster.

2.2.1 The domestic energy model environment

The domestic energy module includes three elements: the photovoltaic production component, the rechargeable battery model with the inverter, and the consumption model, which calculates the self-consumption of the produced energy and the flows from and into the public grid (see Fig. 2-1). The residual load of a domestic energy system R_D [kW] is defined as the difference between the residential consumption E_D [kW], the production of the PV-panel P_{PV} [kW] and charging/discharging power of the battery P_B [kW] (see Eq. (2-1)). It is assumed that the PV-system and the battery are directly coupled in a DC topology and their performances are converted to alternative current with a constant inverter efficiency η_{It} [-]. The power flows of the PV-panel to the residential grid are limited to 70% of the peak power to meet the restriction of EEG 2017 (Bundesministerium für Wirtschaft und Energie 2017). Thereby, the effects of a feed-in restriction on the battery utilization can be evaluated.

$$R_D = E_D - (P_{PV} + P_B) \cdot \eta_{It} \qquad (2\text{-}1)$$

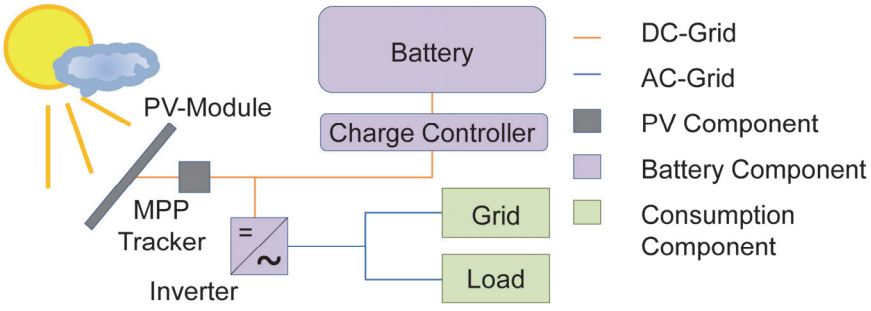

Fig. 2-1: Structure of the domestic energy module containing the energy production of the PV-panels, the battery with its environment and the grid power flows.

The following three chapters describe the determination of the components of Eq. (2-1): The hourly residential consumption E_D is explained in Section 2.2.3, the computation of the PV-performance P_{PV} is given in Section 2.1.1, and the battery model used to determine the battery power in

terms of the physical condition is shown in Section 2.2.4. The determination of the battery performance P_B including the constraints of the charging strategies is described in Section 2.2.5. The parameterizations of the variables, which are used in the presented study case, are described in Section 2.5.2 and Tab. A. 2-1.

2.2.2 The production model

The production of electric energy calculated in the PV-model is driven by the meteorological input, which consists of station measurements for air humidity, air temperature, precipitation and wind speed (see Section 2.5.1). Based on these meteorological boundary conditions, the direct and diffuse radiation fluxes are simulated on pixel resolution considering topographical impacts and cloud cover (Mauser et al. 2009). The incoming fluxes correspond to the amount of hourly direct and diffuse radiation on the horizontal plane E_{Dir} [W/m²] and E_{Dif} [W/m²] used for the determination of the PV-production rates.

At each time step, the incidence angle of the sun on the inclined planes of the PV-panel θ_{ic} [deg] is calculated as shown in Eq. (2-2) (Quaschning 2013):

$$\theta_{ic} = cos^{-1}(-\cos\gamma_S \sin\gamma_P \cos(\alpha_S - \alpha_P) + \sin\gamma_S \cos\gamma_P) \quad (2\text{-}2)$$

The parameter γ_S denotes the solar zenith [deg], γ_P is the inclination angle of the solar panel [deg], α_S is the solar azimuth [deg] and α_p is the orientation of the solar module plane [deg].

The total radiation $E_{tot,P}$ [W/m²] on the inclined planes of the solar panels is calculated from the direct solar irradiation $E_{Dir,P}$ [W/m²], the diffuse solar irradiation $E_{Dif,P}$ [W/m²] and the background reflection $E_{Ref,P}$ [W/m²] following the approach of Quaschning (2013) according to Eq. (2-3):

$$E_{tot,P} = E_{Dir,P} + E_{Dif,P} + E_{Ref,P} \quad (2\text{-}3)$$

The determination of the direct irradiation on the inclined plane $E_{Dir,P}$ [W/m²] of the solar panels is shown in Eq. (2-4):

$$E_{Dir,P} = E_{Dir} \cdot \cos\theta_{ic} / \sin\gamma_S \quad (2\text{-}4)$$

The indirect irradiation $E_{Dif,P}$ [W/m²] is calculated using the model of Klucher (Quaschning 2013) (see Eq. (2-5) and (2-6)).

$$F = 1 - \left(\frac{E_{Dir}}{E_{Dir} + E_{Dif}}\right)^2 \quad (2\text{-}5)$$

$$E_{Dif,P} = E_{Dif} \cdot 0.5(1 + \cos\gamma_P)(1 + F \sin^3(0.5\gamma_P))(1 + F \cos^2\theta_{ic} \cos^2\theta_{ic} \cdot \cos^3\gamma_S) \quad (2\text{-}6)$$

The reflective share of the incoming irradiation on the inclined planes is estimated from the albedo A [-] as shown in Eq. (2-7).

$$E_{Ref,P} = (E_{Dir} + E_{Dif}) \cdot A \cdot 0.5(1 - \cos\gamma_P) \quad (2\text{-}7)$$

The production of electric power P_{PV} is calculated considering size of the PV-panels A_{PV} [m²], the efficiencies of the PV-panels η_{PV} [-] considering the influence of the module temperature T [°C] and aging [a] and the efficiency of the MPP-tracker (see Eq. (2-8)). A snow coverage of more than 2 cm and a solar irradiation angle of less than 3° leads to a stop of the production of electric energy.

$$P_{PV} = E_{tot,P}/1000 \cdot A_{PV} \cdot \eta_{PV}(T, a) \cdot \eta_{MPP} \quad (2\text{-}8)$$

The PV-model was successfully validated in the study region by measurement data with a 15 min resolution from three PV-plants for the year 2016.

2.2.3 The consumption model

The yearly domestic demand in electrical energy is determined as the annual consumption of the community divided by the amount of residential buildings.

The hourly energy demand of the household E_D is determined from the annual domestic consumption E_{Da} [kWh] hourly load curves $h_f(S,doW)$ [-], which distinguish between seasonal S [-] and daily profiles doW [-] (see Eq. (2-9) and Fig. A. 2-1).

$$E_D = E_{Da} * h_f(S, doW) \quad (2\text{-}9)$$

It is assumed that the load is always supplied either by the energy production of the PV-module and the discharging of the battery or the energy suppliers. Restrictions and further losses from the electric grid are not considered.

The results of the applied consumption model were validated on municipal scale by 15 min measurement data for the city of Bad Tölz and 2016, which is located in the study region.

2.2.4 The battery model

In this paper, the term battery stands for a rechargeable, stationary accumulator, which is always connected to the grid. The battery and integrated charge controller model follows the approach of Weniger et al. (2014) using a lithium ion accumulator system.

The useable capacity of the accumulator C_t [kWh] is calculated by Eq. (2-10) from the nominal capacity C_N [kWh], the maximum state of charge at the end of the lifetime SOC_{tmax} [-] and the utilization degree of the battery, which is defined as the current number of cycles nc_{act} [-] and the maximum number of cycles nc_{max} [-].

$$C_t = C_N \cdot (1 - (1 - SOC_{tmax}) \cdot nc_{act}/nc_{max}) \quad (2\text{-}10)$$

The hourly losses due to self-discharging E_{BL} [kW] are determined as a constant percentage L [-] of the nominal capacity of the battery (see Eq. (2-11)).

$$E_{BL} = C_N \cdot L/\Delta t \quad (2\text{-}11)$$

When charging the battery device, the amount of stored energy is increased by the computed delta regarding the free capacity, the maximum charging power, and the efficiency. If the battery is discharged, the amount of stored energy is decreased taking again into account the maximum discharging power, the amount of stored energy, and the efficiency of the discharging process. The dependency of the current, ageing, temperature on the charging and discharging power P_B [kW] is considered by a constant efficiency parameter η_B [-]. Eq. (2-12) shows the determination of the battery charging performance P_B [kW] with $P_{B,max}$ [kW] denoting the maximum battery performance, C_B the stored capacity and ΔE [kW] the available excess energy from the PV-plant.

$$P_B = min\left(P_{B,max}, (C_t - C_B), \Delta E\right) \cdot \eta_B \quad (2\text{-}12)$$

For discharging the battery (see Eq. (2-13)), the efficiency η_B is used in inverse form to supply the deficit ΔE [kW].

$$P_B = min\left(P_{B,max}, C_B, \Delta E\right) / \eta_B \quad (2\text{-}13)$$

The number of charging cycles is counted during the model run in a simplified form, which only depends on the direction of the hourly grid flows from or to the battery. As soon as the battery starts with charging after discharging, a charging cycle is defined as completed.

2.2.5 The charging strategies

Three different charging strategies are applied in this study:

1. Maximization of the self-consumption rate (MSC)

The first approach maximizes the self-consumption rate of the households. This means that in times the production of the PV-panels exceeds the domestic consumption, the battery is charged. If the battery capacity is full, the excess energy is fed into the grid. As soon as the delta between consumption and production becomes positive, the battery is discharged. In case the state of charge is zero, the residential energy demand is supplied by the grid.

2. Fixed-feed in limit (FFL)

This strategy is based on the objective to overcome the power excess peaks by limiting the grid feed-in to a fixed maximum. As the German statutory provisions of EEG 2017 restrict the PV feed-in to 70% of the PV-peak performance (Bundesministerium für Wirtschaft und Energie 2017), this limit is chosen as the threshold for the battery management: The battery starts off with charging of the surplus energy as soon as the PV-energy production of the PV-panels exceeds the fixed feed-in limit of 70% of the peak performance. When the solar energy production falls below the domestic demand, the battery is first fully discharged before the demand is finally supplied by the grid. Consequently, selecting this threshold also minimizes the losses by the assumed legal restrictions.

3. Daily dynamic feed-in limit (DFL)

The third strategy has the purpose to combine the maximization of the domestic self-consumption on the one hand and the reduction of the losses due to potential grid restrictions on the other hand. The approach implies a perfect forecast of the weather conditions and the domestic energy consumption. Therefore, a threshold value *DFLV* [-] is previously determined iteratively on daily resolution for each battery with regard to the state of charge *SOC* [-], which ensures the highest possible state of charge on condition that the daily peaks of the grid feed-in are smoothened as shown in Eq. (2-14)

$$DFLV_{n+1} = \frac{\sum_{i=1}^{24} \grave{R}_D(i) - SOC \cdot C_t}{SP \cdot P_{PV}}, \qquad \text{with } n = 0,1,2,\ldots \tag{2-14}$$

$$\text{with } \grave{R}_D(i) = \begin{cases} -R_D(i), & R_D(i) > 0 \\ 0, & R_D(i) \leq 0 \end{cases}$$

with *SP* [kW] being the minimum residual delta of the selected residual deltas $R_D(i)$ larger than the value $DFLV_n$ [-]. The starting values for the *DFLV* and the *SP* parameters are set to zero and the iteration process is stopped as soon as the minimum residual delta exceeds the *DFLV*-value.

Therefore, the battery starts to charge as soon as the delta between consumption and production exceeds the daily threshold value. The discharge strategy follows the first approach: When the domestic delta becomes positive, the demand is supplied first by discharging the battery device and then by the grid operators.

2.3 Evaluation parameters

The model results are evaluated with regard to the battery parameters like the states of charge, the number of cycles, the curtailment losses in [kWh] but also the influence on the grid in pixel resolution. The degree of self-supply *DSS* [-] of a domestic energy system *D* is defined according to Eq. (2-15) and the degree of self-consumption *DSC* is given in Eq. (2-16). The degree of autarky *DA* [-] determines the rate of energy flows related to the energy flows without storage system, which corresponds to the annual energy demand, as shown in Eq. (2-17).

$$DSS_D = 1 - \frac{\sum R_{D+}(i)}{E_{Da}} \tag{2-15}$$

$$DSC_D = \frac{E_{Da} - \sum R_{D+}(i)}{\sum P_{PV}} \tag{2-16}$$

$$DA_D = \frac{\sum |R_D(i)|}{E_{Da}} \tag{2-17}$$

R_{D+} [kW] denotes the positive hourly resolved grid power flows and R_D [kW] the grid power flows of the domestic energy system *D* [-].

2.4 The study area

Fig. 2-2 shows the selected research area "Bavarian Oberland", which is located in the south of Germany and covers an area of 2944 km² (Statistisches Bundesamt (DESTATIS) 2016). The three administrative districts Weilheim-Schongau, Bad Tölz-Wolfratshausen and Miesbach are divided into 72 municipalities with a total population number of 356,122 people (Statistisches Bundesamt (DESTATIS) 2016).

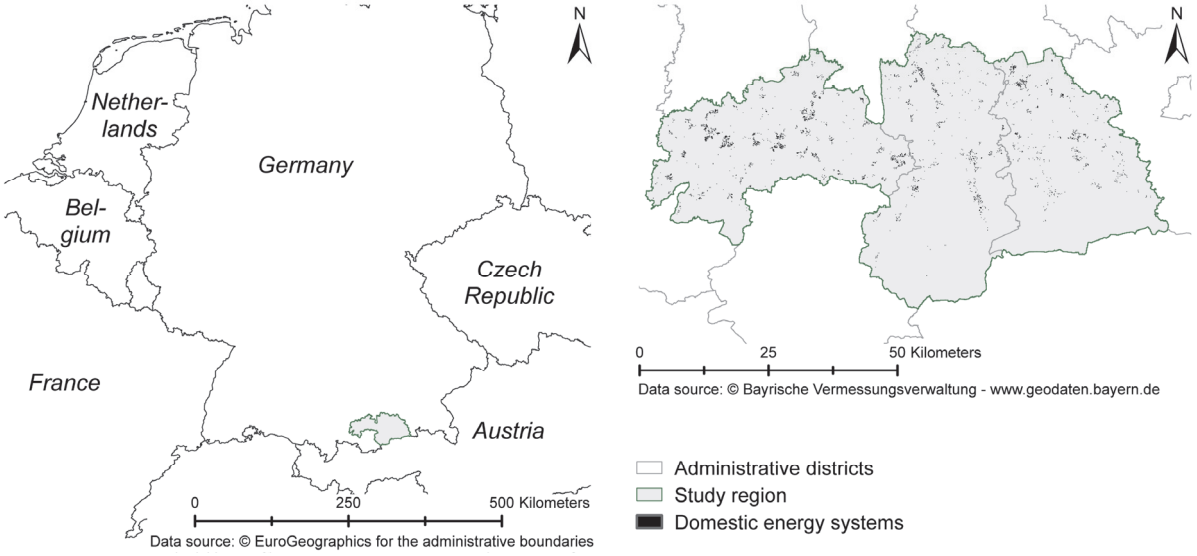

Fig. 2-2: Study region with a total area of 2,944 km², 356,122 inhabitants, and the distribution of 4,906 PV-systems selected in this study. (Data source: Bayerische Vermessungsverwaltung (2018); EuroGeographics (2018))

In 2016, the total electric energy consumption of the model region was 2168.25 GWh/a, of which the domestic electricity demand accounts for 21.1% with an annual domestic consumption of 5127 kWh in average (Lechwerke 2017; Bayernwerk 2017; Elektrizitätswerke Tegernsee 2017; Gemeindewerke Holzkirchen 2017; Gemeindewerke Peißenberg 2017; Stadtwerke Bad Tölz 2017; Elektrizitätswerke Böbing e.G. 2017). 13,409 PV-systems are installed in the three districts (Bayerisches Landesamt für Statistik 2017; Deutsche Gesellschaft für Sonnenenergie e.V. (DGS) 2015), of which 56.1% were classified as residential systems using the information of the Bavarian data model for buildings (Bayerisches Landesamt für Digitalisierung 2015a). The total global radiation from 1981 to 2012 ranges from 1137 to 1196 kWh/m² within the study area with a seasonal variation of the long-term monthly mean from 166 kWh/m² in July to 30 kWh/m² in December (DWD CDC 2015).

2.5 Input data

2.5.1 Meteorology

The meteorology input including air humidity, precipitation, air temperature and wind speed is taken from hourly measurements from 79 stations of the German and Austrian Weather Service network (DWD and ZAMG) covering the south of Bavaria and Austria. The simulation is performed for the year 2016 and the temporal resolution is set to 1 h. The cubic spline method is used to interpolate the meteorological input regarding the altitudinal gradients of the model region.

2.5.2 Input of the domestic energy model

The general input data for the PROMET-model are described in detail in Mauser (2016). The spatial and temporal resolution is set to 100 m and one hour. 4906 PV-systems with a nominal power between 3 and 10 kWp are selected and classified as private systems, which is a share of 65.2% of the households owning a PV-plant. The inclination of the PV-panels is assumed to match the roof pitches, which are obtained from a digital building model (Bayerisches Landesamt für Digitalisierung 2015a). The selected systems have an average area of 44.17 m^2 with a rooftop inclination angle of 27.36 deg and an orientation of 3.59 deg in southeast direction. The efficiencies of the PV-panels vary from 10.7% to 16.4% with a mean of 14.5% depending on the starting year (Fraunhofer ISE 2019b). The inverter has an average efficiency of 94.0% (Quaschning 2013).

The nominal capacities of the 4906 batteries are determined from the rated power of the PV-plants according to Weniger et al. (2014) with a usable capacity of 60% of the nominal capacity. This means a total nominal capacity of 77 MWh and a mean size of 6.3 kWh per household. The hourly loss rate is set to 6.25E−8 of the nominal capacity (Schoop 2013). The maximum power of the battery modules is set to 0.3 kW/kWh with a charging and discharging efficiency of 0.99 (Opiyo 2016) (see supplementary data).

The annual residential consumption of electric energy is determined from the measurement data of local energy suppliers in 2016 and the number of domestic buildings of the 72 communities (Lechwerke 2017; Bayernwerk 2017; Elektrizitätswerke Tegernsee 2017; Gemeindewerke Holzkirchen 2017; Gemeindewerke Peißenberg 2017; Stadtwerke Bad Tölz 2017; Elektrizitätswerke Böbing e.G. 2017). The households selected for this study have a total annual energy demand of 25,115.51 MWh in 2016, which means 5119.35 kWh per household. The hourly load profiles are categorized in three seasons of winter, summer, and spring/autumn as well as into three daily types of profiles for working day, Saturday and Sunday (Stadtwerke Unna 2015). The daily energy demand varies between 13.08 kWh and 15.52 kWh for an average household. The nine profiles are generally characterized by two load peaks in the early midday and evening, whereas in the early morning they become minimal (see supplementary data).

2.6 Results

2.6.1 The grid power flows and curtailment losses without battery storages

Fig. 2-3 shows the cumulated curve of the residual loads and the curtailment losses before considering the battery storage systems of the selected households.

The PV-plants of the selected households produce enough power to cover their annual energy demand, although the total delta of those households is positive at 6121 h of the year. During 2663 h, the production rates of the PV-systems exceed the total consumption. The generated backflows into the grid reach values that are up to three times higher than the maximum simulated overall hourly demand. During 4054 h of the year, there are simultaneous power excesses and deficits of the domestic energy systems observable. The balancing residual grid power loads have a size of 138 kWh in average, which is 4.8% of the total power flows.

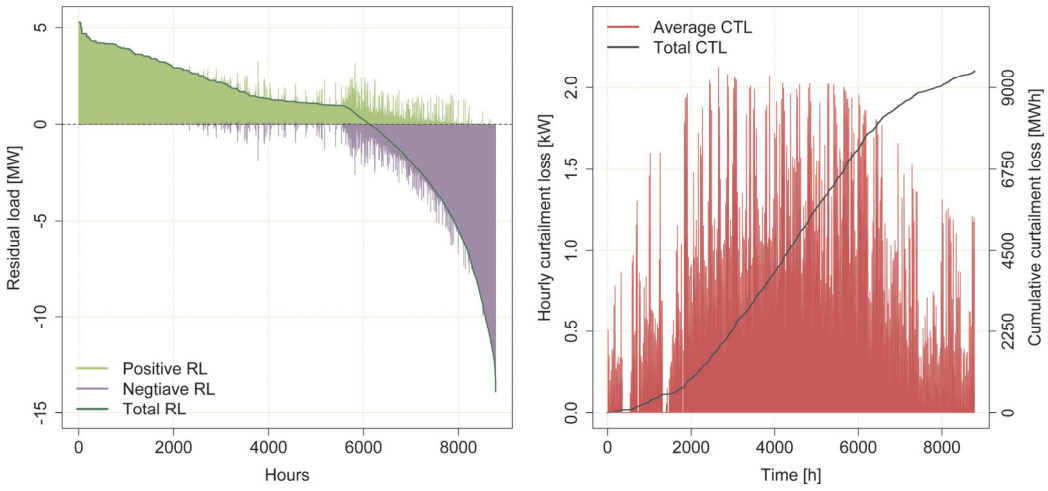

Fig. 2-3: Hourly power excesses (purple) and deficits (light green) of 4906 domestic energy systems without the influence of battery storages and the obtained regional balancing effect of the residential residual loads RL (dark green line) (left) and hourly curtailment losses CTL at average (red) and cumulated (grey line) (right).

The curtailment losses accumulate to 9470 MWh over the year, which equals the annual demand of 2000 households (see Fig. 2-3). Even during the winter months with low radiation intensities, curtailment losses up to 7.2 kWh per day for an average system are observed.

The map in Fig. 2-4 illustrates the residual loads of the domestic energy systems on 5 March 2016 at 2 p.m., which is the time step with the highest balancing effect. The grid power flows vary between -20.50 kW and 8.35 kW with an average of -0.40 kW before considering the curtailments at 70% peak power. 38.4% of the pixels containing the 4,906 households feed their power-excess into the grid, whereas 61.6% are supplied by the electricity grid with 4.56 MW. On regional scale, the sum of the deltas accounts for 1.40 MW at total amount of 7.73 MW domestic grid power flows.

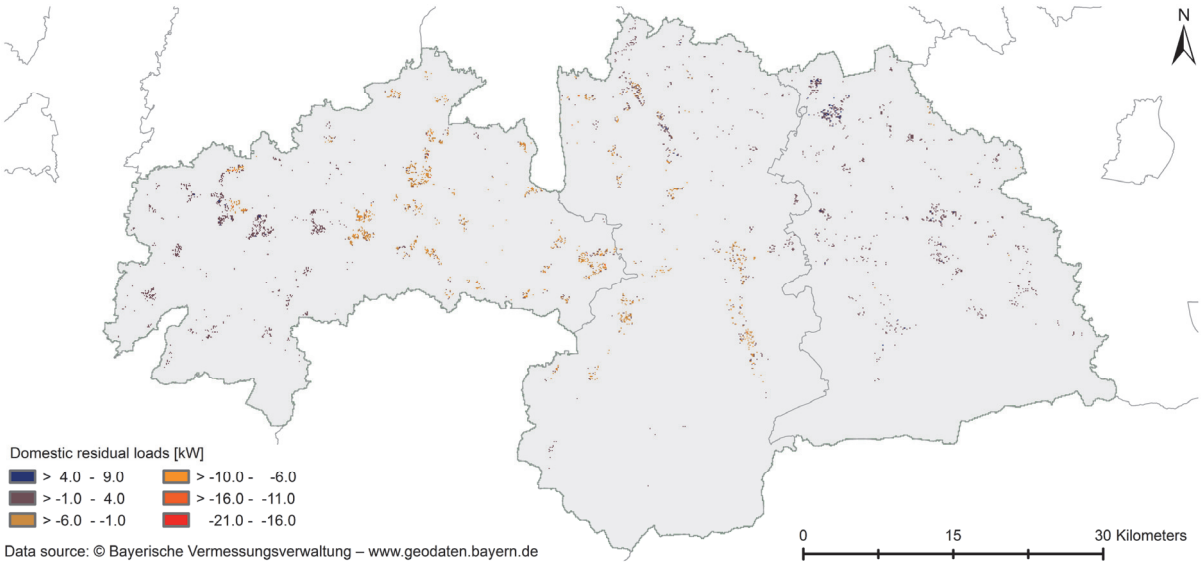

Fig. 2-4: Spatial distribution of the grid flows from the domestic energy systems at the hour with the highest regional balancing effect.

2.6.2 Influence of the charging strategies on the grid flows

The use of battery storage systems generally, but the selected charging strategy in particular, have different effects on the residual loads and curtailment losses. Fig. 2-5 shows the sums of the residual loads for the three applied charging strategies compared to the simulation without storages when the power flows are not reduced to 70% of the rated PV-plants.

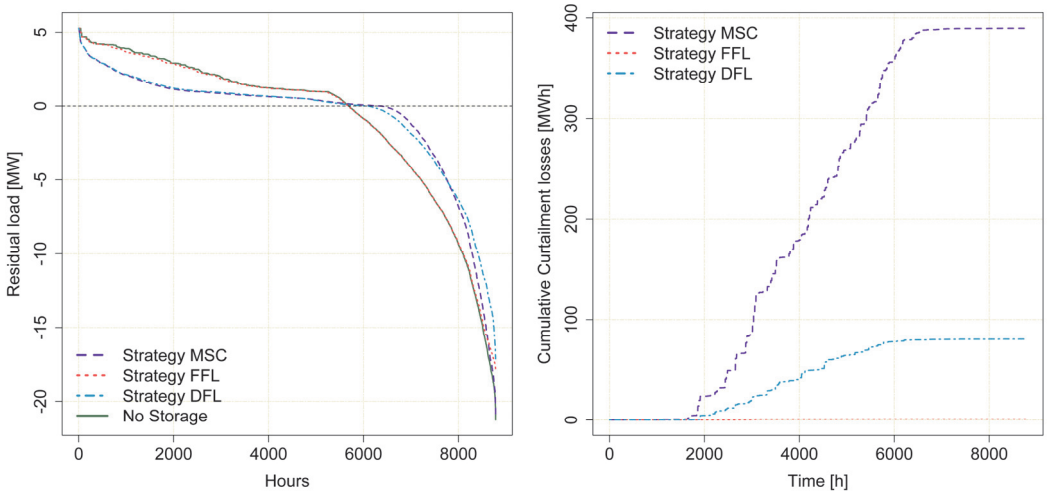

Fig. 2-5: Residual loads including curtailment losses (left) and curtailment losses (right) using the charging strategies maximization of the self-consumption rate (MSC), fixed feed-in limit (FFL), and daily dynamic feed-in limit (DFL) when compared to no battery storage systems.

The charging strategy Maximization of the self-consumption leads to a significant decrease of low grid feed-ins, but the results correspond to the residual power loads without storage systems for the high peaks. The second analyzed charging strategy applying a fixed feed-in limit leads to a reduction of the extreme deltas, but it has no effects on the lower residential residual loads. The

strategy Daily dynamic feed-in shows similar values as strategy MSC for the lower residual loads and converges to the result of strategy FFL for the highest deltas.

The application of battery storage systems leads to a decrease of the curtailment losses between 9076 MWh and 9465 MWh. The strategy Maximization of self-consumption can reduce the curtailment losses by 95.9% compared to the scenario without storage systems, whereas a higher reduction of the curtailment losses is obtained by strategy DFL with 99.2% and strategy FFL with 99.9%.

The day with highest daily energy delta, Monday, May 23, 2016, shows high differences of up to 48.2 kWh in peak between the pixels containing the domestic profiles. For the simulation without storage systems, the maximum grid feed-in is obtained by eight domestic energy systems located on one pixel (see Fig. 2-6a). The 5% and 95% quantiles vary between a minimum range of 0.6 kWh at 4 a.m. and a maximum span of 11.3 kWh at noon. The highest demand is observed at 9 p.m. varying between 0.6 kWh and 8.4 kWh. At midday, all domestic energy systems feed excess energy into the grid with a mean of 4.5 to 5.7 kWh. The first turnaround points of the grid power flows occur between 5 a.m. and 11 a.m. when the PV-production starts to exceed the demand. In the evening, the second turnaround is reached between 3 p.m. and 9 p.m. when the production falls below the consumption.

Compared to the simulation without the battery storages, the use of batteries with charging strategy MSC leads to a delay of the feed-ins by two hours in average. However, the influence on the heights decreases within in the next four hours (see Fig. 2-6a and b). From 12 a.m. to 5 p.m. the mean and the ranges of the quantiles and extrema are similar. After this time span, the deltas significantly decrease in the evening due to the discharge of the storages. The turnaround of the power flows, at which the discharging process is started, varies between 6 p.m. and 8 p.m. compared to a span of 3 p.m. to 9 p.m. in the basic scenario.

Strategy FFL leads to a cut-off of the peaks at midday compared to the residual loads without storage systems (see Fig. 2-6a and Fig. 2-6c). The damping effects of this charging strategy are higher with increasing negative residual loads. The minimum and 5% quantile of the residual loads for instance are not affected. The highest influence is observable for the maximum load with a reduction of up to 20.8 kWh from 10 a.m. to 2 p.m. In the evening, the reduction of the positive deltas follows a similar pattern: the highest influence of this strategy is obtained on the reduction of the maximum positive energy deltas, whereas the effects decrease with decreasing deltas. The turning points in the morning and evening are not shifted.

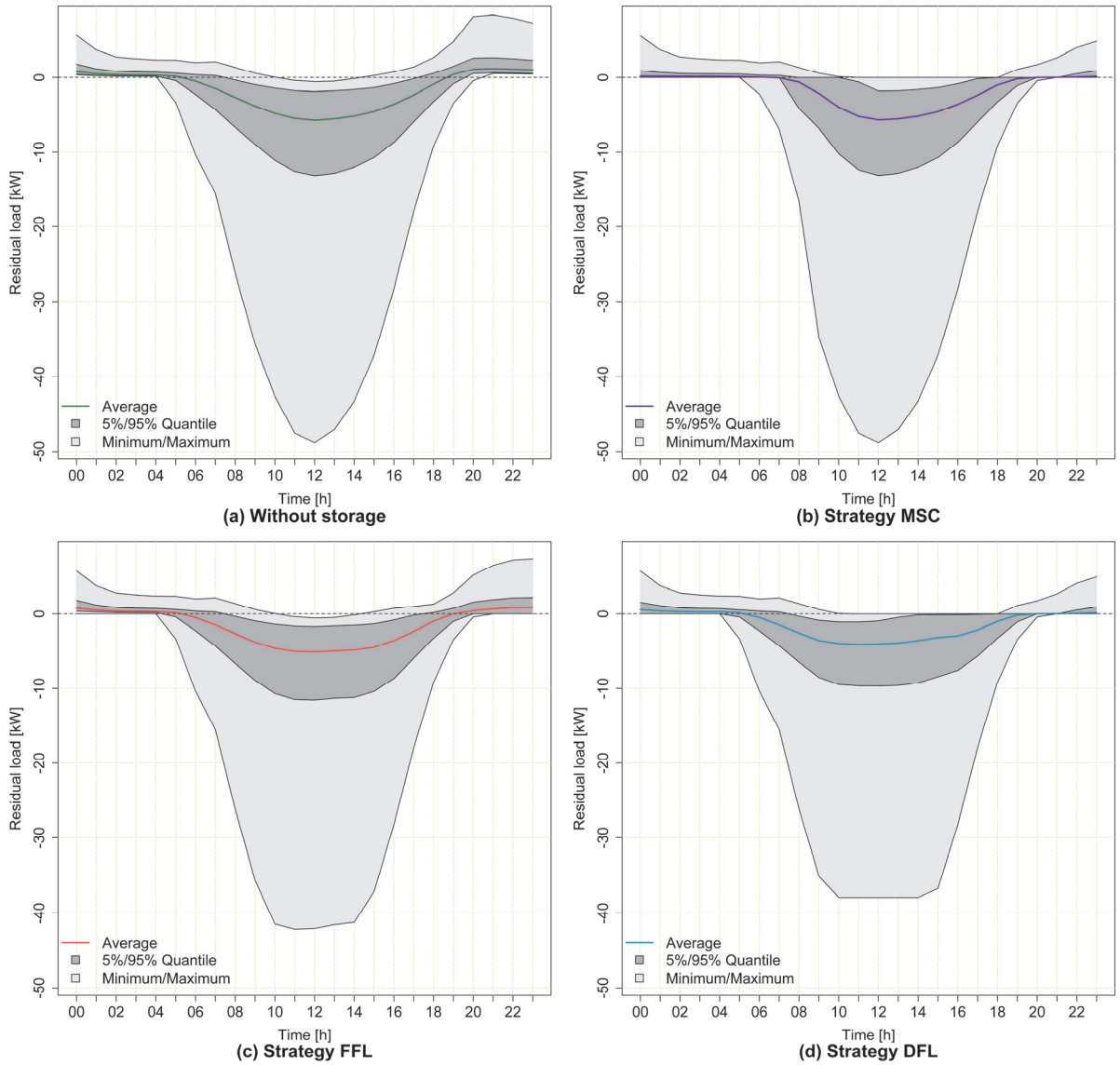

Fig. 2-6: Average, range of minimum, maximum and range of 5% / 95% quantile of the domestic residual loads at daytime with maximum negative delta in 2016 with (a) no battery storage, (b) charging strategy Maximization of self-consumption (MSC), (c) charging strategy Fixed feed-in limit (FFL) and (d) charging strategy Daily dynamic feed-in limit (DFL).

Fig. 2-6d shows the residual loads for charging strategy DFL, which uses daily dynamic feed-in limits. The damping effect, which is also observable at charging strategy FFL is higher. Even the minimum residual loads become zero during midday. The peak of the maximum feed-ins is cut to a threshold of 37.9 kW for five hours, which means a total reduction of 39.8 kWh. In the morning, the turnarounds occur similar as for the basic scenario without charging strategy. However, the turning points in the evening are similar to charging strategy MSC.

2.6.3 The influence of the charging strategies on the domestic energy systems

Table 1 shows the evaluation parameters obtained on pixel resolution, which are relevant for the domestic battery storage systems.

Tab. 2-1: Average number of battery cycles, degree of self-consumption, self-supply and autarky without storages and with batteries applying strategy Maximization of the self-consumption, Fixed feed-in limit of 70% kWp power and Daily dynamic feed-in limit.

Average	No Storage	Strategy MSC	Strategy FFL	Strategy DFL
Degree of self-consumption	0.505	0.795	0.521	0.785
Degree of self-supply	0.443	0.726	0.459	0.716
Number of cycles	-	528.26	78.51	538.51
Degree of autarky	1.432	0.858	1.398	0.835

On average, half of the power produced by the PV-plants is consumed by the households if no storage systems are used. Battery storage systems increase the degree of self-consumption further by 29.0% for strategy MSC, by 1.6% using the strategy fixed feed-in limit and 28.0% for strategy DFL.

The charging strategy with the approach of maximizing the self-consumption increases the degree of self-supply in average by 28.3%. This is a similar result compared to the strategy DFL. In contrast, strategy FFL can increase the domestic consumption only by 1.6% compared to systems without storage.

The highest utilization of the battery storage systems is obtained for strategies MSC and DFL, at which the charging processes of the battery is started 1.44 and 1.47 times per day, respectively. When applying charging strategy FFL, the charging processes of the batteries are started every 4.66 days in average.

The degree of autarky shows that the domestic grid flows are increased by 43.2% in average, when a PV-system is used without storage effects. This result is also obtained by the charging strategy FFL, which only becomes active when the feed-in of the PV-systems is cut. Consequently, only the excess energy is used, which does not reach the grid due to the current regulations. Strategy MSC and DFL lead to a higher degree of autarky of the domestic energy systems, as the grid flows are reduced by 20% compared to households without PV-system nor battery storage.

2.7 Discussion

2.7.1 Assessment of the charging strategies

The results show that the production and storage sizes have crucial influence on the residual loads on regional scale apart from the weather conditions. As the useable capacities of the batteries are thoroughly dimensioned to 1 kWh per 1 kW peak power of the PV-plant, the size of the PV-plant obviously limits not only the maximum possible feed-in rate but also the grid relief effects of the

battery. Consequently, the choice of the charging strategy is less important for domestic energy systems having smaller PV-plants and therefore excess energy productions than for larger systems.

The charging strategy Maximization of self-consumption leads to the highest domestic utilization of the PV-power compared to all analyzed charging strategies. The high self-supply reduces the grid flows by 20% on average compared to a household without storage. However, the high feed-in peaks, which lead to corresponding power excesses, cannot be reduced significantly. Consequently, this charging strategy has only little benefits for the grid suppliers. Apart from this, the losses due to the curtailment at 70% of the peak power are the highest among the three strategies.

The second charging strategy, which uses a fixed feed-in limit of 70%, leads to the lowest utilization of the batteries, although the energy produced by the PV-plants over the year can be fully used. Furthermore, the residual loads are significantly decreased for extreme hours by this charging strategy, which can help to integrate the PV-power into the regional energy system. However, the rates of self-consumption and self-supply are not influenced by the storages, which does not comply with the request of the households for rising consumption rates. The obtained results for charging strategy FFL depend in this case on the threshold set by the German government. A lower feed-in limitation would lead to higher cycle numbers and self-consumption rates but also to a potential increase of curtailment losses. This shows the strong influence of this threshold and the need for a careful selection if applied.

The best results in terms of self-supply and damping of high grid excesses are obtained by the charging strategy Daily dynamic feed-in. The parameters for self-consumption and self-supply are comparable to charging strategy MSC. In addition, the negative residual loads can be damped at hours with extreme excesses similar to strategy FFL. This means that both the demands of the households can be satisfied to increase their self-consumption and the fluctuations of the PV-production is balanced out to a certain degree. This result affirms the recommendation of favoring the use of dynamic thresholds (Resch et al. 2015).

As the determination of the daily feed-ins is calculated from an ideal forecast, undesirable feed-in peaks or suboptimal SOCs due to prediction errors were not simulated in this study. However, this result emphasizes the relevance of the current research in the field of charging strategies, which regulate the feed-in dynamically based on predictions to reach the perfect balance of grid feed-ins and consumption rates.

The dimensioning rate of PV-performance to battery capacity of 1 to 1 is relatively large compared to the economic optimum of 1 to 1.4 recommended in Weniger et al. (2014). With an increased capacity, the batteries generally cause higher balancing effects on the domestic grid flows, when

using charging strategy MSC or DFL. This means that the study is based on conservative assumptions concerning the grid relief effects.

The self-consumption rates obtained in this study exceed previous findings by 5% in average with 79.5% for strategy MSC and 78.5% for strategy DFL (Luthander et al. 2015). This can be reasoned in the sizes of the assumed storage capacities. The dimensioning approach of 1 kWh per kWp power gives a mean useable battery capacity of 6.2 kWh for the selected domestic energy systems, which exceeds the system configurations evaluated in Luthander et al. (2015). This illustrates the relationship between self-consumption rates and the sizes of the PV-plants and storages.

The analysis of results from the feed-in restrictions shows that the two charging strategies FFL and DFL, which compared to strategy MSC significantly decrease the curtailment losses, also lead to a more effective reduction of extreme grid excesses. A fixed feed-in restriction as given leads to the lower utilization of the installed systems if no storage systems are installed. However, it could indirectly motivate the owners of PV-coupled batteries to prefer charging strategies with grid-relieving effects.

2.7.2 Evaluation of the raster-based approach for modeling domestic energy systems with battery storages

The results of the residual loads and the utilization of the batteries reveal a distinct spatial variation for the selected domestic energy systems on regional scale. These differences can be explained by the diverse sizes and inclination angles of the PV-panels, as well as the charging capacities of the batteries adjusted to the PV-plants, differences in the efficiency parameters and the domestic demands, which vary on municipal scale. The variations are also caused by the meteorological conditions, which determine the amount of incident radiation collected by the panels, and therefore the PV-production rates. From these observations, we conclude that for an assessment of the influences on the domestic consumption rates and grid flows it is not sufficient to examine the charging strategies on one average system. Rather, it is recommended to apply a sample size in a quantity that the meteorological and technical variations of the set-ups are taken into account.

The raster-based method is a suitable approach for the performed analysis offering the easy integration of the specifications for each domestic system. In contrast to vector based methods, large areas regardless of the building density and the amount of domestic systems can be covered with reasonable effort. However, a sufficient spatial resolution is required if the obtained results should be attributed to single energy systems. This implies an increased computing time so that the optimal balance between resolution and computing performance has to be found for each application.

A further advantage of the presented approach is the extension of solar cadasters by battery systems. Similar to the assessment of potential locations for rooftop PV-plants and their penetration amounts, the effects from domestic storage systems on the grid integration can be evaluated with

regard to backflows and utilization. Further research may extend the analyzed approach by integrating the grid infrastructure. This includes the identification of periods, positions, and amounts of critical energy flows from the domestic energy systems under grid constraints. This paves the way for vector-based analyses of critical grid segments knowing the relations and the state of the regional energy system. With the comprehensive understanding, appropriate measures could be examined on local scale taking the effects on larger scale into account. This could further support the local planners by integrating the decentralized energy producers into the energy system.

2.8 Conclusion

The decreasing feed-in compensations for small-scale, rooftop mounted PV-systems raised the interest in higher self-consumption rates by the owners of the PV-systems. This will drive the request for domestic battery storage systems in the near future to balance the discrepancies between PV-production and consumption. The utilization of domestic energy storages could offer a cost-efficient way for grid suppliers to reduce harmful peaks occurring at hours with high excess PV-production. The key factor, which decides upon the benefits for households or grid suppliers, is the applied management strategy of the battery storage system.

In terms of self-consumption rates and grid flow reductions, the best results are obtained by charging strategy Daily dynamic feed-in limit. The choice of the charging strategy becomes more important the larger the PV-plant and battery devices are dimensioned. This shows that the collaboration of grid suppliers and households, which consider purchasing battery storage systems, is necessary if a better integration of PV-systems is desired. A fixed feed-in limitation could support the decision for grid-stabilizing charging strategies due to their substantial reduction in curtailment losses.

In this study, the influence of the consumer behavior has undergone some shortcomings as only standard load profiles and averaged annual demands are applied in this study. The inclusion of different consumption rates, increasing efficiencies and demand-side management effects could further contribute towards the understanding of the impacts of charging strategies. The energy production of the PV-plants will also undergo transitions due to shifts in temperature, cloud cover rates, and irradiation intensities induced by climate change. This can also be simulated by the proposed approach.

The high regional variance also shows that it is not sufficient to analyze the effects of a charging strategy on one representative system under averaged conditions neglecting the spatial patterns. For a detailed assessment of the impacts, the meteorological variations, different sizes, and parameters for the batteries and PV-systems and different consumption rates have to be considered. The presented method is developed for raster-based approaches, which enable the simultaneous

analysis of spatially distributed domestic energy systems on larger scales. The inputs of the production, demand, and storage components are specified individually for each system to obtain a comprehensive understanding of the power flows. A careful choice of the pixel size is suggested to obtain a sufficient resolution of the domestic grid power flows but to save computational time on the other hand. Thus, the presented approach is a suitable tool for assessing the influence of domestic interventions on regional energy systems. This could contribute to the development of regulations and funding opportunities by the local authorities, which are targeted to the specific requirements of the households and the local systems.

Acknowledgement

This study is done in the framework of the project “INOLA – Innovationen für ein nachhaltiges Land- und Energiemanagement auf regionaler Ebene” (grant code 033L155AN), which is supported by the German Federal Ministry of Education and Research (BMBF).

Supplementary materials

Tables

Tab. A. 2-1: Technical input parameters for the domestic energy model (Sources: Weniger et al. (2014); Quaschning (2013); Opiyo (2016); Fraunhofer ISE (2019b))

Component	Parameter	Value
Inverter	Nominal power	1 kWh/kW
	Efficiency	0.92 – 0.97
Battery	Nominal voltage	3.6 V
	Nominal power	0.3 kW/kWh
	Dis-/charging efficiency	0.99
	Max number of cycles	30,000
	Initial useable capacity	0.60
	Maximum lifetime	20 a
	Hourly loss rate	0.00000625
PV-system	Ageing parameter	0.003
	Temperature coefficient	0.45
	PV-constant	31.25
	Efficiency MPP-tracker	0.99

Figures

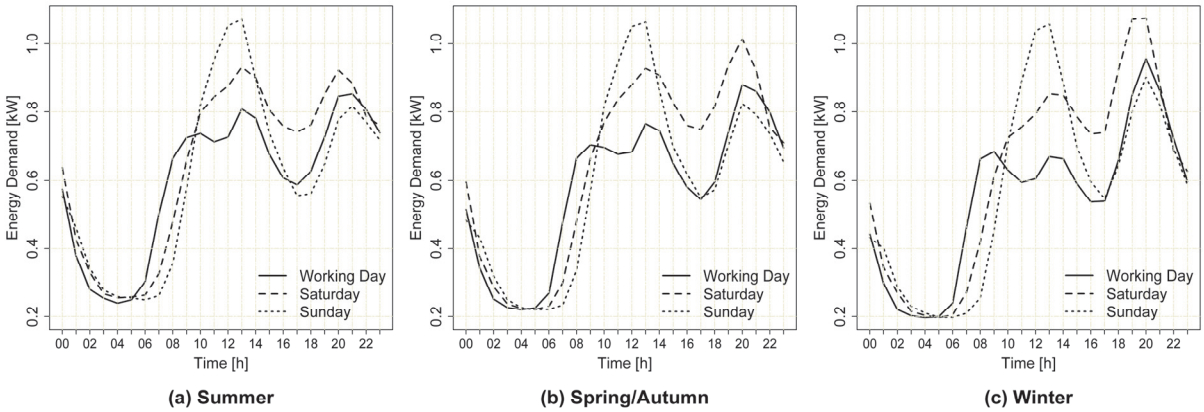

Fig. A. 2-1: Load profiles of a household with an average annual electrical energy demand of 5119.35 kWh

3 How does the rate of photovoltaic installations and coupled batteries affect regional energy balancing and self-consumption of residential buildings?

This chapter was published in the MDPI journal *Energies*:

Reimuth, Andrea, Veronika Locherer, Martin Danner, and Wolfram Mauser. 2020. "How Does the Rate of Photovoltaic Installations and Coupled Batteries Affect Regional Energy Balancing and Self-Consumption of Residential Buildings?" *Energies* 13 (11): 2738.

Abstract

The strong expansion of residential rooftop photovoltaic (PV) and battery storage systems of recent years is expected to rise further. However, it is not yet clear to which degree buildings will be equipped with decentral energy producers. This study seeks to quantify the effects of different PV and battery installation rates on the residential residual loads and grid balancing flows. A land surface model with an integrated residential energy component is applied, which maintains spatial peculiarities and allows a building-specific set-up of PV systems, batteries, and consumption loads. The study area covers 3163 residential buildings located in a municipality in the south of Germany. The obtained results show minor impacts on the residual loads for a PV installation rate of less than 10%. PV installation rates of one third of all residential buildings of the study region lead to the highest spatial balancing via the grid. The rise in self-consumption when utilizing batteries leads to declined grid balancing between the buildings. For high PV installation rates, regional balancing diminishes, whereas energy excesses rise to 60%. They can be decreased up to 10% by the utilization of battery systems. Therefore, we recommend subsidy programs adjusted to the respective PV installation rates.

3.1 Introduction

The global energy supply has been identified as a major driver of anthropogenic climate change. In 2010 for instance, the generation of electricity and heat accounted for 26% of the anthropogenic greenhouse gas emissions (Bruckner et al. 2014). In recent years, the global CO_2-emissions arising from the combustion of fossil fuels have continuously increased by 1% p.a. on average (IEA 2019a). Therefore, the transformation of the energy systems to renewable sources is an essential mitigation measure (Rogelj et al. 2018).

The expansion of non-fossil resources will increase the demand for space. In contrast to conventional combustion plants, renewable production systems usually have a low energy density (Layton 2008). This means that a larger area is needed to produce the same amount of electrical energy as by a conventional plant. The expansion of renewables can especially in highly populated regions raise the potential for land-use conflicts (Huber et al. 2017). As an exception, photovoltaic (PV) systems mounted on rooftops can significantly contribute to the reduction of greenhouse gas emissions in the residential electrical sector (Schram et al. 2019) but their installation does not intensify this competition for land. Thus, this renewable energy resource belongs to the most accepted by the public (Sütterlin et al. 2017). Consequently, the expansion of rooftop PV is an integral part in the energy policies of many countries. Germany for instance, has introduced a law, which includes a fixed minimum remuneration for PV energy (EEG 2019). China has enacted the 13th Five Year Plan for energy, which offers special feed-in tariffs for small-scale, residential systems (Gosens et al. 2017).

Due to the attractive economic conditions, more and more PV systems have been installed on rooftops. In 2018 for instance, the worldwide performance of rooftop PV accounted for 27.9 GWp in total (SolarPower Europe 2019). Until 2023, it is expected that the installation rates continue to rise by between 14.3 GW and 46.8 GW in total (SolarPower Europe 2019). However, the growing decentralization of the energy production presents a challenge to the local electricity networks. This development fundamentally changes the structure of the regional energy systems (Bauknecht et al. 2020). Rising amounts of grid-connected PV systems can lead to poor power quality, when the residential PV excesses are fed into the grid (Haque et al. 2016).

Coincidently with the expansion of rooftop PV, the utilization of residential battery storage systems has also strongly increased. In Germany, every second newly installed PV system was coupled to a battery storage in 2017 (Figgener et al. 2018). This may be reasoned in the higher profitability of the residential PV systems when additionally utilizing batteries (Malhotra et al. 2016). The storages increase the degree of self-consumption by 13–24% (Luthander et al. 2015), as they balance mismatches between the production rate of the PV system and the residential consumption. Due to this, they have the potential of decreasing harmful backflows into the grids (Moshövel

et al. 2015). The potential impact of PV and battery systems on the grids is assessed by detailed analyses of single systems or small parts of the local voltage grids. Various pricing schemes and management strategies for residential batteries have been developed, which target the integration into the grids apart from maximizing the benefits for the owners (Resch et al. 2015; Young et al. 2019; Fares et al. 2017). These studies offer detailed analyses of single systems and their effects on grid flows.

Emerging challenges of the expansion of PV systems and the impact of batteries are also analyzed on a larger spatial scale. In these regional analyses, the interrelations of the residential energy systems can be assessed when multiple buildings are equipped with PV and residential batteries. The PV energy yields are subject to significant spatial variations when regarding technical, meteorological, social, and economic constraints (Lee et al. 2018; Hong et al. 2017). Even on neighborhood level, the PV potential is subject to strong variation, which also influences the integration of rooftop PV (Litjens et al. 2018). The spatial variations in the potential consequently affect the residual loads, which can be partly balanced via the grids (Reimuth et al. 2019).

The majority of the studies focus on high PV installation rates on the selected rooftops. However, it is not clear when and to which extent consumers will decide for the installation of residential PV and additional battery systems (Agnew et al. 2015). Therefore, the future role of rooftop PV production in the energy systems is still unknown. This raises the question how the energy flows are influenced in a regional energy system if the residential buildings are partially equipped with PV and batteries. There is still a lack of understanding of the influence of the PV and battery installation rate on the relation between regional grid balancing, energy excesses and self-consumption rates on regional scale. In this context, the study sets out to quantify the influence of the PV and battery installation rate on the regional energy excesses and self-consumption of residential buildings. We evaluate how far the residual energy flows can be balanced in dependency of the degree of PV and battery installation due to spatial variations in the potentials. The study further aims to assess how far the partial utilization of PV and residential batteries affects the residual loads of the residential buildings on a regional scale.

To address these objectives, we apply a land surface model with an integrated domestic energy system component. This tool enables the simulation of power flows from various residential buildings considering local differences in consumption, PV plants and batteries designs, as well as the topographical and weather conditions. We use statistical data combined with spatial information to dimension residential consumption rates and PV systems. In this way, we are able to evaluate the effects of different PV installation and battery-coupling rates on self-consumption, regional balancing, and the energy excesses in a regional energy system.

3.2 Materials and methods

3.2.1 Model environment

In order to simulate the residential energy flows of the residential buildings we apply the Processes of Radiation, Mass, and Energy Transfer (PROMET) land surface model. It offers an integrated residential energy system component and has been tested successfully in various study areas at different scales (Mauser et al. 2009; Mauser et al. 2015). The PROMET model is fully spatially distributed and raster-based. This means that each building in the study area can be attributed to a grid point in the raster and the processes are simulated in spatially explicit way. This model approach allows the assessment of regional PV and battery effects with physically based simulations of PV production rates and battery flows.

The temporal and spatial resolution in the following study is set to 1 h and 100 m. The meteorological input for the PROMET model includes temperature, precipitation, wind speed, cloud cover, and air humidity. Provided as point values at installed stations, the weather conditions are interpolated to the raster points with the inverse squared distance weighting method considering local statistical dependencies of the meteorological parameters on topographical conditions. The radiation fluxes relevant for the PV model are determined on the raster resolution from air temperature and degree of cloudiness using a simple atmospheric radiative transfer model. Snow depth and coverage impeding the production of PV energy are estimated from the precipitation sums, radiation fluxes, heat fluxes, and air temperature (Mauser et al. 2009; Mauser et al. 2015).

The domestic energy system component embedded in the PROMET model consists of three submodules (Reimuth et al. 2019), which are interconnected in the following way: First, the hourly electrical energy production is simulated by the PV model considering the building-specific slopes and orientations of the roofs. The amount of direct and diffuse solar irradiation and the reflection striking the PV panels is determined from the spatially resolved radiation fluxes derived from the meteorological input data. The electrical energy yield is calculated from the hourly irradiation conditions following the method of Quaschning (2013) under the constraints of temperature effects, module efficiencies, ageing losses. At snow depth exceeding 2 cm it is assumed that the PV systems are fully covered by snow and the production is stopped due to suboptimal radiation conditions (Giddings et al. 1961; Andrews et al. 2013). The losses from the MPP-tracker are considered by constant efficiency parameters. The PV model is further described comprehensively in a technical report (Locherer 2018). The PV model was successfully validated with hourly measurement data of several PV systems located in the study area.

In the consumption module, the magnitude of the residential energy load is determined on hourly scale. The input of this component includes the average, annual consumption rates, which are spatially resolved to raster resolution according to the building locations. The yearly consumption rates are calculated from these reference values using annual adjustment parameters. The temporal course of the energy consumption is determined from the obtained annual consumption rates by hourly load profiles (Stadtwerke Unna 2015; VDEW 1999). The derivation of hourly consumption rates is further described in a dedicated modelling documentation (Prasch et al. 2018). The consumption component was successfully validated with 15 min measurement data of the study area.

In the next step, the differences between production and consumption rates are determined on building scale. The PV energy is transformed to alternative current (AC) via inverter assuming a constant efficiency. The PV self-consumption is determined as the amount of energy produced by the PV panel which is simultaneously consumed by the building.

The third submodule also includes the simulation of the battery storages, if coupled to PV systems. The battery model calculates the charging and discharging flows of the battery storages from the available energy excess or deficit of the residential energy system before the conversion to AC (Reimuth 2017a, 2017b). It is assumed that the battery systems are rechargeable and always connected to the grid. The magnitude of the charging and discharging flows are determined considering the maximum charging and discharging power, self-discharging, ageing effects, and the influences of temperature and current. The selected operation strategy maximizes the self-consumption of the PV production, which is currently the common management strategy for residential buildings employed by the battery retailers (Olaszi et al. 2017). This means that the battery is charged as soon as excess energy is generated by the PV system and discharged when the hourly energy consumption exceeds the production.

The residual load is defined as the energy flow between the public and residential grid network. Grid supply is defined as a positive residual load, whereas negative loads denote PV excesses fed into the grids. The amount of PV excesses available in the grids and consumed by the other residential buildings is termed as regional balancing flow. It is assumed that the energy flows between the buildings are not constrained by grid limitations. In this way, the upper bounds for the supply with regionally generated PV energy from rooftop-mounted systems can be quantified. PV self-consumption is defined as the annual share of PV energy that can be directly consumed by the building, whereas self-sufficiency denotes the percentage of consumption that is produced by the residential PV plant per year. The energy production, which is neither consumed by the own household nor by the other residential buildings is termed as energy excess.

Three different energy supply options exist for each building in the study area: (1) full grid supply, (2) supply by a rooftop PV system and the grid, and (3) supply by PV, an additional battery and the grid. It is assumed that PV and battery systems are jointly used in buildings with multiple households, so that only one PV and battery system is potentially installed per building. The regional effects of the partial equipment with PV systems and coupled batteries are assessed sequentially by the increase of the installation rates in increments of 1%. The buildings, which are equipped with PV systems and additional batteries, are selected randomly. The resulting energy flows are first determined on building scale and then aggregated to raster resolution.

3.2.2 Description of the study area

The study area covers the district town Bad Tölz, which is located in the Alpine foreland in the southeast of Germany (see Fig. 3-1). The study area belongs to a region in Germany characterized by a high potential for photovoltaic energy production. Within the municipal area, the average global incoming irradiation ranges between 1.167 kWh/m² in the north and 1.145 kWh/m² in the south at higher elevation levels (DWD CDC 2019).

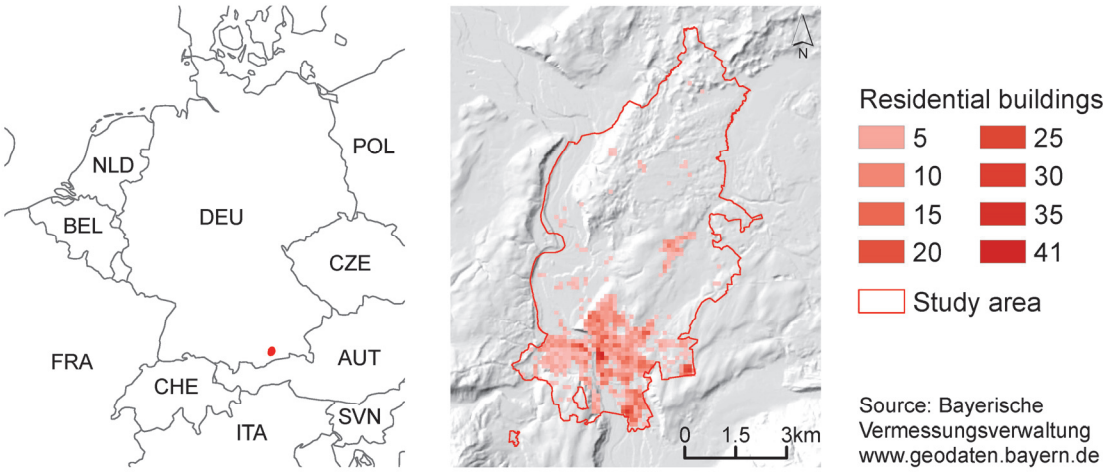

Fig. 3-1: Location of the study area and distribution of residential buildings (Data source: Bayerisches Landesamt für Digitalisierung (2015b, 2015a); Bayerische Vermessungsverwaltung (2018)).

The city covers 3080 ha with an average population density of 564 persons per km² (Bayerisches Landesamt für Statistik 2019b). In total, 20.1% of the study region is classified as residential and traffic area, of which 233 ha belong to residential settlements. In 2017, 18,647 inhabitants living in 3289 residential buildings were registered in Bad Tölz (see Figure 1). One or two person households account for the most common form of housing (Bayerisches Landesamt für Statistik 2019b). An average building has 2.75 apartments with 84.2 m² and 5.67 residents. The city of Bad Tölz has an annual energy consumption of 69.693 GWh (measured between 2013 and 2016), of which 38.0% are contributed to the residential sector (Stadtwerke Bad Tölz 2019). On average, the

households in the study region consumed 3093 kWh of electrical energy per year, which is similar to the German mean of 3168 kWh/yr (Statistisches Bundesamt (DESTATIS) 2019).

3.2.3 Input data

The period of five years from 2014 to 2018 is simulated using hourly climate data from 1236 measurement stations of the German weather service, of which 44 are located within or in max. 50 km distance to the study region. The essential input for the land surface model PROMET includes spatially resolved data sets for elevation (Bayerisches Landesamt für Digitalisierung 2015b) and land use (Arbeitsgemeinschaft der Vermessungsverwaltungen der Länder der Bundesrepublik Deutschland 2015). The domestic energy system component needs further input data for the PV, battery and consumption component. Tab. 3-1 shows the values of the PV and battery parameters, which are kept constant for all systems. We assumed that the PV systems featured crystalline silicon type solar panels, which is the dominant configuration used in the past few years (Fraunhofer ISE 2019b). The use of lithium-ion accumulators is simulated, as this is currently the primarily purchased type for residential applications (Figgener et al. 2018).

Tab. 3-1: Specification of the input parameters of the PV and battery model.

	Parameter	Value	Source
PV model	Efficiency module [–]	0.173	(Fraunhofer ISE 2019b)
	Efficiency inverter [–]	0.98	(Fraunhofer ISE 2019b)
	Temperature coefficient [–]	0.45	(Quaschning 2013)
	Constant [–]	30.5	(Quaschning 2013)
	Ageing factor [–]	0.001	(Fraunhofer ISE 2019b)
Battery model	Nominal voltage [V]	3.6	(Opiyo 2016)
	Power energy density ratio [W/Wh]	1	(Opiyo 2016)
	Maximum number of cycles [–]	3000	(Opiyo 2016)
	Hourly losses [–]	0.00000625	(Schoop 2013)
	(Dis-) Charging Efficiency [–]	0.99	(Opiyo 2016)
	Initial maximum depth of discharge [–]	0.60	(Opiyo 2016)

3.2.4 Temporal and spatial downscaling of the consumption rates

For the presented analysis we use 3163 residential buildings located in our study region, which we extracted from a digital building model provided by the Bavarian Agency for Digitization, High-Speed Internet and Surveying (Bayerisches Landesamt für Digitalisierung 2015a).

This data set contains georeferenced, building-specific information as construction heights, base areas, roof shapes, and the types of utilization for instance. It was generated from airborne laser scanning data and the national real estate cadaster.

The annual residential consumption rates are provided by the local energy supplier and cover the years 2014 to 2016 (Stadtwerke Bad Tölz 2019). As the energy consumption of electrically based heating systems is reported separately in this data set, the applied residential consumption loads exclude the additional energy demand from heating pumps. The energy consumption rates for the years 2017 and 2018 are extrapolated using the moving average of the previous two years. Standardized load profiles for households are applied to temporally downscale the annual consumption rates (see Fig. A. 3-1) (Stadtwerke Unna 2015; VDEW 1999).

As the use of building-specific energy loads allows the determination of the PV self-consumption, the annual consumption rates are spatially downscaled from the municipal to the building level. The method applied in this study is based on the assumption that the electrical energy consumption is proportional to the living space. The exact positions of the buildings provided by the digital building model are transformed to the grid system used in the applied land surface processes model.

The building-specific consumption rates are derived in the following way:
In the first step, the number of floors N_F is determined for each building B of the study area according to Eq. (3-1).

$$N_F(B) = (H_E(B) - H_B(B) - H_0)/(H_R + H_C) \quad (3\text{-}1)$$

The altitude of the building is calculated from eaves heights H_E and the ground level H_B provided by the building data set. For H_0, which is the distance from the ground surface to the first floor, we use a height of 0.85 m. This value is reasonable for regions, which are prone to flooding and have consequently raised ground floors for flood protection. We further assume an average room height H_R of 2.50 m. This is in line with the room heights of the dwellings constructed in Germany in the recent decades. Since more than 70% of the residential buildings in Bad Tölz were built in the second half of 20th century (Statistische Ämter des Bundes und der Länder 2014), the assumed room height is a reasonable value for the study area. We further assume a thickness of 0.4 m for the height of the ceiling construction H_c as the sum of 20 cm height for the load-bearing layer and 20 cm for the floor construction. These are typical heights for the current construction heights of German dwellings.

Eq. (3-2) shows the determination of the total living area A_L based on the obtained numbers of floor N_F, the effective area for living N_{ea}, and the gross floor A_B, which is provided by the digital building model. According to the guidelines of the Association of German Engineers (VDI), the

percentage of the effective living area to the gross floor is between 59% and 71% for residential buildings (VDI 2013). Based on this, we assume an effective area for living N_{ea} of 65%:

$$A_L(B) = N_F(B) \cdot N_{ea} \cdot A_B(B) \tag{3-2}$$

The applied dimensioning approach results in a high share of residential buildings with two floors (see Fig. 3-2a)). This seems plausible, as the study area is characterized by a large number of detached two-story houses. The resulting living area of 229.87 m² per building is in line with the statistical mean of 229.61 m² obtained in the municipality of Bad Tölz for 2014 (Bayerisches Landesamt für Statistik 2019a).

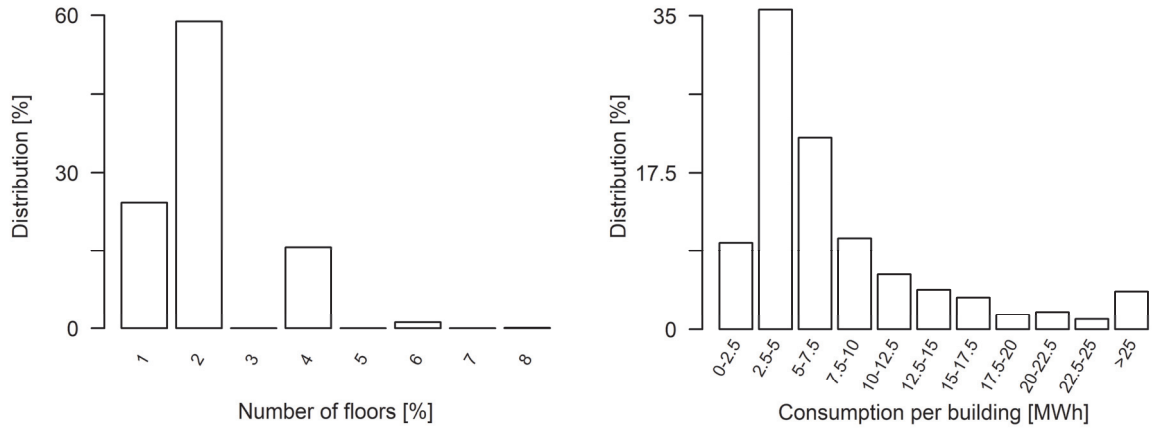

(a) *(b)*

*Fig. 3-2: (**a**) Distribution of floor numbers used for the estimation of the living areas; (**b**) distribution of the average consumption rates per building.*

In the next step, the consumption rate is spatially distributed based on the obtained living areas of the buildings. It is assumed that the annual, municipal energy consumption is equally distributed over the living areas. In total, the residential energy use of the municipality accounted for 26,603.86 MWh on average and varies by 0.3%, which amounts to 36.10 kWh/m² between 2014 to 2016 (Stadtwerke Bad Tölz 2019). The obtained annual consumption rates presented in Figure 2 range between 0.88 MWh and 67.70 MWh per building at an average of 8.30 MWh.

3.2.5 Dimensioning of the PV systems and batteries

The installed capacities of residential PV systems underlie a high variability, as they are influenced by several factors. The installation of rooftop mounted PV systems is not allowed for buildings kept under a preservation order. This applies to 1% of the residential buildings located in the study region, which are excluded from the potential for a PV and battery expansion.

PV sizes are subject to technical and spatial constraints concerning the inclination angels of the roofs, the available areas, and the orientations of the buildings relative to the sun. Apart from these limitations, different motivations with the purchase but also the development of the incentives

and prices have a strong influence on the installation capacities of the PV systems (Figgener et al. 2018). In our study, we consider both aspects by dimensioning the PV system sizes in two steps.

First, the spatial constraints of the potential PV systems are determined individually for each building. For this purpose, we calculate the statistical energy yields PV_{pot} for the available rooftops R of each building B (see Eq. (3-3)). The information for areas A_R, orientations O_R, and inclination angels θ_R of the roofs is taken from the building model (Bayerisches Landesamt für Digitalisierung 2015a):

$$PV_{pot}(R,B) = 0.9 \cdot A_R(R,B) \cdot \sum_{s=1}^{12} IR(s) \cdot c\big(s, O_R(R,B), \theta_R(R,B)\big) \qquad (3\text{-}3)$$

The size of the potential PV system is curtailed to 90% of the roof area A_R to consider roof areas covered by windows, snow guards, chimneys, and the space needed for installation and access. It is assumed that the orientation O_R and the inclination of the PV panels θ_R correspond to those of the rooftops. The statistical irradiation striking the roof areas is based on the average monthly incoming global irradiation IR on the horizontal plane (DWD CDC 2019). The inclinations between the solar irradiation and the PV panels are considered through seasonal correction factors c, which are adjusted for Bavarian conditions (Bayerisches Staatsministerium für Wirtschaft und Medien 2015).

For each building, we determine the rooftop with the highest estimated energy yield as the technical potential. The nominal potential PV power is derived from the available roof area assuming a rated power of 170 W/m² (Fraunhofer ISE 2019b).

To consider the actual variability of the PV installation capacities and not only technical constraints, we use the statistical distribution of the nominal PV power rates obtained from central registry of renewable energy systems, which is operated by the German Federal Network Agency (Bundesnetzagentur 2019). Based on this data set, the panel areas of the selected PV systems are further reduced to reproduce the different shares of the PV sizes. Fig. 3-3a) shows the resulting distribution of the PV installation rates with an average nominal power of 9.30 kWp. For almost half of the buildings the ratio between the PV production capacity and annual electrical energy demand is 1.0−1.5 kWp/MWh (see Fig. 3-3b)).

The sizes of battery storages are dimensioned from the nominal PV power of the systems with one kWp per kWh useable battery storage capacity. This ratio follows the average dimensioning rate of the new-installations in 2017 (Figgener et al. 2018).

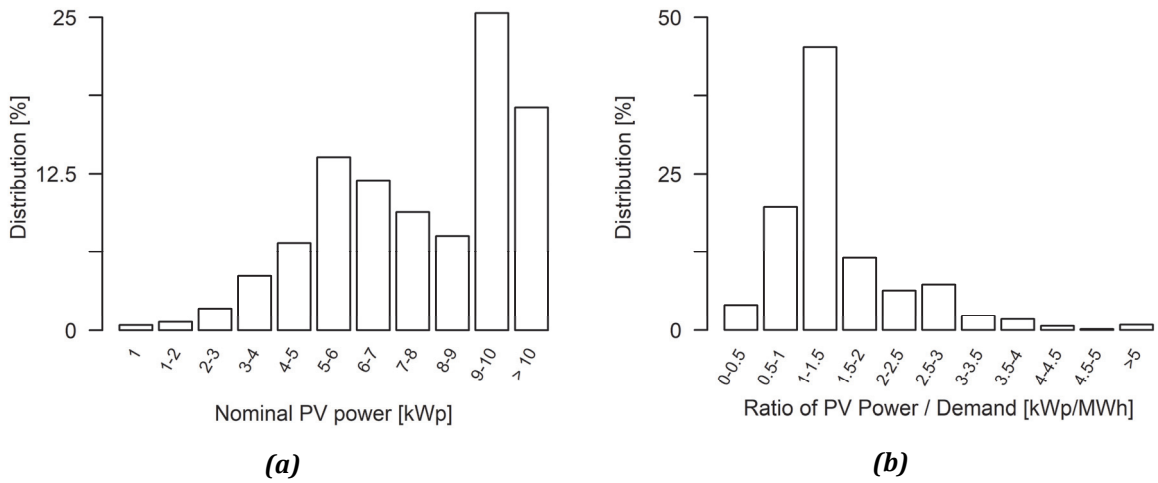

*Fig. 3-3: (**a**) Distribution of the nominal PV power dimensioned according to the current German distribution considering the technical constraints of the buildings; (**b**) distribution of the ratios between nominal PV power and annual demand (right side).*

3.3 Results

3.3.1 Regional balancing and self-sufficiency

In order to assess the impact of the PV and battery installation rate on municipal scale, the rate of installed PV systems and coupled battery storages is increased in 1% steps leading to 10,201 simulation runs.

The PV installation and battery-coupling rate has different effects on the regional balancing and self-sufficiency. Fig. 3-4 shows the share of regional balancing and self-sufficiency of the total energy consumption as functions of the PV installation rate and the percentage of battery coupling.

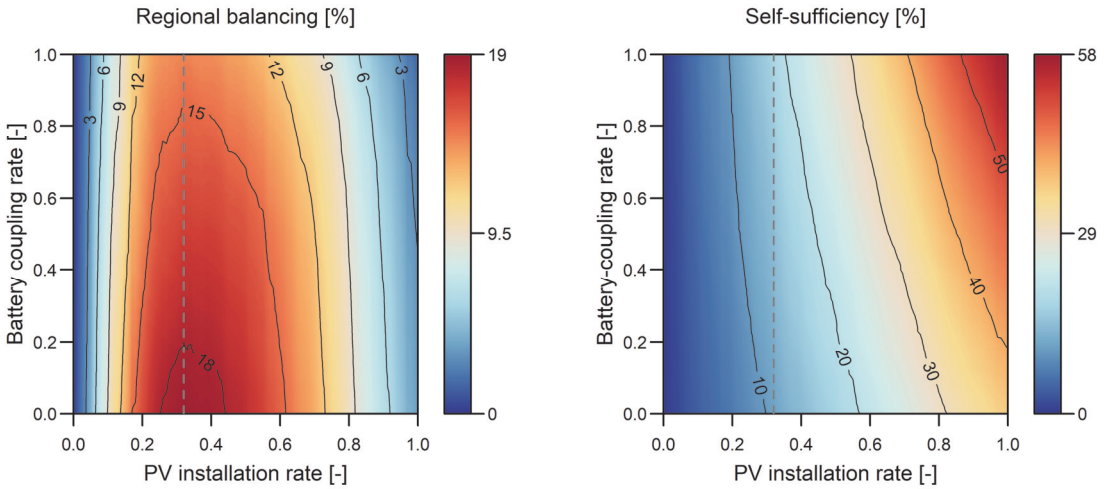

*Fig. 3-4: (**a**) Regional balancing and (**b**) self-sufficiency for different PV installation and battery-coupling rates as percentage of consumption (with the PV installation rate of 32% in dashed grey).*

The degree of rooftops with installed PV systems has a higher impact on the regional balancing than the additional utilization of batteries. As presented in Fig. 3-4 left, the PV installation rate influences the regional balancing of the residual loads in a non-linear way. The maximum amount of the consumed energy, which is produced externally by the PV systems of other residential buildings, reaches 18.7% at a PV rate of 32%. With the further increase of the PV rate, the regional balancing effect declines. At a PV installation rate of 99% for instance, the regional balancing is marginal with a value of only 3.5%.

The utilization of residential batteries reduces the regional balancing effects as the mismatches between PV production and consumption are already levelled within the building. The impact of batteries is apparent in particular for the PV installation rates around 30%. The balancing effects are decreased by 4.4% by equipping all PV systems with additional batteries. At high PV installation rates, a change of the battery coupling rate has only minor influence.

In contrast to the regional balancing, the degree of residential self-sufficiency rises linearly with increasing the PV or battery installation rates (see Fig. 3-4 right). If only PV-systems are expanded, the regional self-sufficiency reaches a maximum of 36.3%, when all buildings are equipped with PV systems. Batteries additionally raise the self-supply due to the balancing of residential energy excesses and deficits. The strongest effect of the storages is observable at a PV installation rate of 99%. The additional utilization of batteries increases residential self-sufficiency by 21.3% to 57.6%.

3.3.2 Self-consumption and energy surplusses

The PV installation rate and the share of systems coupled to storages influence the PV self-consumption and excesses in different ways as presented in Fig. 3-5. The degree of direct self-consumption stays more or less constant at 28.9% on average for all PV rates (Fig. 3-5a)). For higher shares of buildings equipped with PV, the charging and discharging of residential storages increases the self-consumption from 28.9% to a mean value of 46.8% depending on the battery-coupling rate. However, for low PV installation rates the degree of self-consumption reaches its maximum at 55.8%.

In contrast, the energy excesses are strongly determined by the PV installation rate. At PV installation rates of less than 10%, the total amount of generated PV power is so low that the residential buildings fully consume the available production rates by either self-consumption or regional balancing. If the PV installation rate exceeds this threshold, the degree of energy surpluses rises linearly. At an installation rate of 99%, the highest share of excesses is obtained with 67.9%.

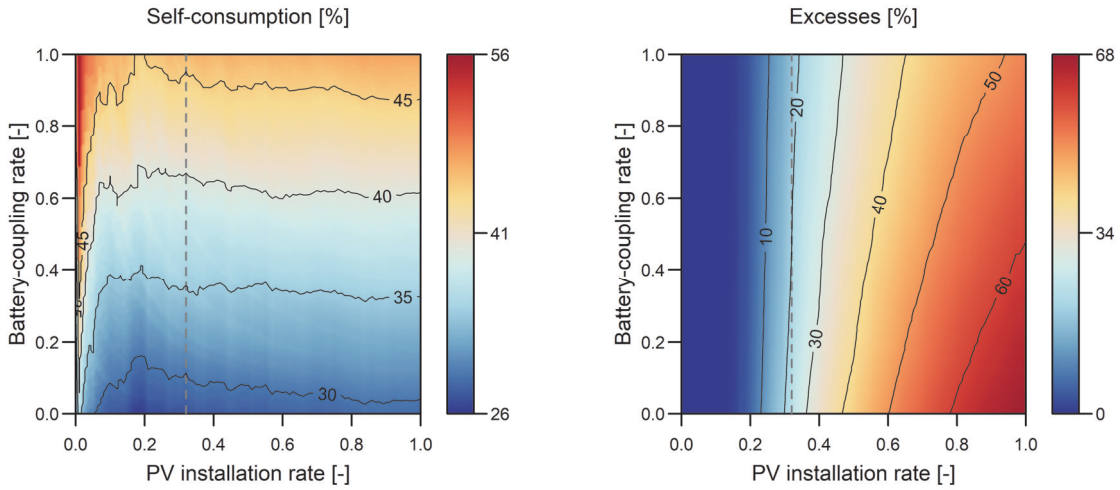

(a) *(b)*

*Fig. 3-5: (**a**) Self-consumption and (**b**) energy excesses for different PV installation and battery-coupling rates as percentage of consumption (with the PV installation rate of 32% in dashed grey).*

With the additional equipment of the residential energy systems with battery storages, the production surpluses are partially damped, as mismatches between PV production and consumption of the residential energy systems are balanced by the storages. With a reduction of 16.3% to 51.2%, the highest effect of battery utilization is obtained for a PV installation rate of 99%.

3.3.3 Residual loads and regional balancing flows

We first analyze the impact of the PV installation rate on the energy flows without the utilization of the residential storage systems. Fig. 3-6 shows the distributions of the total residual loads and regional grid balancing flows between the residential buildings by indicating the number of hours, at which a certain value is exceeded.

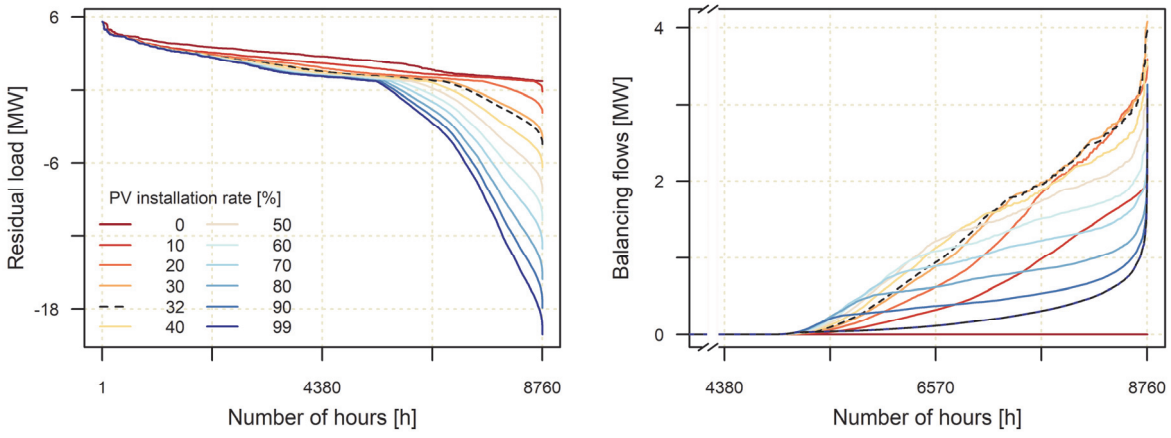

(a) *(b)*

*Fig. 3-6: Duration curves of (**a**) residual loads of the residential buildings and (**b**) balancing flows between the buildings for different PV installation rates without the utilization of battery storage systems. The residual load and distribution of the balancing flows for PV installation rate leading to the highest regional balancing are marked in black.*

Increasing PV installation rates raises the hours and the magnitudes of energy excesses. The expansion of PV systems leads to a reduction of the positive residual loads in the medium range between 4.0 MW and 2.0 MW, whereas the peak hours with maximum consumption are not significantly affected. In contrast, the magnitudes and hours of negative residual loads rise with increased PV capacities. At an installation rate of 99% for instance, the maximum excess is equivalent to 69.1% of the installed capacity.

The balancing flows are in contrast to the distribution of the residual load. Whereas an installation rate of 32% leads to the maximum total balancing effects, the highest magnitude of power flows between the buildings is obtained at PV installation rate of 40%. A further increase of the PV rate reduces the balancing flows in the medium range, whereas the extrema stay more or less constant.

Fig. 3-7 shows the residual loads and balancing flows for different battery-coupling rates for the PV installation rate of 32%. The impact of residential battery storages systems is analyzed exemplarily for this degree of PV expansion as it shows in the highest regional balancing effects.

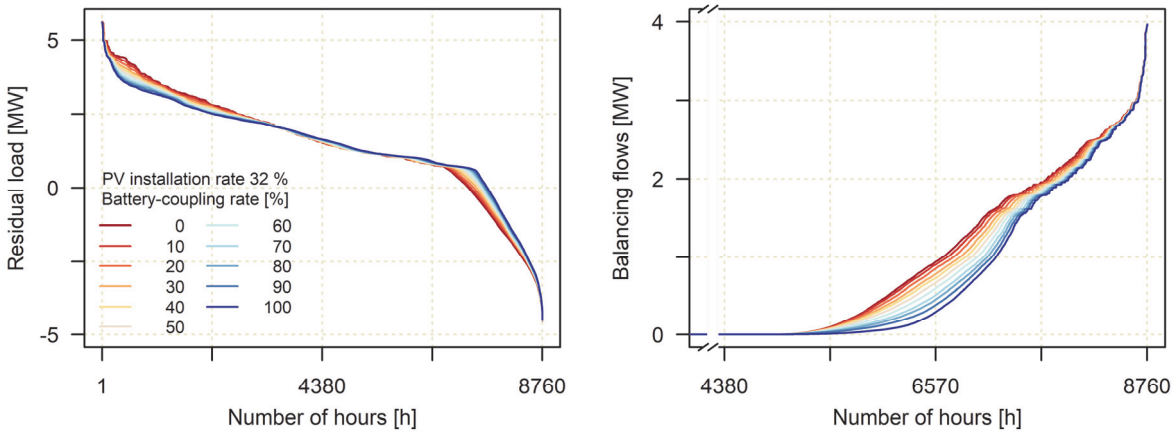

(a) ***(b)***

*Fig. 3-7: Duration curves of (**a**) residual loads and (**b**) balancing flows for different battery-coupling rates at a PV installation rate of 32%.*

As the batteries partially balance the energy excesses and deficits already within the buildings, the utilization of the storages leads to a decrease of the residential residual loads. However, this effect is not equally distributed over the year. Fig. 3-7 shows that the residual loads are mainly reduced in hours of medium residential deficits between 2.5 MW and 5.0 MW. The additional equipment of battery storages reduces the remaining energy demand by up to 22.2%. The fraction of hours per year with energy excesses declines from 16.8% to 12.5% when additionally using batteries. However, hours with peak demand are not affected by the utilization of batteries. The analysis of the regional residential energy excesses follows a similar distribution. The utilization of batteries significantly reduces the lower positive excesses flows of less than 2.5 MW. Feed-in peaks remain unaffected if residential buildings are additionally equipped with batteries that are managed with the goal of maximizing self-consumption.

Similar to the residual load, the storage operations of the batteries influence the flows between the residential buildings mainly in the medium range. They reduce the regional balancing by up to 90%, if all PV systems are coupled to batteries. The balancing flows peaking 3.0 MW remain constant independently of the degree of coupled batteries.

Fig. 3-8 shows that for high PV expansions, the impact of storages on residual load and balancing flows is reversed. The residual loads are reduced in a much stronger way than the balancing flows if the PV systems are additionally coupled to batteries. Especially the energy excesses in the medium ranges are decreased by the utilization of batteries. The decline of the negative grid flows between 0 MW and −16.5 MW ranges from 0.5 kW to 2.5 kW if all residential buildings are equipped with PV systems and batteries. However, the highest PV excesses of less than −16.5 MW remain constant independently of the degree of battery utilization. When analyzing the energy deficits, the storage effect becomes also visible for the range of positive residual loads by a reduction of 19.5% on average.

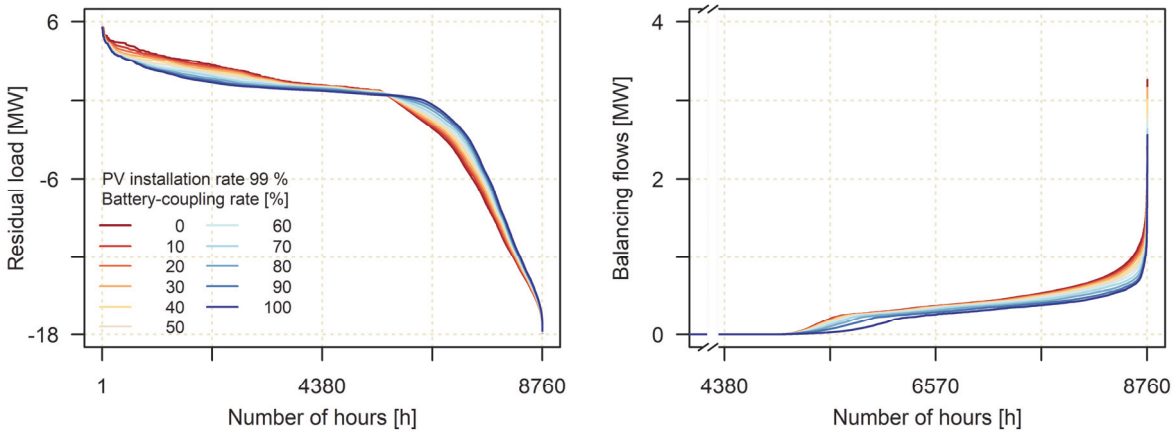

(a) ***(b)***

*Fig. 3-8: Duration curves of (**a**) residual loads and (**b**) balancing flows for different battery-coupling rates at a PV installation rate of 99%.*

In contrast to the residual loads, the balancing flows are marginal at the PV installation rate of 99%. Consequently, the decreasing effect of the battery storages on grid balancing is much weaker than for lower PV installation rates. Especially, in the medium range, the balancing flows decline by less than 1% when simulating the additional utilization of the battery storages. The highest reduction from 3.26 MW to 2.56 MW is obtained at the peak load when all PV systems are additionally equipped with batteries.

3.4 Discussion

3.4.1 Relation between regional balancing, energy surplusses and self-consumption

In this paper, we analyzed the effects of PV installation rates and battery coupling on self-consumption and excesses in a regional case study. We used the example of a real distribution of houses in Southern Germany and the hourly electricity consumption patterns to study through simulations the effects.

The integration of residential PV energy and the potential effects of battery storages are strongly dependent on the installation and coupling rates. At PV installation rates of less than 10%, the decentral energy production has limited impact on the residual load of the residential buildings. As the majority of buildings are entirely supplied by the grid, backflows arising from PV surpluses can be fully consumed by the residential buildings. As the PV production is low compared to the total energy consumption, the influence of PV systems and residential batteries on the energy flows is marginal on regional scale.

This is different for a higher PV installation rate as balancing effects and self-sufficiency rise when increasing the PV installation rate. In our example, the spatial grid balancing due to differences in the residual loads reaches its maximum if one third of the buildings are equipped with PV systems. Residential buildings with positive residual loads can partly consume PV excesses from the grids. For this reason, a higher share of PV energy can be used for the supply of the residential buildings additionally to self-consumption.

The additional utilization of battery storage systems reduces these grid-balancing effects by raising self-consumption, which is especially observable at PV installation rate around 30%. Energy excesses, which would supply the other residential buildings, are then used for charging the batteries. The shifts in the energy flows also become apparent in the distribution of the residual loads. The utilization of batteries generally reduces the negative residual loads. However, the hours with residential energy deficits are increased by up to 4%, as the higher self-consumption leads to less energy surpluses in the grids available for regional balancing. Consequently, the share of energy consumption covered by residential PV energy production remains at the same level. The decrease of the total energy excesses through the storages is limited.

As the grids are not simulated in our study, bottlenecks impeding the energy exchange between the buildings are not considered. It is assumed that the grid enables the full energy exchange between the residential buildings. This means that the obtained values are upper bounds for the spatial balancing effects, which can be reached if the grid infrastructure is adjusted to the obtained flows.

For a high PV installation rate of more than 80%, the grid balancing effects diminish, whereas self-sufficiency rises. This can be explained by the increasing number of buildings equipped with PV systems. The high self-supply reduces the residential energy deficits, so that rising PV surpluses can be less effectively balanced via the grid. For PV rates of 99% for instance, the consumption of the PV power production is solely dependent on residential self-consumption, as the regional balancing effect decreases to almost zero.

Consequently, high PV installation rates have strong effects on the residual loads leading to an extreme rise of backflows. At full PV expansion, the maximum negative residual load is increased up to three times the peak demand.

The utilization of batteries significantly reduces the arising energy excesses to the benefit of increasing self-consumption rates. As the regional balancing effect diminishes for high PV installation rates, the storages are charged by PV surpluses, which would otherwise entirely lead to excesses in the grids. Especially negative residual loads in the lower and medium range are decreased when using the batteries.

The average increase in self-consumption of 29% obtained in this study exceeds the values found in Ref. (Luthander et al. 2015). This may be explained by increased efficiency rates of PV and battery systems compared to earlier studies. We consider the obtained results to be robust due to the large numbers of buildings with varying PV sizes, battery capacities, and consumption loads. The temporal extent of the simulations set to five years is also long enough in order to represent average meteorological conditions for PV production.

However, the utilization of residential battery storage systems does not contribute to the reduction of extreme backflows, as the highest negative residual loads remain unaffected by the utilization of storages. This can be explained by the selected battery charging strategy optimized for maximizing self-consumption. The obtained peaks usually occur in summer days, when the inclinations between panels and sun have reached the optimum and a large amount of PV energy is produced. During these days, the PV surplus of the late midday hours is completely fed into the grids as the batteries are already fully charged by the energy excesses of the morning hours. Our results are in line with previous studies (Reimuth et al. 2019; Young et al. 2019; Resch et al. 2015) showing that on sunny days reverse power flows are likely despite the utilization of the storages.

3.4.2 Applicability of the results to other municipalities

Two factors decide about the direct transferability of the obtained findings to other regions: The first aspect is the irradiation potential, which decides on the productivity of the PV systems. With an average annual irradiation of 1150 kWh/m^2, the study region is representative e.g., for the midlatitudes of Central Europe. For areas with higher PV potentials, grid-balancing effects will

probably reach their maxima already at lower PV installation rates. Residential energy excesses occur at lower shares of buildings equipped with PV systems, which are available for the other households of the community. In order to understand how far grid balancing effects and the PV installation rate are influenced under higher natural potentials, further research is necessary at this point. However, the impact of residential battery storages, which increase self-consumption rates at declining grid-balancing effects, remains similar.

One aspect, which is not considered in this study, is the effect of shading of neighboring buildings, vegetation, or obstacles on the roofs. Their incorporation would impose unsatisfiable requirements to the availability of data and computational resources and is thus neglected in the study design. Although it is assumed that these effects are eliminated as far as possible by the optimal selection of the PV location, they still can reduce the PV production of a building especially in months of low solar inclination angles. It is not yet clear, how far these effects become apparent on regional scale.

The second factor affecting the transferability to other municipalities is the distribution of the residential energy consumption. The results obtained in this study are valid for regions with a similar relation between PV potential and energy consumption rates shown in Fig. 3-2b). This accounts for municipalities in rural or suburban areas with high shares of detached and terraced houses. In these regions, shading effects by neighboring buildings could be of lower impact compared to cities which are commonly characterized by much smaller site areas.

The results cannot be directly applied to heavily urbanized communities with high shares of multistory buildings. These types of buildings have smaller ratios of their PV production potentials to consumption rates due to the limited space for rooftop mounted PV systems at a high number of residents. This indicates that the degree of self-consumption is much higher compared to detached houses, which reduces regional balancing effects. In these cases, the PV installation rate, which maximizes grid balancing, is shifted from 30% as obtained for the study region to higher values.

Apart from the utilization of batteries, heat pumps or electric cars also have the potential to decrease residential PV energy excesses within a house grid network. The utilization of an electrically powered heating or car raises consumption rates and varies residual loads due to different load profiles. These two parameters strongly influence the degree of self-consumption of a building and the magnitude of energy excesses fed into the grids. For this reason, at a high degree of electrification of traffic and heating in a municipality, the presented approach will need to undergo an update of the framework condition.

3.4.3 Policy implications

Several conclusions can be drawn concerning political incentives facilitating the transition to renewable energy systems in regions dominated by detached or terraced residential buildings. At low shares of residential PV systems, financial support for PV systems can be offered without leading to significant changes in the residential residual loads in a regional energy system. The expansion of net metering models could contribute to the PV integration more efficiently than subsidies for battery storages. At medium PV-rates of 30%, the financial support of residential batteries would not lead to an enhanced grid integration of PV systems, as the batteries raise self-consumption at the expense of the regional balancing. A sufficiently large grid infrastructure between the residential buildings leads to similar effects as the broad utilization of batteries. Therefore, potential funding could better focus on the expansion and reinforcement of the local grids than on the expansion of batteries, if regional balancing flows are limited by an insufficient grid infrastructure.

If a large share of residential buildings is already equipped with PV systems, the utilization of the residential storages can help to reduce energy excesses. In this case, incentives for battery systems could be a suitable instrument to motivate households to purchase residential storages. If the energy systems are dominated by the residential sector, additional measures like central storages or feed-in limits are necessary in order to reduce the extreme energy excesses.

3.5 Conclusions

In the transition to renewable energy systems, residential PV and battery storage systems are among the most popular technologies for house owners. Consequently, they are often fostered by governmental institutions. The expansion of rooftop PV power fundamentally changes the structure of the energy systems posing new challenges to the grid suppliers. The impact of the prosumers on the residential residual loads and resulting requirements for their integration is thereby dependent on the PV and battery installation rate:

- If less than 10% of the residential buildings are equipped with PV systems, the prosumers induce minor changes of the residential residual load on regional scale under the assumption of an adequate grid infrastructure. This is also valid, if batteries are additionally utilized. State subsidies for residential PV can be fully offered without constraints.
- For PV installation rates of one third, the balancing arising from differences in the residual loads of the buildings reaches a peak value. At the maximum, 18% of the total residential consumption is produced on other buildings. The utilization of decentral battery storage systems mainly decreases this balancing effect while raising self-consumption. The magnitudes of energy excesses are not significantly reduced by the storages. Due to this, financial supporting schemes should concentrate on grid expansion and the removal of bottlenecks to enable the

full energy exchange between the buildings. Incentives for residential storages do not lead to the further integration of the PV systems.

- For high degrees of buildings equipped with rooftop mounted PV systems, two third of the produced PV power cannot be consumed by the residential buildings. In this case, residential batteries can contribute to a better grid integration of residential PV by reducing low and intermediate negative residual loads. With the utilization of batteries, the residential degree of self-sufficiency reaches the maximum of 58%. The energy excesses, which cannot be consumed by the residential buildings, still account for half of the total PV production. If the residential PV expansion has already reached these high levels, state incentives should set the focus on the increased purchase of battery storage systems instead of single PV systems, as the storages help to reduce backflows into the local grids. Additional mitigation measures become mandatory for energy systems dominated by the residential sector in order to prevent power quality issues.

The obtained results are valid for rural or suburban municipalities at mid-latitudes with high shares of detached or terraced houses and sufficient potential for installing PV systems on their roofs. For these areas of application, we recommend a flexible adjustment of governmental subsidies for battery systems to the current levels of residential PV expansion in order to push the energy transition forward and reduce the efforts for the grid integration of rooftop PV. For rural regions with higher PV potentials, the maximum of regional balancing flows will be obtained at lower PV installation rates. This paper shows that further research is necessary to assess the needs for grid strengthening between the residential buildings for the partial PV expansion and battery utilization.

Author contributions: Conceptualization, A.R. and M.D.; Data curation, A.R. and V.L.; Formal analysis, A.R.; Funding acquisition, W.M.; Investigation, A.R.; Methodology, A.R.; Project administration, M.D.; Resources, W.M.; Software, A.R., V.L. and W.M.; Supervision, W.M.; Validation, V.L.; Visualization, A.R.; Writing – original draft, A.R.; Writing – review & editing, V.L., M.D. and W.M. All authors have read and agreed to the published version of the manuscript.

Funding: This research was funded by the German Federal Ministry of Education and Research (BMBF), grant number 033L155AN.

Acknowledgments: The authors would like to thank Dr. Monika Prasch (LfL) and Bürgerstiftung Energiewende Oberland (EWO) for their support and the German weather service DWD for the data provision.

Conflicts of interest: The authors declare no conflict of interest. The funders had no role in the design of the study; in the collection, analyses, or interpretation of data; in the writing of the manuscript, or in the decision to publish the results.

Appendix

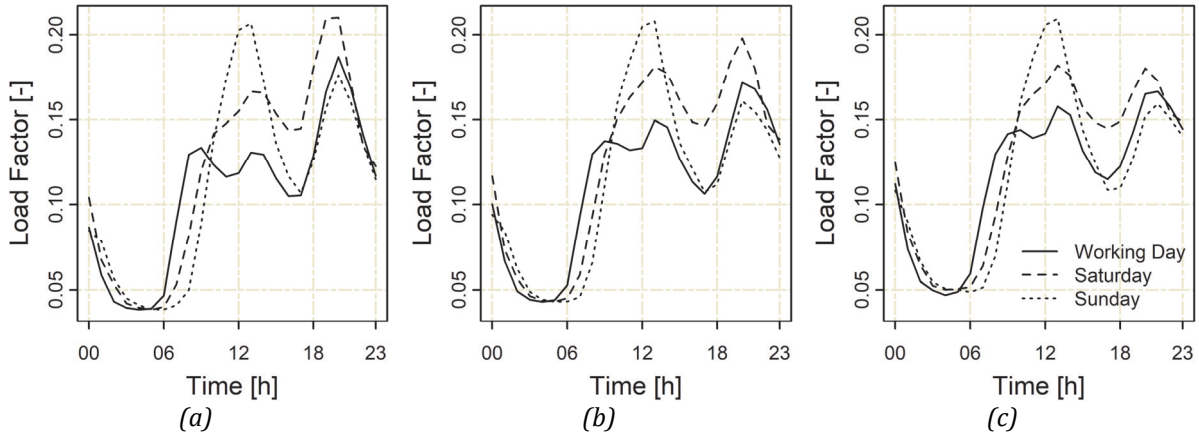

(a) *(b)* *(c)*

*Fig. A. 3-1: The load factors for three different daily profiles and the seasons (**a**) winter, (**b**) spring, and (**c**) summer represent the hourly percentage of the annual consumption in 1.000kWh/a of a residential building (Source: Stadtwerke Unna (2015); VDEW (1999)).*

4 How do changes in climate and consumption loads affect residential PV coupled battery energy systems?

This chapter was published in the Elsevier journal *Energy*:

Reimuth, Andrea, Veronika Locherer, Martin Danner, and Wolfram Mauser. 2020. "How do changes in climate and consumption loads affect residential PV coupled battery energy systems?" *Energy* 198: 117339.

Abstract

Weather conditions and domestic consumption belong to the essential boundary conditions in the optimal dimensioning of residential battery storage systems. In future, both factors will undergo transitions due to climate change and efficiency enhancement of domestic appliances. This study seeks to assess potential developments in climate and consumption loads on the battery flows and residual loads for the near-time future. For this purpose, a land surface processes model with an integrated domestic energy system component is applied. Three scenarios project changes in consumption loads and meteorological conditions for the year 2040. The study area includes 4906 buildings located in the south of Germany. The results show a general rise of grid feed-in rates between 21% and 27% due to increased photovoltaic production. Climate change is expected to raise battery utilization during the winter months, whereas decreasing effects from efficiency enhancement dominate in the summer. The self-consumption rate declines between 4% and 12%, whereas self-sufficiency rises up to 6%. Consequently, in the assessment of battery dimensioning approaches maximizing self-consumption or profitability, we recommend including the shifts in battery utilization and residual loads arising from future changes in climate and consumption loads.

- Analysis of three future scenarios for efficiency enhancement and climate change.
- Impacts of scenario conditions on battery flows depend on the season.
- Decline of average battery flows under more sustainable conditions.
- Rising grid flows due to increasing power excesses in the summer months.
- Degree of PV self-consumption declines between 4% and 12%.

4.1 Introduction

In recent years, residential battery storage systems have gained growing popularity among the owners of rooftop mounted photovoltaic (PV) systems. Taking Germany as an example, already every second newly installed PV system with less than 30 kWp was coupled to a storage system in 2017 (Figgener et al. 2018). Consequently, residential batteries are expected to influence the flows in the energy systems significantly.

Apart from the ability of increasing the PV self-consumption rates, battery storages have the potential of reducing harmful feed-in peaks into the local grids (Moshövel et al. 2015). Therefore, much research has been undertaken in the dimensioning of residential battery storage capacities for cost-effective and grid-friendly operation modes. A variety of studies presents optimization techniques for the battery size aiming at different goals like the maximization of economic benefits for the PV owners under different tariffs (Li 2019; Sharma et al. 2019; Talent et al. 2018; Koskela et al. 2019), the reduction curtailment losses under feed-in restrictions (Colmenar-Santos et al. 2019) or the additional utilization for frequency regulation apart from self-consumption (Gomez-Gonzalez et al. 2020). In these fields of application, the profitability of a battery system is driven by the excess energy production of the domestic PV plants and the residential consumption loads apart from economic parameters. Apart from the future technological development of the PV and battery systems, these two factors will undergo severe transitions in the next decades.

Climate change will influence the operation temperature of PV systems, but also the availability of the bottom-of-atmosphere solar irradiation due to shifts in cloud cover and humidity (Huber et al. 2016). Several studies have examined how far the PV production rates will be affected by the changing meteorological conditions. In a first approach, the potential changes in PV energy are quantified from daily temperature and solar radiation means of global climate projections for 208 (Crook et al. 2011). This approach has been adopted in subsequent studies, which used improved climate projection data in order to determine the future annual changes in PV production and their variance for different spatial extents and scales (Wild et al. 2015; Jerez et al. 2015; Soares et al. 2019). Their spatial resolutions of PV production scenarios originate from the grid sizes of the underlying climatic projections. The results provide a general estimate of potential changes in the production of residential PV systems up monthly temporal scale (Müller et al. 2019). In order to increase the temporal resolution, the meteorological parameters of the climate projections have been temporally downscaled from monthly means to daytime values assuming sinusoidal curves of the daily courses for temperature in Ref. Crook et al. (2011) or irradiance in Refs. Müller et al. (2019). However, the impacts of changing PV production rates resulting from the future shifts in the meteorological conditions on the charging and discharging quantities of battery storage systems have not yet been investigated closer.

The mitigation of global warming implies a transformation of the residential energy sector, which belongs to the considerable contributors of greenhouse gas emissions (Nejat et al. 2015). Apart from the conversion to renewable energy resources, potential measures also include energy savings by changes in behavior or improvements in energy efficiency (Lucon et al. 2014). Significant reductions in the electrical energy demand can be achieved if appropriate regulative instruments are implemented (Allouhi et al. 2015). Recent research has shown that the residential consumption profile has a strong influence on the self-consumption of PV systems coupled to battery storages (Nyholm et al. 2016). Thus, a decrease of the energy demand arising from increasing efficiency rates of domestic appliances will induce changes in the residual loads and battery utilization.

These future developments of climate and efficiency enhancement will affect PV production and consumption loads in adverse ways. To the authors' knowledge, the effects of changes in consumption loads and climatic conditions on the residential storage systems have not yet been analyzed.

In this context, the study sets out to assess their impacts on the charging and discharging quantities of batteries. The paper seeks to answer the following questions: Firstly, in which way will the battery flows and utilizations be influenced by changes in climate and consumption loads in the course of the year? Secondly, how far will the local grid flows be affected that have to be managed by grid suppliers? Third, to which degree will self-consumption, self-supply, and battery cycles be influenced? The parameters are analyzed as changes in the battery utilization and grid flows potentially shift the optimal dimensioning.

In order to answer these questions, a spatially distributed land surface model with an integrated residential energy system component is applied. This model enables the assessment of multiple residential systems on regional scale with building-specific PV inclination angels and orientations, energy demands and battery sizes. As currently available climate projections provide insufficient temporal resolutions needed for an assessment of battery flows, a statistical climate generator is applied, which downscales the meteorological drivers to an hourly time step. Three different scenarios for the future development of climate change and efficiency enhancement are assessed to gain a comprehensive understanding of the impacts on the energy flows in the residential systems in the near-term future.

4.2 Materials and methods

4.2.1 Model environment

The simulation environment of the domestic energy systems is embedded into the land surface processes model PROcesses of Radiation, Mass, and Energy Transfer (PROMET) (Mauser et al.

2009). The PROMET model was originally developed for analyzing hydrological and agricultural processes. It uses a raster-based approach, which means that each domestic energy system is referenced to a grid point in the simulation domain. It is spatially explicit and strictly conserves mass and energy in all components. The presented simulation results were carried out with a temporal and spatial resolution of 1 h and 100 m. The basic input includes hourly meteorological point data for air temperature, air humidity, wind speed, cloud cover, and precipitation (Mauser et al. 2009). These parameters are spatially interpolated with the inverse squared distance weighting method considering topographical conditions. The incoming direct and diffuse radiation relevant for the hourly PV generation is calculated according to the approaches of McClatchey et al. (1972), and Möser et al. (1983). A detailed description of the general model and application is given in Mauser et al. (2009), and Mauser et al. (2015).

The domestic energy system simulating the residential energy flows consists of three components (see Fig. 4-1).

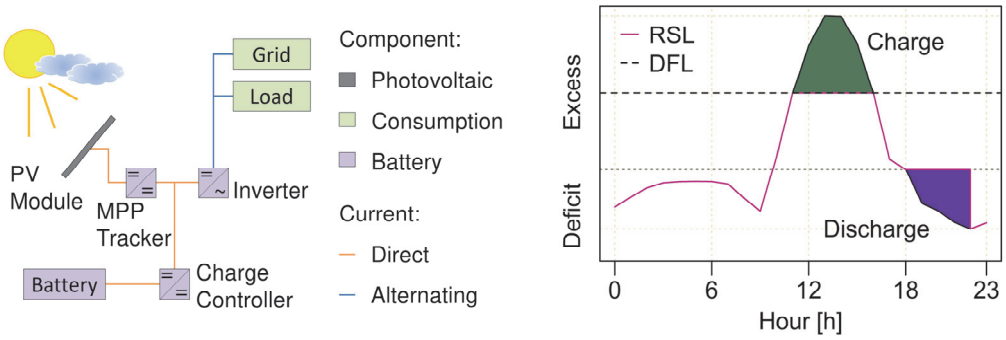

Fig. 4-1: Structure of the domestic energy module including the energy production of the PV panels, the battery with its environment and the grid power flows (left) and selected charging and discharging strategy (right). RSL denotes the residual loads, DFL the dynamic feed-in limit.

The PV model calculates the energy production rate P_{PV} from the solar direct and diffuse irradiation E_{Dir} and E_{Dif} and background reflection E_{Ref} on the inclined PV panel area A_{PV} following the method of Quaschning (2013) (see Eq. (4-1)). Temperature effects T, and aging a are considered by the efficiency parameters η_T *and* η_A. Snow coverage exceeding 2 cm impedes the PV production.

$$P_{PV} = \left(E_{Dir} + E_{Dif} + E_{Ref}\right)/1000 \cdot A_{PV} \cdot \eta_T(T) \cdot \eta_A(a) \qquad (4\text{-}1)$$

The temporal course of the energy consumption E_D is calculated from the annual consumption E_{Da}, which is downscaled by hourly load profiles hf depending on season S and day of the week doW (see Eq. (4-2)).

$$E_D = E_{Da} \cdot h_f(S, doW) \qquad (4\text{-}2)$$

The PV model and the consumption component were validated with measurement data on hourly resolution obtaining determination coefficients of 0.58 respectively 0.56.

The battery model includes the simulation of the flows within the accumulator as well as the grid conversion. The battery is assumed as rechargeable, always connected to the grid, and directly

coupled to the PV module. The performance of the battery P_B is determined from the available energy excess or deficit ΔE, the state of charge SOC, the useable capacity C_N, and the maximum charging or discharging power $P_{B,max}$ (see Eq. (4-3)). The influences of temperature and current are considered by a constant efficiency rate η_B. The battery model includes self-discharge and aging effects.

$$P_B = \min\left(P_{B,max}, SOC \cdot C_N, \Delta E\right) \cdot \eta_B \quad (4\text{-}3)$$

The battery management is based on daily dynamic feed-in limits (DFLs) as shown in Fig. 4-1. The battery starts to charge as soon as the PV production rate, which is not immediately consumed by the household, exceeds the DFL, and stops, when the residual load falls below this threshold. In this way, the selected battery charging strategy both optimizes the self-consumption rate and decreases the feed-in peaks. The DFL thresholds have been previously determined assuming a perfect forecast. The battery is discharged when the hourly energy consumption exceeds the production.

The residual load of a domestic energy system RSL_B, which is supplied by or fed into the grid, is defined as the difference between the consumption rate and the power flows of PV panel and battery. The efficiencies of the MPP-Tracker η_{MPP} and inverter η_{Inv} are considered as shown in Eq. (4-4).

$$RSL_B = E_D - (P_{PV} \cdot \eta_{MPP} - P_B)\eta_{Inv} \quad (4\text{-}4)$$

The degree of self-consumption (DSC) assesses the percentage of production used by the domestic energy system (see Eq. (4-5)). The degree of self-sufficiency (DSS) quantifies the annual percentage of the total consumption that is supplied by the domestic PV production (see Eq. (4-6)). The degree of autarky (DA) represents the changes in the grid flows in comparison to the state without a residential energy generation and storage system (see Eq. (4-7)). RSL_+ denotes the hourly energy flow supplied by the grid.

$$DSC_B = 1 - \sum RSL_+ / \sum E_D \quad (4\text{-}5)$$

$$DSS_B = \left(\sum E_D - \sum RSL_+\right) / \sum P_{PV} \quad (4\text{-}6)$$

$$DA_B = \sum |RSL| / \sum E_D \quad (4\text{-}7)$$

A detailed description of the model setup and structural embedding into the PROMET model is given in Reimuth et al. (2019) and in its associated technical notes (Locherer 2018; Prasch et al. 2018; Reimuth 2017a, 2017b).

4.2.2 Generation of the meteorological scenarios

The effects of anthropogenic emissions on the future climate are studied extensively under the umbrella of the Intergovernmental Panel on Climate Change (IPCC) (IPPC 2014). The IPCC established four Representative Concentration Pathways (RCPs), which project different future developments of the greenhouse gas concentrations. The impacts of these RCP emission scenarios on the future climatic conditions are assessed using global climate models. The generated output data sets of the global climate models as well as those of derived regional models often have a grid size of several kilometers and low temporal resolutions (Flato et al. 2013). Since local climatic conditions can considerably deviate from the coarse-grid model representations, we downscale the meteorological drivers to a resolution of 100 m and 1 h. In this way, the small-scale variation of the weather conditions, which induce relevant differences in the energy flows within a regional system (Reimuth et al. 2019), can be adequately considered in this study.

From the variety of downscaling processes (Bhuvandas et al. 2014) we chose the statistical climate generator of Mauser (2016), which uses the general regional future climate change trends to rearrange measured historical data sets in a way that they represent future climatic conditions. This method relies on climate parameters measured by a station network and therefore produces spatially and physically consistent meteorological data sets with a temporal and spatial resolution identical to the measured data. Thus, the full comparability of the results for the current and future states of the domestic energy systems is ensured and local peculiarities are preserved.

Precondition for this method is an hourly data set with a sufficiently high number of observation years. The approach further assumes a continuance of the current climate regime, which can be presumed in Central Europe for the near-time future (Rubel et al. 2010). In this manner, robust correlations representing the local weather characteristics can be derived. Therefore, the historical weekly sums of precipitation and weekly averages of temperature measurements are analyzed with respect to their annual variation and covariance. In the next step, the annual future trends in temperature and precipitation are extrapolated for the study region from the selected IPCC climate projection. A two-dimensional statistical random generator is applied to mimic the natural variability of the future climate. The final projection is obtained by rearranging the historical data set according to the future synthetic weeks. In this way, the projected meteorological scenario follows the future temperature trend of the IPCC scenario but maintains the measured consistency of the region. A detailed description of the method and its restrictions is presented in Ref. Rubel et al. (2010) and the supplementary material.

4.3 Case study

4.3.1 Description of the study area

The research area "Bavarian Oberland" is located in the south of Germany and covers the administrative districts Miesbach, Bad Tölz-Wolfratshausen, and Weilheim-Schongau (see Fig. 4-2). The region consumes 2161 GWh of electrical energy in the annual average (2013–2016), of which 21.6% can be attributed to the private sector (Lechwerke 2017; Bayernwerk 2017; Elektrizitätswerke Tegernsee 2017; Gemeindewerke Holzkirchen 2017; Gemeindewerke Peißenberg 2017; Stadtwerke Bad Tölz 2017; Elektrizitätswerke Böbing e.G. 2017). This corresponds to a mean consumption of 5127 kWh per building for an average household with 4.3 persons.

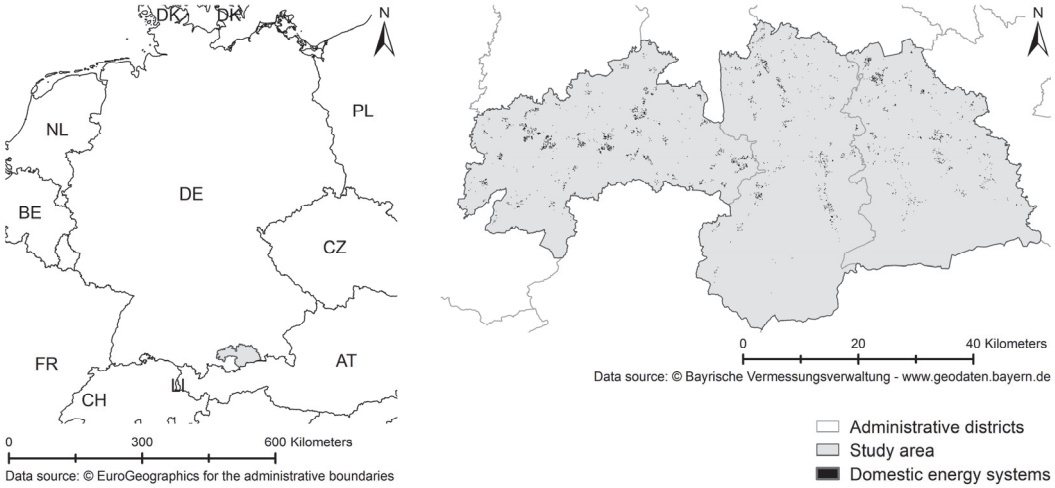

Fig. 4-2: Location of the study area (left) and distribution of the 4906 selected households (right) (Data source: Bayerische Vermessungsverwaltung (2018); EuroGeographics (2018)).

Between 1994 and 2016, a total of 13,940 PV systems feeding into the local grids have been registered within the study area (Deutsche Gesellschaft für Sonnenenergie e.V. (DGS) 2015; Bayerisches Landesamt für Statistik 2017). 7522 plants mounted on residential houses could be identified as domestic systems by using an airborne laser scanning data set containing the building outlines (Bayerisches Landesamt für Digitalisierung 2015a). With an annual incoming solar irradiation of 1167 kWh/m², the study area belongs to the regions of Germany with the highest PV potentials under the current climate (DWD CDC 2016).

4.3.2 Basic input for the domestic energy model

To consider the variability of the energy system setups, 4906 residential buildings with existing, rooftop mounted PV systems are selected having a nominal power between 3.0 kWp and 10.0 kWp. The inclinations and orientations of the panels are derived from the corresponding roof pitches of the building outlines provided by (Bayerisches Landesamt für Digitalisierung 2015a). On average, the panels have a nominal power of 6.3 kWp, a size of 44.17 m² at an inclination of

27.36° aligned towards the southeast. The efficiencies are estimated from the date of installation and an efficiency curve (Fraunhofer ISE 2019a) and range between 10.7% and 16.4%. Further parameters for the PV model are taken from Quaschning (2013) (see also Tab. A. 4-1).

The load curves used to determine the hourly domestic energy consumption rates are based on standardized consumption profiles (Stadtwerke Unna 2015; VDEW 1999). Three types of season and day are distinguished (see Fig. A. 4-1).

The domestic energy storage devices are assumed as lithium-ion accumulators, which have become the common type for domestic applications (Figgener et al. 2018). The battery systems are limited to a useable capacity of 60% and a maximum power of 0.3 kW/kWh at an hourly loss rate of $6.25 \cdot 10^{-8}$ of the nominal capacity (Schoop 2013; Opiyo 2016). The converter efficiency is set to 94% and the losses of dis-/charging to 1% of the power flow (see also Tab. A. 4-1).

The useable capacities of the battery systems are dimensioned according to the nominal power of the corresponding PV systems following Weniger et al. (2014). Thus, the nominal battery capacities of the domestic energy systems range between 5.0 kWh and 16.7 kWh at an average value of 10.5 kWh.

These parameters are kept constant for all scenarios to quantify the influence of climate change and efficiency enhancement of domestic appliances. The basic input needed to drive the land surface model PROMET is described in Mauser et al. (2009).

4.3.3 Input required for the climate generator

The hourly measurement data used for the statistical analysis and the reassembling process are taken from 377 weather stations German and the Austrian Weather Service network covering the years 1960–2006.

The future local climate trend is developed from bias-corrected projections for precipitation and temperature of five global climate models from the ISIMIP Fast Track input-data catalogue for each RCP scenario (Warszawski et al. 2014; Hempel et al. 2013a, 2013b).

The mean decadal temperature increases serving as input for the climate generator were determined from the five projections of the grid cell representing the study area. The annual temperature trend of each RCP scenario relevant for the study region was finally found by fitting a polynomial curve of third order to the ensemble average of the temperature trends (see Tab. A. 4-2 and Fig. A. 4-2).

The changes of the weekly temperature averages and precipitation sums were calculated from the five data sets for each RCP scenario in the following way: First, the long-term average for precipitation sums and temperature means were obtained from the time spans 1961 to 1990 and 2021

to 2050. The differences between past and future time span were smoothened by taking the moving average over 10 weeks. The differences in the weekly temperature means and ratio of the precipitation sums were finally determined as the ensemble average of the smoothened values from the five projections (see Fig. A. 4-3).

4.3.4 Scenario generation

The baseline scenario simulates the current state of the energy system as reference using the year 2016. This year is characterized by average annual energy consumption rates (Lechwerke 2017; Bayernwerk 2017; Elektrizitätswerke Tegernsee 2017; Gemeindewerke Holzkirchen 2017; Gemeindewerke Peißenberg 2017; Stadtwerke Bad Tölz 2017; Elektrizitätswerke Böbing e.G. 2017) and a global irradiation sum deviating only marginally from the long-term average (DWD CDC 2016). The domestic consumption is obtained in a top-down approach from the number of buildings and the annual consumption of the municipalities (Lechwerke 2017; Bayernwerk 2017; Elektrizitätswerke Tegernsee 2017; Gemeindewerke Holzkirchen 2017; Gemeindewerke Peißenberg 2017; Stadtwerke Bad Tölz 2017; Elektrizitätswerke Böbing e.G. 2017). The simulation is carried out with hourly measurement data from 79 weather stations of the German and the Austrian Weather Service network.

Three future scenarios are applied considering potential developments of the annual domestic energy consumption and climatic conditions. The year 2040 is chosen as projected year, since a time interval of 25 years corresponds to the performance guarantees of the PV manufacturers (Fraunhofer ISE 2019a).

The first varied component is the underlying global climate trend, which is used to project the meteorological conditions in 2040. Three out of four available RCP pathways of IPCC are selected (van Vuuren et al. 2011):

- RCP 2.6 represents the lower bound of a warming climate. It assumes that the radiative forcing undergoes the lowest total increase of 1.27 W/m2 until 2050.
- RCP 4.5 includes ambitious efforts in reducing temperature increase. The scenario projects a rise of the radiative forcing by 2.04 W/m2.
- The third scenario is based on RCP 8.5 assuming the highest rise of global temperature. For the first half of the 21st century the radiative forcing is projected to rise by 3.04 W/m2.

The time span from 2038 to 2042 is simulated assuming constant climatic conditions within five years. The year with median PV production is assumed to represent average meteorological conditions for the respective climate scenario (see Fig. A. 4-4-Fig. A. 4-6).

In terms of efficiency enhancement, scenario "Strong" and "Medium" follow the story lines developed in Prognos AG et al. (2014), who outlined two scenarios for the energy consumption rates in Germany. These scenarios already include the additional prospective energy consumption arising from the growing use of air conditioning and changes in behavior, which counteract the decrease in energy consumption from efficiency enhancement. The differences between the residential consumption of 2040 and 2016 (obtained by linear interpolation between 2011 and 2020) represent the future, potential increases in energy efficiency used in this study. Scenario "Strong" supposes that the goals of the official energy concept are realized. This means a reduction of 17.1%. Scenario "Medium" projects the German trend of the recent years leading to 15.5% in 2040. Scenario "No" assumes that the domestic energy consumption is not reduced.

As the assumptions in the RCP scenarios already include explicit projections of the global energy use, a consistent development of energy enhancements and the greenhouse gas emissions is assumed in this study (see Tab. 4-1). Scenario A is characterized by strong efforts in climate change mitigation, which is consistent to strong improvements in energy efficiency. Scenario B projects a medium range future with major emission reductions and medium success in raising energy efficiency. Scenario C assumes a business-as-usual, non-sustainable development, which projects the current emission path and consumption into the future.

Tab. 4-1: Boundary conditions for three future scenarios concerning the IPCC emission scenarios and the progresses in energy efficiency.

		Greenhouse gas emission path		
		RCP 2.6	RCP 4.5	RCP 8.5
Efficiency improvements	17.1%	A		
	15.5%		B	
	0%			C

4.4 Results

4.4.1 Temporal course of the energy flows

Fig. 4-3 shows the average annual course of the cumulated energy flows and the cumulated differences of the future scenarios in relation to the baseline.

The energy consumption rates do not show significant seasonal variations in all four scenarios, as they accumulate almost linearly during the year. The reductions of the annual consumption result in a decline of 868.83 kWh in scenario A and 786.97 kWh in scenario B compared to the baseline and scenario C with 5110.48 kWh.

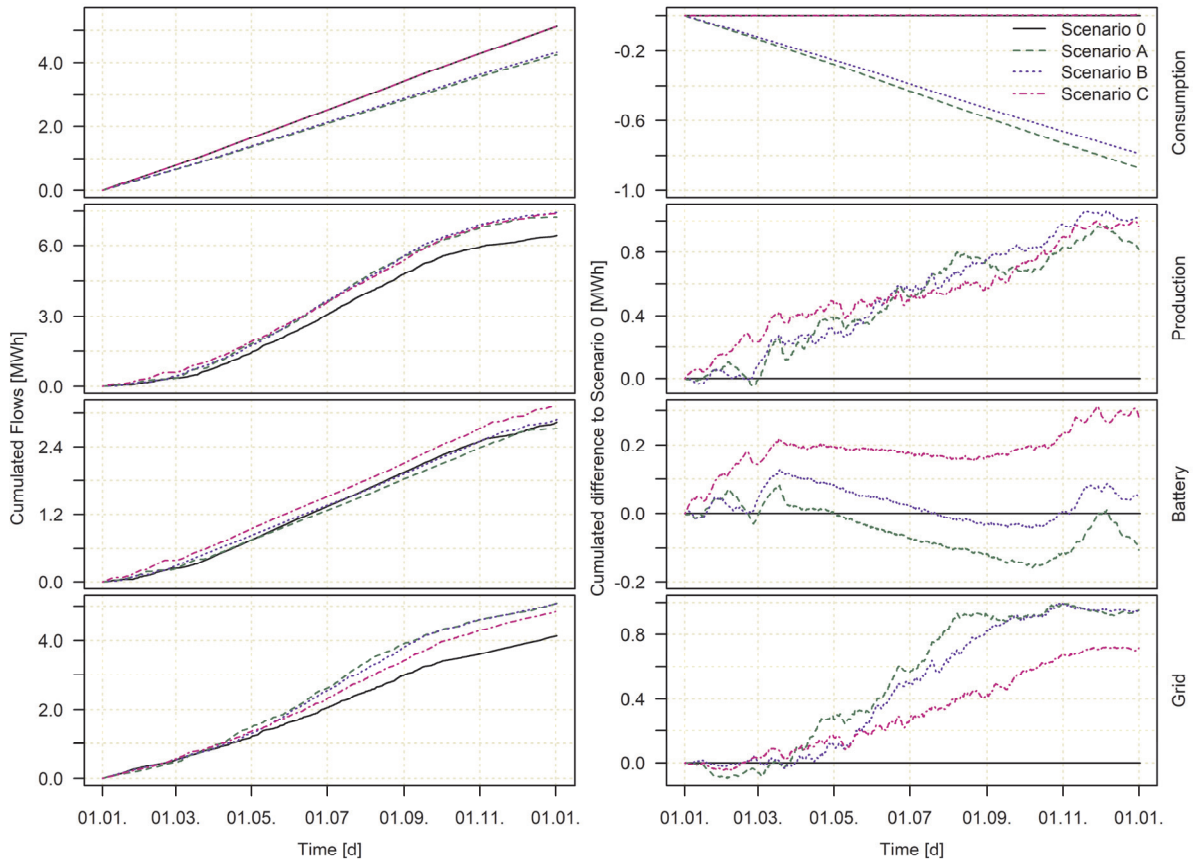

Fig. 4-3: Cumulated energy flows of consumption, production, battery and grid flows for an average domestic energy system (left), and cumulated differences between the future energy flows of Scenario A, B, and C and the baseline scenario (right).

In contrast, the courses of the PV production rates are characterized by sigmoid shapes caused by the steeper solar inclinations angles in the summer months. Under conditions of scenario 0, the average PV production rate exceeds the total energy consumption with an annual yield of 6419.26 kWh. Due to the changing climate conditions, the electrical energy generation is further raised between 12.5% and 17.5%. The deviations to scenario 0 have different seasonal courses. In spring, the changes in scenario A and B underlie a higher variability than the scenario C. In the further course of the year, scenario B and C are characterized by a linear daily increases in contrast to A, which continues to fluctuate.

The differences, which can be observed in the production and consumption rates, consequently lead to varying changes of the battery flows. Scenario A is characterized by an annual, average reduction of 105.96 kWh compared to the battery flows of the baseline scenario 0 with 2832.31 kWh. In contrast, the battery flows of the two future scenarios B and C increase by 46.81 kWh and 280.61 kWh. In the spring and summer months, the deviations in the battery flows follow the form similar to the linear variation of the projected consumption rates. Scenario A decreases by 6.7%, scenario B by 4.5%, and scenario C shows more or less no deviation. However,

at the beginning and end of the year, the changes in the battery flows between scenarios and baseline converge to those of the PV production rates. This time span is characterized by higher fluctuations as the batteries cannot always be fully charged.

The average flows between the domestic energy systems and grids are collectively raised between 717.97 kWh in scenario C and 952.11 kWh in A, compared to 4121.80 kWh in the baseline year. The courses of the grid flows are also subject to seasonality. During the first and last months of the year, all three scenarios are similar to the baseline. However, the varied boundary conditions lead to significant changes between the scenarios in spring and summer. Scenario A and B show the strongest increase of grid flows with a daily average of 17.05 kWh and 17.95 kWh. This is caused by the increased PV excesses and the lower battery utilization. In contrast, the differences in the grid flows of scenario C show a more or less constant daily increase of 15.93 kWh.

4.4.2 Variance of the energy flows

Fig. 4-4 represents statistical parameters of the annual energy flows for the PV production, consumption, battery, and grid flows referenced to their PV peak performance (see Tab. A. 4-3).

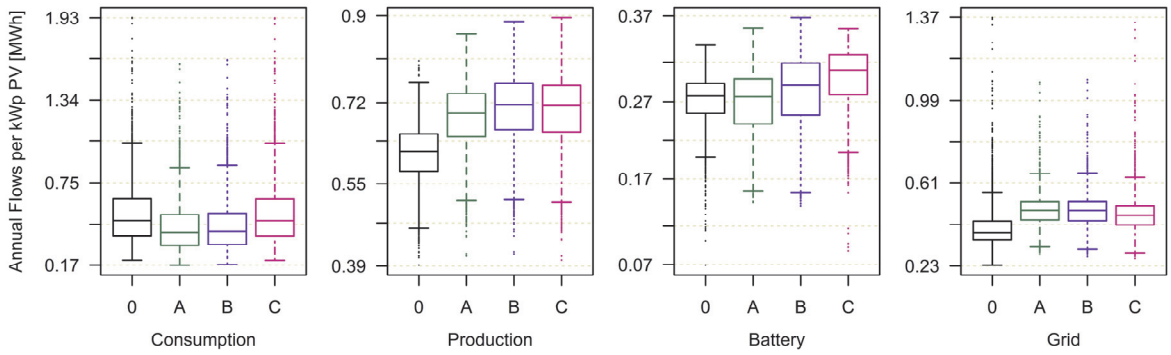

Fig. 4-4: Quantiles of the domestic annual energy flows for consumption, production, battery, and grid per kWp-PV power for Scenario 0, A, B, and C.

Scaled by the PV power, the annual consumption rates show the largest deviations among the 4906 domestic energy systems varying by 2.93 MWh. The high number of outliers is caused by households with small PV plants and high annual energy consumption rates. According to the efficiency increases of 17.1% and 15.5%, the medians of the consumption rates decline by 140.07 kWh for scenario A and 127.10 kWh for scenario B related to the baseline with 812.40 kWh per kWp PV. The distribution of scenarios C is identical to 0, as no shifts in the consumptions are assumed.

The scaled PV production shows a more or less constant increase between 12.8% and 15.3% of median and quartiles for all future scenarios. Climate change increases the PV production but not the variance among the domestic energy systems.

The scaled battery flows are generally characterized by lowest variance of the analyzed parameters, as the interquartile range varies only by 63.77 kWh per kWp in the baseline year for instance. However, in scenario A and B the spread between the annual battery flows is increased under future conditions by up to 110.96 kWh. For smaller battery systems, the battery flows increase, whereas for larger systems they decline.

This is different for the residual loads: The median increases between 26.7% in A, and 20.8% in C compared to the baseline scenario. However, the future interquartile ranges are decreased. Thus, the total grid flows of the domestic energy systems rise but the variances between the energy systems decreases under the future scenario conditions.

4.4.3 Development of the residual loads

The residual loads presented in Fig. 4-5 are obtained from a subset of 2505 simulated domestic systems, which exclusively occupy a raster grid point so that the energy flows can be directly linked to a single building.

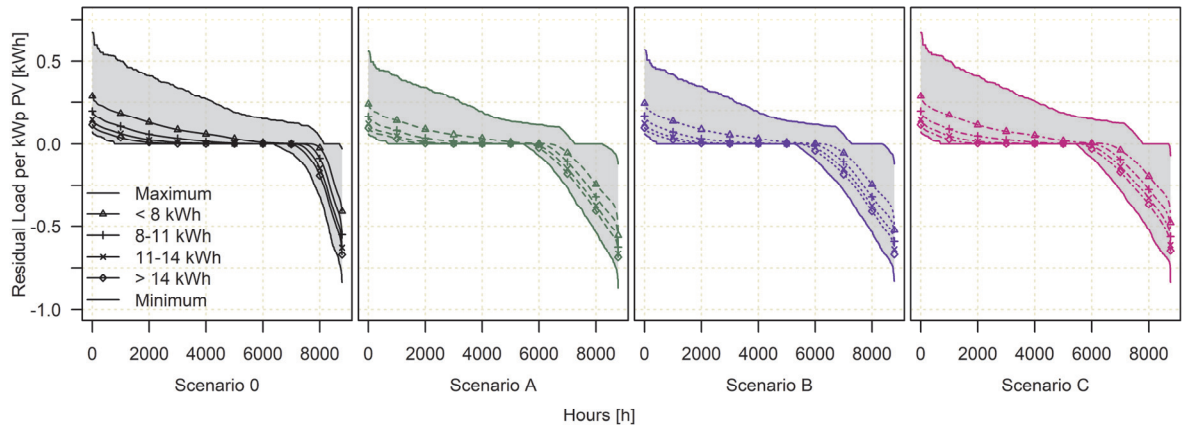

Fig. 4-5: Distribution of the hourly residual loads of 2505 selected domestic energy systems with the minimum and maximum extrema enclosing the average flows for the battery systems having capacities of less than 8 kWh, 8–10.99 kWh, 11–14.99 kWh, and larger than 14 kWh.

The maximum and minimum residual loads represent the range of hourly power flows per kW-peak, which are supplied by or fed into the grid. All four scenarios show that the feed-in peaks exceed maximum consumption. The power excesses are also raised in all three future scenarios in their quantities. In addition, the maximum positive residual loads decrease in scenarios A and B due to the reductions of the consumption rates. In all scenarios, the maximum power flows of the households are defined by the PV excesses.

The extreme grid flows flank the average loads of the four classes of storage capacities (<8 kWh, 8–11 kWh, 11–14 kWh, >14 kWh). All three future scenarios are characterized by an increase of hours with medium and maximum excesses. This can also be observed when analyzing the number of hours without grid flows. In the baseline scenario, the domestic energy systems with less

than 8 kWh capacity have 47 h without grid interaction in contrast to 1640 h with systems of more than 14 kWh. Under the future scenario conditions, the hours of autarky decrease for all sizes of the battery systems. Scenario C is characterized by the highest decline for all battery sizes showing only 12 h without grid interaction for the smallest and 1071 h for the largest category of battery capacities.

4.4.4 Self-consumption and self-supply

Fig. 4-6 shows the degrees of self-consumption (DSC), self-supply (DSS), autarky (DA), and the number of cycles (NoC) as a function of the domestic battery capacities (see also Tab. A. 4-4-Tab. A. 4-5). The curves are interpolated from the subset of 2505 domestic energy systems.

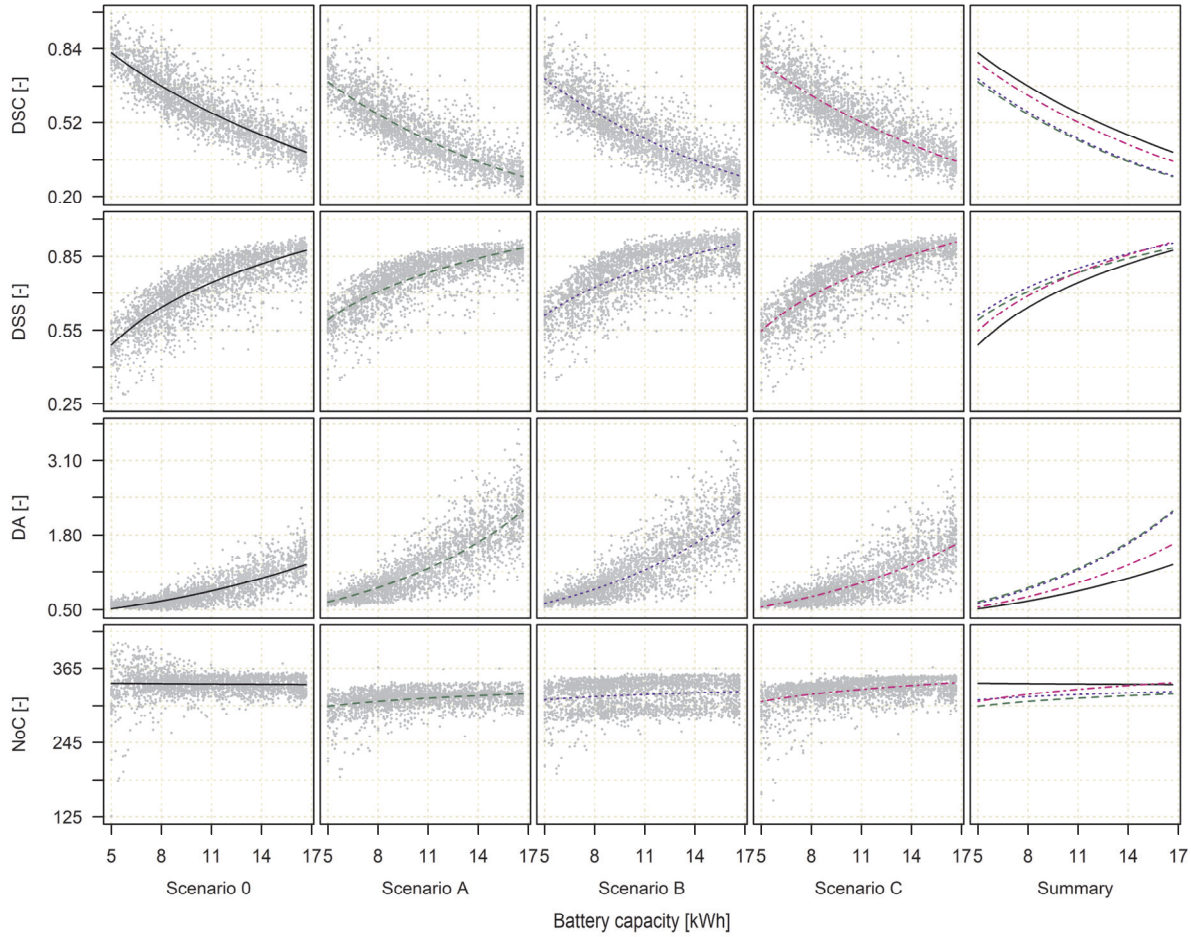

Fig. 4-6: Degree of Self-Consumption (DSC), Degree of Self-Supply (DSS), Degree of Autarky (DA), and Number of Cycles (NoC) in dependency of the battery capacity. The lines represent the fitted curves, which are in logarithmic form for DSC and DA, and exponential form for DSS and NoC.

In the baseline scenario 0, the degree of self-consumption ranges between 82.2% at a storage capacity of 5.0 kWh and 39.4% at the maximum capacity of 16.7 kWh. In the future scenarios, the DSC decreases constantly by 11.9% in scenario A, 11.1% in B, and 4.1% in C.

Whereas the degree of self-supply varies between 49.2% and 87.5% in the baseline scenario, the DSS increases under the future scenarios. With 79.0%, scenario B is characterized by the highest

DSS rates for an average storage size, which means an increase of 6.2% compared to the baseline scenario. However, the sensitivity of this parameter to the capacities declines. The range of the DSS between the smallest and largest battery sizes decreases from 38.3% for the baseline to a 29.4% in scenario A and B.

Analyzing the degree of autarky shows a high dependency of the battery size. Whereas the influence of climate change and efficiency enhancement is low for small battery systems, the DA is very sensitive to the future developments of efficiency improvements and climate change for larger systems. At the smallest battery size of 5.0 kWh, the DA increases only up to 12.0% compared toscenario 0. For the largest analyzed battery storage size of 16.7 kWh, the DA rises from the baseline result of 127.8%–222.3% in A, 220.4% in B, and 163.5% in C.

The threshold of 100% is the point at which the annual grid flows of the building are equivalent to grid supply. In the baseline scenario, an energy system with a peak power of 8.1 kW and storage capacity of 13.5 kWh has the same magnitude of grid flows as without a production and storage component. Scenario A reaches this threshold already at 9.2 kWh, Scenario B at 9.5 kWh and Scenario C at 11.4 kWh.

While the DA increases under futures conditions, the cycle numbers decline. In the baseline scenario, the NoC shows almost no dependency on the battery size with 340.0 battery starts. In scenario C in contrast, the NoC has the highest sensitivity to the battery capacity with annual cycle numbers ranging from 321.2 to 341.9. Scenario C is also characterized by the lowest decline of the NoC from the future scenarios.

4.5 Discussion

4.5.1 Battery utilization

The results obtained in this study show that the influence of efficiency enhancement and climate change on the battery flows is both significantly and strongly dependent on the season.

The summer months are characterized by the rising PV production of up to 13.7% under RCP 4.5 (see Fig. 4-3). This leads to an increased availability of excess energy in a time span, which is already in the baseline year characterized by higher back flows and fully charged batteries. Consequently, the discharging quantities enabling the intake of surpluses gain more influence. Since a reduction of the consumption impedes the full discharging, efficiency enhancement will lead to the decrease of the battery flows in the summer months.

This is different in the winter times, when the changes in the production rates determine the battery flows. The availability of excess PV power will continue to play the decisive role on the battery flows in winter. On the one hand, climate change will lead to increasing precipitation events and

therefore a reduced availability of solar irradiation. On the other hand, the days with snow coverage and therefore the blocking of radiation absorption will decrease under rising temperatures. Under a high climate change scenario the positive effects of decreasing snow days exceed the reduced availability of solar irradiation in the study region, which leads to increasing PV production and battery flow rates.

However, the potential development of the battery flows is also dependent the capacity. The battery flows will rise under the conditions of high efficiency improvements and low climate change only for small capacities. This is also reflected by the decrease of the cycle numbers, which is caused by fewer and longer lasting energy surpluses of the small systems.

The projected developments of the battery flows suggest that the analysis of the future utilization requires scenarios containing both the changing climate conditions and efficiency improvements as their influences are subject to opposing temporal courses: The effects of climate change dominate in the winter months, whereas those of efficiency enhancement prevail in the summer.

The spatial patterns of the meteorological drivers are less relevant, as the annual flows of battery systems are characterized by the smallest regional variance. The results indicate that a sufficient temporal resolution of the energy efficiency and climate projections plays a more important role in the regional assessment of the changes in the future battery utilizations than the choice of the grid size.

4.5.2 Residual loads

Similar to the battery flows, the projected deviations in the grid flows underlie seasonal effects. In the winter months, all three future scenarios are characterized by only small differences. Despite the reductions in energy demand under scenario A and B, the grid flows do not decline at the same magnitude as the energy consumption. This indicates that also in winter the grid suppliers have to deal with rising power excesses.

In the summer months, the feed-in rates are significantly raised when compared to the baseline scenario 0. These shifts arise from several factors: Despite adverse effects of rising temperatures, the PV production rates will increase due to more stable high-pressure systems, which lead to reduced cloudiness and intensified shortwave irradiance. The buffering function of the batteries balancing PV production and consumption remains more or less constant or even declines if the consumption is reduced. Therefore, the increasing energy excesses have to be fully balanced by the grid suppliers. Consequently, scenario A with the strongest reduction of the battery flows is characterized by the highest increase of the grid power flows. Scenario C assuming no efficiency improvements and the climatic conditions of RCP 8.5 shows the lowest rise of grid flows, as the increased PV production can be better balanced under the higher consumption rates.

The distributions of the residual loads, which shift to more extreme PV excesses, also reflect this development. Stresses in the local grids caused by high PV production rates will further intensify, if no countermeasures are taken. The annual grid flows scaled by kWp PV show a high spread between the domestic energy systems, which is caused by the variance in the consumption rates (see Fig. 4-4). This can be explained by the divergence of PV sizes, which were primarily dimensioned to maximize the grid-feed in recent years.

The average increase of the PV production obtained in this study exceeds the projected rates of the discussed literature findings (Müller et al. 2019; Wild et al. 2015; Jerez et al. 2015). One reason for this divergence could be that the selected study area belongs to a part in Germany with high PV potential but also large sensitivity to climate change. Lying at the fringe of the Temperate and Mediterranean climate, it will increasingly come under the influence of Mediterranean climate with milder winters and dry, hot summers. This effect may be generally underrepresented in climate models with larger grid sizes.

The deviations are further reasoned in the lower temporal resolutions of the climatic projections used in previous studies (1h in our study vs. 3h in Ref. Jerez et al. (2015) or 1d in Ref. Wild et al. (2015)). Temperature rise and irradiation conditions, but also the influence of the continuously changing inclination angles between panels and sun are not distributed linearly during daytime. Temporally coarser meteorological drivers using daily or even monthly values for assessing changes in PV production rates cannot capture these effects due to their coarse simulation of atmospheric processes. Consequently, we recommend the utilization of climate data with a sufficiently high temporal resolution or downscaling methods when analyzing potential effects on residual loads.

4.5.3 Limitations of the study

The study is subjected to several limitations concerning the temporal and spatial variability of the consumption loads. As the annual energy consumption is averaged on municipal scale and temporally downscaled by standard load profiles, the variance between the individual buildings cannot be represented with high precision. That means that the obtained results for battery utilization and grid flows are valid for residential buildings constructed in recent decades but not new buildings like zero-energy homes.

The validity of the study is further restricted to buildings without electrically based heating or cooling systems. Their electrical consumption is additionally dependent on the supply with thermal energy, which is driven by the heat demands, insulating properties of the building materials and outside temperatures. Consequently, the hourly consumption rates of buildings with heat pumps strongly vary from the load profiles used in this study.

Apart from this, the modeling of the efficiency enhancement applied to scenario A and B leads to further shortcomings. The hourly decline of the consumption rate is depending on the single efficiency improvements of the running devices. However, the progresses in efficiency enhancement will differ between the electrical goods. The varying developments in the improvements will possibly induce unsteady changes of the hourly load profiles. The assumption of a temporally constant decrease insufficiently reflects these shifts. Nevertheless, the approach applied in this study offers a concise assessment on the battery and grid flows.

4.5.4 Implications for the battery dimensioning

The obtained results indicate that the current assumptions in terms of battery utilization and grid flows will have to be adjusted to the future developments when investigating optimal storage sizes.

Climate change and efficiency enhancement will reduce the self-consumption rates between 4% and 12% depending on the scenario conditions. The independency from the battery size is reasoned in the point that climate change rises the PV production constantly for all PV sizes as described in chapter 4.2. In contrast, the development of the self-supply is strongly influenced by the scenario assumptions, which thus have to be carefully selected. When applying dimensioning approaches with the goal of a high self-consumption or self-supply in the future, we recommend considering these future changes of the boundary conditions in the optimization methods.

Another important factor for the system sizing under economic constraints is the magnitude and time of the residual loads as the cost savings are also indirectly dependent on the charging and discharging amounts of the batteries. The results of this study indicate that the balancing effect of the batteries will be weakened for the majority of the systems. Especially during the summertime with high PV excesses, the battery flows of the systems will be generally reduced if consumption declines. At these times, a significant increase of excessive grid feed-in rates has to be expected. This will further raise curtailment losses if feed-in limits are imposed by the government. These changes can have crucial impacts on the profitability apart from the future development of economic parameters and technological improvement of the PV and battery systems.

4.6 Conclusion

In recent years, small-scale battery storage systems have been increasingly installed in households with rooftop mounted PV systems. In the development of appropriate dimensioning approaches with different optimization goals, weather conditions and energy consumption belong to the essential boundary conditions. However, climate change and efficiency enhancement of domestic appliances affect PV production and consumption rates, which consequently induces

changes in battery and grid flows. We conducted a regional model simulation study of three future scenarios for the year 2040, which combines projected changes in climate and consumption loads to assess the annual course of their impact on 4906 spatially distributed households with PV systems and battery storages.

The results of the study show a rising PV production and a reduction of the charging cycles but rising battery flows for small battery systems. However, a decline in the utilization of larger residential batteries has to be expected with increasing sustainability of the boundary conditions. The changes in the battery flows are subject to a strong seasonal influence: In summer with higher PV production, they are driven by the reduction of the energy consumption. In winter, they are induced by the changes of the PV production rates, due to the lower availability of energy excesses. A decrease of the self-consumption between 4% and 12% independently from the battery and PV size has been found in this study, which is reasoned in the constant increases of the PV production rates.

The reduced buffering effect of the batteries and the increasing PV-production also affect the grid flows. The residual loads are shifted to more and higher energy excesses under future climate change and efficiency scenarios. Especially the summer months are characterized by high PV excesses, which cannot be stored by the residential energy systems. This will increase the probabilities of bottlenecks in the grids and therefore the need for grid adjustment.

The projected changes should be considered in the application and development of dimensioning approaches optimizing self-consumption and cost-efficiency. For a robust sizing, we recommend the usage of scenarios, which include the potential developments of both weather conditions and consumption apart from economic parameters.

Apart from the impact of climate and energy efficiency analyzed in this study, residential energy flows will also be affected by rising rates of electrically based heating and cooling systems and the launch of electric vehicles. These future developments highlight the need for further research in the assessment of challenges and options for the grid integration of residential PV systems under a changing climate.

Acknowledgement

This study was carried out in the framework of the project “INOLA – Innovationen für ein nachhaltiges Land- und Energiemanagement auf regionaler Ebene” (grant code 033L155AN), sponsored by the German Federal Ministry of Education and Research (BMBF).

Supplementary materials

Description of the Statistical Climate Generator

The statistical climate generator of Mauser (2016) regroups historical measurement data sets following the future temperature trend and precipitation changes of the coarse-grid projections of the selected global or regional climate models. The approach consists of three steps:

Firstly, the weekly precipitation sums P_w and temperatures T_w for the whole historical data set consisting of M meteorological stations and N measurement years are calculated and spatially averaged. From the $M \cdot N$ value pairs of T_w and P_w the covariance ($Cov(T,P)_w$) between temperature and precipitation is determined for the 52 weeks (w) of the year as shown in Eq. (A. 4-1). The obtained covariance matrices represent the current regional climatic conditions and their seasonal variations throughout the year.

$$Cov(T,P)_w = \sum_{i=1}^{N} \frac{\left(T_{i,w} - \bar{T}_w\right) \cdot \left(P_{i,w} - \bar{P}_w\right)}{N-1} \qquad (A.\ 4\text{-}1)$$

In the next step, the climatic changes in temperature and precipitation are assessed using the meteorological projection from the pixel of the global or regional climate change model, which represents the study area. The meteorological projection follows the IPCC Representative Concentration Pathways (RCP) scenarios, which translate greenhouse gas emission pathways into changes in radiative climate forcing and hence essential climate variables like temperature, precipitation, wind, and incoming shortwave radiation. The average annual temperature trend $T_{a,t}$ for the scenario period 2038 to 2042 is derived from the decadal means. The changes in temperature means and the precipitation sums are determined as the weekly differences from the scenario period to the historic period of the climate projection. The obtained values represent the weekly changes D in temperature $D_{w,T}$ and precipitation sum $D_{w,P}$.

To realistically construct future climate drivers for spatially resolved PV simulations, the regional climate variability obtained from the historic measurements has to be considered together with the future changes of temperature $D_{w,T}$ and precipitation $D_{w,P}$. This is done by using a coupled normal distribution random generator, which connects random temperature variation with variations in precipitation based on the weekly covariance matrices $Cov(T,P)_w$ of Eq. (A. 4-1). The obtained variations are added to the average weekly development of temperature and precipitation to create a random $T_{w,F(y)}$ - $P_{w,F(y)}$ pair for each week in the future climate record.

In the third step, the obtained weekly temperature and precipitation pair is fed into a maximum-likelihood search algorithm, which identifies the week in the measurement data set with the min-

imum Mahalanobis distance. This is the historical T_w - P_w pair, which has the most similar temperature mean and precipitation sum as the synthetic $T_{w,F(y)}$ - $P_{w,F(y)}$ pair. The data set of all measurement stations M of this week then represents the projections of the future week.

These two steps are carried out for all weeks of the projection period to create a temporally and physically consistent point data set of a meteorological network with M stations. It follows the changing, average, regional temperature and precipitation trend of the chosen RCP scenario. The relation of temperature to precipitation corresponds to the historical weekly covariance $Cov(T,P)_w$, so the regional specific variability is kept in the projection data set.

The approach of the statistical climate generator is based on the following assumptions:

1. Weather conditions already observed in the past will also occur in the near term future, but with changing frequencies and probabilities. In a warmer climate, weeks similar to past warm weeks will most likely happen more frequently, and earlier or later in the year. To be more precise, warmer and at the same time drier summer weeks are likely to be more frequent in a future climate because the covariance analysis reveals a negative correlation between temperature and precipitation in summer. Whenever the climate trend feeds the random generator with higher summer temperatures it will, based on the covariance matrix, create lower precipitations on average. This leads to the search of hot/dry weeks in the historical record.
2. In order to create meaningful covariance matrices, the weekly averages should reflect a persistent atmospheric condition, which is either characterized by a high or low pressure system over the study area. Since these pressure systems have a characteristic diameter of the order of 1000 km, the area of the selected study region should be small in comparison to the size of the pressure system. Since the study area covers several hundred km^2 this assumption is fulfilled.
3. The generator further implies that the covariance between the weekly temperatures means T_w and the average precipitation sums P_w does not change significantly in the future. These assumptions are met as long as the changing future climate in the selected study area does leave the current climate regime. In the next four decades, this can be assumed for the selected RCPs, the analyzed year 2040, and the study region (Rubel et al. 2010).

Tables

Tab. A. 4-1: Technical input parameters for the domestic energy model (Sources: Weniger et al. (2014); Quaschning (2013); Schoop (2013); Opiyo (2016); Fraunhofer ISE (2019b))

Component	Parameter	Value
Inverter	Nominal power	1 kWh/kW

	Efficiency	0.92 – 0.97
Battery	Nominal voltage	3.6 V
	Nominal power	0.3 kW/kWh
	Dis-/charging efficiency	0.99
	Max number of cycles	30,000
	Initial useable capacity	0.60
	Maximum lifetime	20 a
	Hourly loss rate	0.00000625
PV-system	Ageing parameter	0.003
	Temperature coefficient	0.45
	PV-constant	31.25
	Efficiency MPP-tracker	0.99

Tab. A. 4-2: Parameters for adjusted curves for fitted temperature trend of type $y = a \cdot x^3 + b \cdot x^2 + c \cdot x + d$ with x as the days since 01.01.1970 [d]

Parameter	RCP 2.6	RCP 4.5	RCP 8.5
a	1.03110E-13	-7.85838E-14	8.32464E-14
b	-8.98456E-09	2.90214E-09	- 5.26066E-09
c	3.04035E-04	7.61436E-05	2.07931E-04
d	-1.22040E+00	3.99161E-02	- 5.76684E-01

Tab. A. 4-3: Annual average and 5 % / 95 % confidence intervals (CI) for the production, battery and grid flows normalized per kWp PV-power in [kWh/kWp PV]

Parameter		Scenario 0	Scenario A	Scenario B	Scenario C
Consumption	Mean	814.768	676.250	689.302	815.608
	5 % CI	472.108	391.837	399.399	472.585
	95 % CI	1567.085	1300.638	1325.741	1568.667
PV-production	Mean	1023.429	1153.393	1184.565	1177.142
	5 % CI	826.438	936.319	961.893	953.221

	95 % CI	1169.559	1306.819	1363.590	1343.561
Battery flows	Mean	451.557	434.664	459.02	496.295
	5 % CI	355.582	325.401	327.621	379.679
	95 % CI	521.508	526.873	573.379	575.549
Grid flows	Mean	657.142	808.938	808.272	771.609
	5 % CI	496.396	617.118	607.685	588.543
	95 % CI	957.841	974.360	984.119	993.810

Tab. A. 4-4: Parameters for adjusted curves for degree of self-consumption and degree of autarky of type $y = exp(a + b \cdot x)$ with x as the theoretical battery capacity [kWh]

Parameter		Scenario 0	Scenario A	Scenario B	Scenario C
Degree of self-consumption	a	0.1196780	0.0196029	0.0409128	0.0946360
	σ2	0.0082443	0.0100838	0.0103883	0.0098300
	b	-0.0631043	-0.0757177	-0.0762158	-0.0677654
	σ2	0.0007388	0.0009036	0.0009309	0.0008809
Degree of autarky	a	-1.048608	-0.987362	-1.036634	-1.068818
	σ2	0.011524	0.014115	0.014718	0.013958
	b	0.077654	0.107185	0.109627	0.093636
	σ2	0.001033	0.001265	0.001319	0.001251

Tab. A. 4-5: Parameters for adjusted curves for degree of self-supply and cycles numbers of type $y = a + b \cdot log(x)$ with x as the theoretical battery capacity [kWh]

Parameter		Scenario 0	Scenario A	Scenario B	Scenario C
Degree of self-supply	a	-0.020078	0.198747	0.215494	0.066547
	σ2	0.010048	0.008777	0.010655	0.009661
	b	0.318076	0.243780	0.244453	0.299285
	σ2	0.004294	0.003751	0.004553	0.004129
Number of cycles	a	342.599	277.119	297.149	272.465
	σ2	2.629	2.132	3.307	2.529

	b	-1.533	16.879	11.019	24.690
	σ2	1.124	0.911	1.413	1.0810

Figures

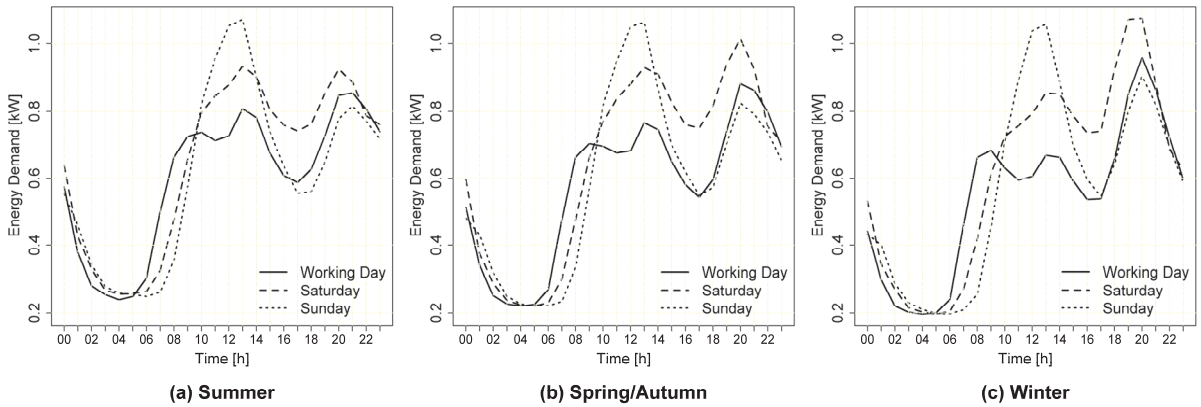

Fig. A. 4-1: Load profiles of an average household with an annual electrical energy demand of 5119.35 kWh.

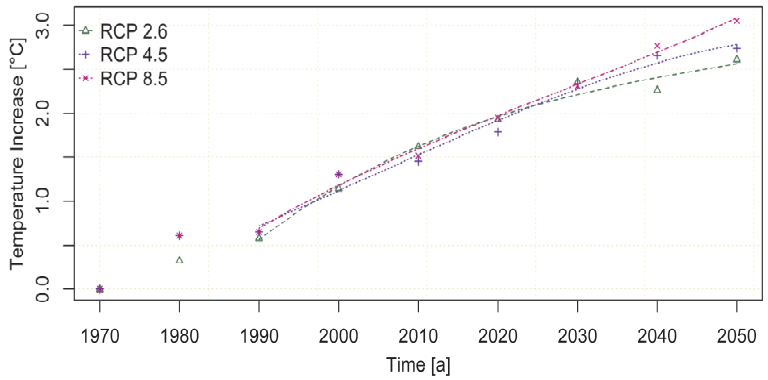

Fig. A. 4-2: Fitted temperature trends to decadal ensemble of the projected temperature increases since 01.01.1970.

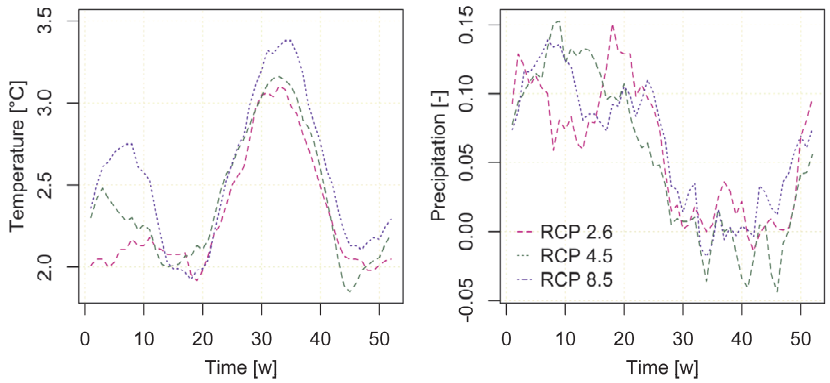

Fig. A. 4-3: Relative changes of the weekly temperatures and precipitation sums from the ensemble means of 2021 to 2050 compared to 1961 to 1990

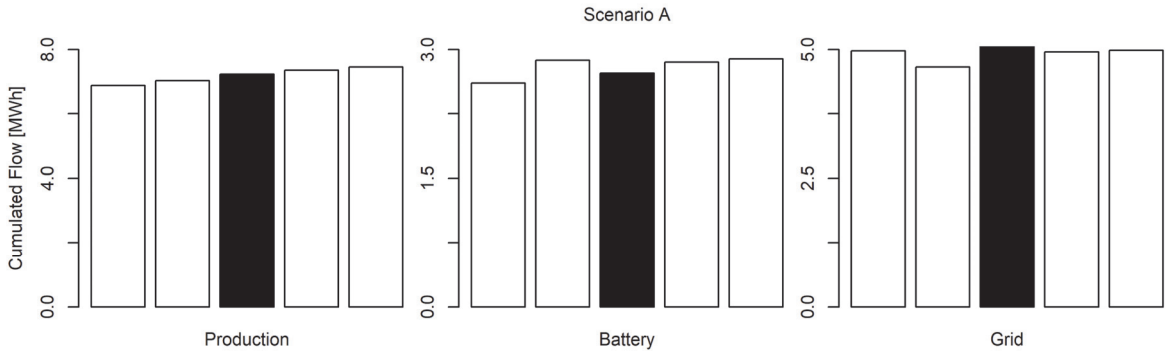

Fig. A. 4-4: Annual mean production rates, battery flows and grid flows with the selected marked in black year representing average meteorological conditions in scenario A

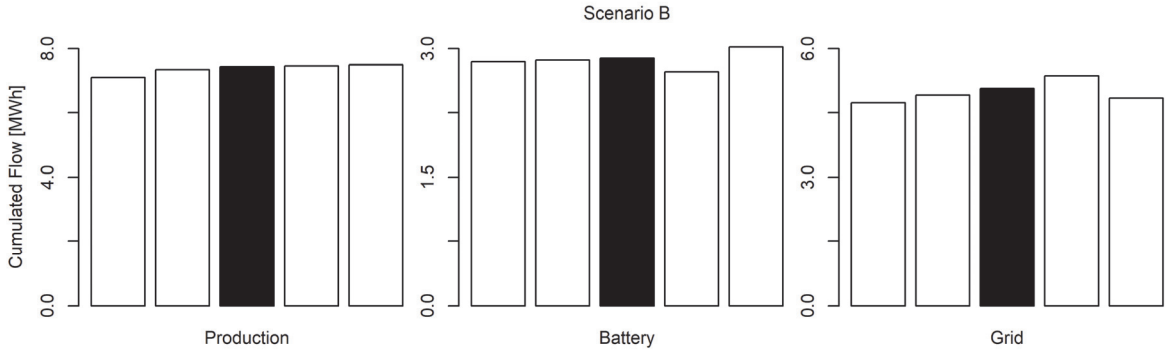

Fig. A. 4-5: Selected year representing average meteorological conditions in scenario B

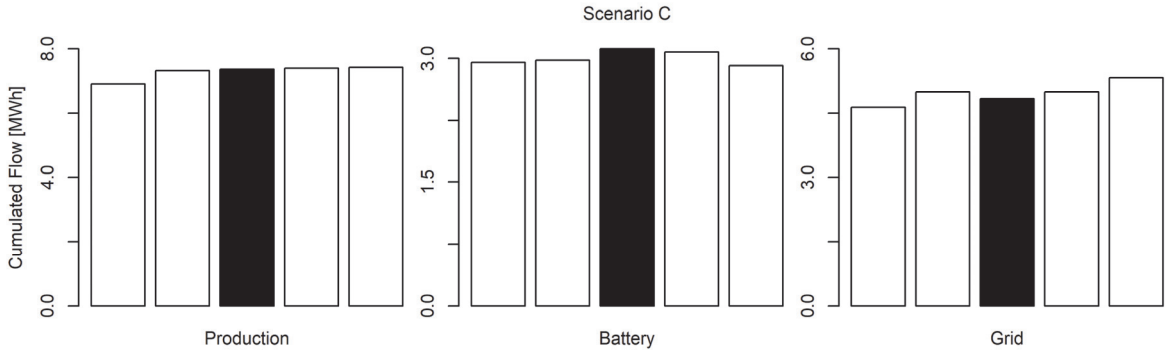

Fig. A. 4-6: Selected year representing average meteorological conditions in scenario C

5 Synthesis

This thesis is focused on the assessment of residential energy systems with PV-coupled batteries from a regional perspective. The large-scale impacts on PV self-consumption and grid flows but also the consequences for the battery utilization under consideration of the spatial peculiarities are the key questions addressed in the three presented publications. The land surface processes model PROMET was therefore extended by a residential energy system model consisting of a consumption, PV production and battery system component. The raster-based approach allows an assessment of the spatial influence of the varying meteorological conditions, PV and battery parameterizations, and loads on regional scale. In this way, residential energy systems and their interrelations can be comprehensively evaluated under both the technical and physical boundary conditions. The methods are applied at the examples of 4906 existing buildings in three administrative districts and 3163 in a municipality located in the south of Germany.

The thesis analyzes three action levels, how residential batteries can contribute to the integration of roof-top PV but also fulfill the request of increasing PV self-consumption.

On building-scale, these two aims are driven by the choice of the battery charging strategy. The utilization of daily feed-in limits, which are adjusted dynamically to consumption and production loads, reduces critical PV excesses fed into the grids but also ensures high self-consumption rates. Residential residual loads spatially deviate largely within the study region, which is reasoned in the different PV- and battery sizes, consumption rates and varying meteorological conditions.

On the superordinate, regional action level, these differences in the residential residual loads can be partly balanced in the grids and therefore contribute to the integration of rooftop PV. The highest spatial balancing effect is obtained if one third of the residential buildings are equipped with PV systems. At these installation rates, the utilization of residential batteries storages decreases grid balancing to the benefit of higher self-consumption rates. At high PV equipment in contrast, residential storages could help to integrate PV into the local energy systems by the in-house buffering of energy excesses and deficits, as grid balancing diminishes.

The third action level refers to the boundary conditions for residential batteries. They play a central role for self-consumption and grid flows in a region and determine the optimal dimension of batteries. Both meteorological conditions and consumption loads are the boundary conditions for residential energy systems, which will undergo considerable transformations in addition to technical developments. Projections for the near-term future indicate an amplification of grid excesses especially in the summer months, which could intensify potential problems with bottlenecks. Climate change with rising PV production rates affects the flows in the batteries mainly in the winter

months, whereas effects from efficiency enhancement dominate in summer. In general, a decrease of the battery utilization is observed for larger systems.

For this reason, several recommendations are given concerning governmental subsidy schemes for the purchase of residential batteries. Firstly, financial support should be adjusted dynamically to the regional PV expansion as batteries have the optimal integration potential at high PV installation rates. The owners of battery storages should be further motivated to use grid-friendly strategies as daily dynamic feed-in limits by additional financial incentives and feed-in limitations. During the dimensioning of batteries, the future developments of climate and efficiency enhancement should be considered to meet the demands for high self-consumption and the request for grid stability.

The obtained results underline the importance of considering both the technical and physical peculiarities individually for each building as well as the small-scale weather patterns in the assessment of the changes in the energy flows. The approach developed in this thesis allows the analysis of potential obstacles and challenges from a regional perspective as the basis for the development of appropriate mitigation strategies for local planners, which are tailored to the physical and technical boundary conditions individual for each region. Further potential applications of the methodology could include building-specific developments concerning the electrical energy systems as the rollout of heat pumps or electric cars for contributing to the comprehensive assessment of the rising decentralization of the energy system.

Bibliography

Agnew, Scott, and Paul Dargusch. 2015. "Effect of residential solar and storage on centralized electricity supply systems." *Nature Climate Change* 5: 315-318. https://doi.org/10.1038/nclimate2523.

Agnew, Scott, and Paul Dargusch. 2017. "Consumer preferences for household-level battery energy storage." *Renewable and Sustainable Energy Reviews* 75: 609-617. https://doi.org/10.1016/j.rser.2016.11.030.

Agora Energiewende. 2014. *Stromspeicher in der Energiewende. Untersuchung zum Bedarf an neuen Stromspeichern in Deutschland für den Erzeugungsausgleich, Systemdienstleistungen und im Verteilnetz.* Agora Energiewende (Berlin, Germany). Accessed 23 May 2018. https://www.agora-energiewende.de/fileadmin2/Projekte/2013/speicher-in-der-energiewende/Agora_Speicherstudie_Web.pdf.

Alboaouh, Kamel A., and Salman Mohagheghi. 2020. "Impact of Rooftop Photovoltaics on the Distribution System." *Journal of Renewable Energy* 2020: 4831434. https://doi.org/10.1155/2020/4831434.

Allouhi, Amine, Youness El Fouih, Tarik Kousksou, Abdelmajid Jamil, Youssef Zéraouli, and Youssef Mourad. 2015. "Energy consumption and efficiency in buildings: current status and future trends." *Journal of Cleaner Production* 109: 118-130. https://doi.org/10.1016/j.jclepro.2015.05.139.

Andrews, Rob W., Andrew Pollard, and Joshua M. Pearce. 2013. "The effects of snowfall on solar photovoltaic performance." *Solar Energy* 92: 84-97. https://doi.org/10.1016/j.solener.2013.02.014.

Angenendt, Georg, Sebastian Zurmühlen, Hendrik Axelsen, and Dirk U. Sauer. 2018. "Comparison of different operation strategies for PV battery home storage systems including forecast-based operation strategies." *Applied Energy* 229: 884-899. https://doi.org/10.1016/j.apenergy.2018.08.058.

Arbeitsgemeinschaft der Vermessungsverwaltungen der Länder der Bundesrepublik Deutschland. 2015. *ATKIS ® Basis DLM (AAA).*

Arvizu, Dan, Palani Balaya, Luisa F. Cabeza, Terry K. G. Hollands, Arnulf Jäger-Waldau, Michio Kondo, Charles Konseibo, Valtentin Meleshko, Wesley Stein, Yutaka Tamaura, Honghua Xu, and Roberto Zilles. 2011. "Direct Solar Energy." In *IPCC Special Report on Renewable Energy Sources and Climate Change Mitigation*, edited by Ottmar Edenhofer, Ramón Pichs-Madruga, Youba Sokona, Kristin Seyboth, Patrick Matschoss, Susanne Kadner, Timm Zwickel, Patrick Eickemeier, Gerrit Hansen, Steffen Schlömer and Christoph von Stechow. Cambridge, United Kingdom and New York, NY, USA: Cambridge University Press.

Bauknecht, Dierk, Simon Funcke, and Moritz Vogel. 2020. "Is small beautiful? A framework for assessing decentralised electricity systems." *Renewable Sustainable Energy Reviews* 118: 109543. https://doi.org/10.1016/j.rser.2019.109543.

Bayerische Vermessungsverwaltung. 2018. *Administrative boundaries.* Accessed 11 November 2019. www.geodaten.bayern.de.

Bayerisches Landesamt für Digitalisierung, Breitband und Vermessung. 2015a. *3D-building model (LoD2).* (Munich, Germany).

Bayerisches Landesamt für Digitalisierung, Breitband und Vermessung. 2015b. *Digital terrain model (25 m).* Accessed 19 March 2015. www.geodaten.bayern.de.

Bayerisches Landesamt für Statistik. 2017. "Energie-Atlas Bayern." Bayerisches Landesamt für Digitalisierung, Breitband und Vermessung. Accessed 08 November 2017. www.energieatlas.bayern.de.

Bayerisches Landesamt für Statistik. 2019a. "Gebäude- und Wohnungsbestand: Gemeinden, Wohngebäude, Wohnungen, Wohnfläche, Stichtag. Fortschreibung des Wohngebäude- und Wohnungsbestandes. 31.12.2014." Accessed 05 December 2019. https://www.statistikdaten.bayern.de/genesis/online/.

Bayerisches Landesamt für Statistik. 2019b. "Statistik kommunal 2018. Stadt Bad Tölz. 09 173 112. Eine Auswahl wichtiger statistischer Daten." Accessed 11 November 2019. https://www.statistik.bayern.de/mam/produkte/statistik_kommunal/2018/09173112.pdf.

Bayerisches Landesamt für Statistik. 2020. *Bevölkerung: Gemeinden, Geschlecht, Stichtag. Fortschreibung des Bevölkerungsstandes.* (Fürth, Germany). Accessed 05 June 2020. https://www.statistikdaten.bayern.de/genesis/online;jsessionid=ABBB4BC0071D2424DA1C291D877EFE19?sequenz=tabelleErgebnis&selectionname=12411-003r.

Bayerisches Staatsministerium für Wirtschaft und Medien, Energie und Technologie. 2015. *Bayerischer Solaratlas. Solare Energiegewinnnung.* (Munich, Germany). Accessed 20 December 2019. https://www.stmwi.bayern.de/fileadmin/user_upload/stmwi/Publikationen/2015/2015-11-09-Bayerischer_Solaratlas.pdf.

Bayernwerk. 2017. *Feed-in data.* Unpublished dataset. (Regensburg, Germany).

Bhattacharyya, Subhes C. 2019. *Energy economics: Concepts, issues, markets and governance*. Springer Nature.

Bhuvandas, Nishi, Prafulkumar V. Timbadiya, Prem L. Patel, and Prakash D. Porey. 2014. "Review of downscaling methods in climate change and their role in hydrological studies." *International Journal of Environmental, Chemical, Ecological, Geological and Geophysical Engineering* 8 (10): 713-718. http://waset.org/publications/9999530.

Bolwig, Simon, Gatis Bazbauers, Antje Klitkou, Peter D. Lund, Andra Blumberga, Armands Gravelsins, and Dagnija Blumberga. 2019. "Review of modelling energy transitions pathways with application to energy system flexibility." *Renewable and Sustainable Energy Reviews* 101: 440-452. https://doi.org/10.1016/j.rser.2018.11.019.

Bruckner, Thomas, Igor Alexeyevich Bashmakov, Yacob Mulugetta, Helena Chum, Angel

De la Vega Navarro, James Edmonds, Andre Faaij, Bundit Fungtammasan, Amit Garg, Edgar Hertwich, Damon Honnery, David Infield, Mikiko Kainuma, Smail Khennas, Suduk Kim, Hassan B. Nimir, Keywan Riahi, Neil Strachan, Ryan Wiser, and Xiliang Zhang. 2014. "Energy systems." In *Climate Change 2014: Mitigation of Climate Change. Contribution of Working Group III to the Fifth Assessment Report of the Intergovernmental Panel on Climate Change*, edited by Ottmar Edenhofer, Ramón Pichs-Madruga, Youba Sokona, Ellie Farahani, Susanne Kadner, Kristin Seyboth, Anna Adler, Ina Baum, Steffen Brunner, Patrick Eickemeier, Benjamin Kriemann, Jussi Savolainen, Steffen Schlömer, Christoph von Stechow, Timm Zwickel and Jan C. Minx. Cambridge, United Kingdom and New York, NY, USA: Cambridge University Press.

Bundesministerium für Wirtschaft und Energie. 2015. *Marktanalyse Photovoltaik-Anlagen.* Accessed 23 May 2018. https://www.bmwi.de/Redaktion/DE/Downloads/M-O/marktanalyse-photovoltaik-dachanlagen.html.

Bundesministerium für Wirtschaft und Energie. 2017. "Erneuerbare Energien Gesetz (EEG)." Bundesministerium für Wirtschaft und Energie - Federal Ministry for Economic Affairs and Energy. Accessed 07 November 2017. http://www.erneuerbare-energien.de/EE/Navigation/DE/Recht-Politik/Das_EEG/das_eeg.html.

Bundesnetzagentur. 2019. "PV data registrations (excluding ground-mounted installations). Data submissions from 1 July 2017 to 31 January 2019." Accessed 11 November 2019. https://www.bundesnetzagentur.de/EN/Areas/Energy/Companies/RenewableEnergy/Facts_Figures_EEG/Register_data_tariffs/EEG_registerdata_payments_node.html.

Chow, Jeffrey, Raymond J. Kopp, and Paul R. Portney. 2003. "Energy resources and global development." *Science* 302 (5650): 1528-1531. https://doi.org/10.1126/science.1091939.

Clarivate Analytics. 2020. "InCites Journal Citation Reports." Clarivate Analytics. Accessed 29 May 2020. https://jcr.clarivate.com/.

Clean Energy Council. 2020. *Clean Energy Australia Report 2020.* Accessed 09 June 2020. https://assets.cleanenergycouncil.org.au/documents/resources/reports/clean-energy-australia/clean-energy-australia-report-2020.pdf.

Colmenar-Santos, Antonio, Mario Monteagudo-Mencucci, Enrique Rosales-Asensio, Miguel de Simón-Martín, and Clara Pérez-Molina. 2019. "Optimized design method for storage systems in photovoltaic plants with delivery limitation." *Solar Energy* 180: 468-488. https://doi.org/10.1016/j.solener.2019.01.046.

Cramton, Peter. 2017. "Electricity market design." *Oxford Review of Economic Policy* 33 (4): 589-612. https://doi.org/10.1093/oxrep/grx041.

Crook, Julia A., Laura A. Jones, Piers M. Forster, and Rolf Crook. 2011. "Climate change impacts on future photovoltaic and concentrated solar power energy output." *Energy & Environmental Science* 4 (9): 3101-3109. https://doi.org/10.1039/C1EE01495A.

Crossland, Andrew, Darren Jones, Neal Wade, and Sara Walker. 2018. "Comparison of the location and rating of energy storage for renewables integration in residential low voltage networks with overvoltage constraints." *Energies* 11 (8): 2041. https://doi.org/10.3390/en11082041.

Deutsche Gesellschaft für Sonnenenergie e.V. (DGS). 2015. *EnergyMap, Anlagen zur Produktion Erneuerbarer Energien. Oberbayern.* Accessed 07 May 2018. http://www.energymap.info/energieregionen/DE/105/111/166.html.

Dufo-López, Rodolfo. 2015. "Optimisation of size and control of grid-connected storage under real time electricity pricing conditions." *Applied Energy* 140: 395-408. https://doi.org/10.1016/j.apenergy.2014.12.012.

DWD CDC. 2015. "Klimadaten für Deutschland." Deutscher Wetterdienst, Climate Data Center. Accessed 17 August 2018. ftp://ftp-cdc.dwd.de/pub/CDC/grids_germany/multi_annual/radiation_global/.

DWD CDC. 2016. "Globalstrahlung in der Bundesrepublik Deutschland basierend auf Satellitendaten und Bodenwerte aus dem DWD-Messnetz. Abweichung der Jahressumme 2016 zum langjährigen Mittel." Deutscher Wetterdienst, Climate Data Center. Accessed 14 May 2019. https://www.dwd.de/DE/leistungen/solarenergie/lstrahlungskarten_ab.html?nn=16102#buehneTop.

DWD CDC. 2019. "Rasterdaten der vieljährigen mittleren Monatssummen und der vieljährigen mittleren Jahressumme für die Globalstrahlung auf die horizontale Ebene für Deutschland basierend auf Boden- und Satellitenmessungen, Version V003. 17 August 2016." Deutscher Wetterdienst, Climate Data Center. Accessed 05 November 2019. https://opendata.dwd.de/climate_environment/CDC/grids_germany/multi_annual/radiation_global/.

EEG. 2019. Erneuerbare-Energien-Gesetz 2017, BGBI. I, p. 1066 (21 July 2014). Bundesministerium für Wirtschaft und Energie.

Elektrizitätswerke Böbing e.G. 2017. *Feed-in data.* Unpublished dataset. (Böbing, Germany).

Elektrizitätswerke Tegernsee. 2017. *Feed-in data.* Unpublished dataset. (Tegernsee, Germany).

Ellabban, Omar, Haitham Abu-Rub, and Frede Blaabjerg. 2014. "Renewable energy resources: Current status, future prospects and their enabling technology." *Renewable and Sustainable Energy Reviews* 39: 748-764. https://doi.org/10.1016/j.rser.2014.07.113.

EuroGeographics. 2018. *Administrative boundaries.* Eurostat/GISCO. http://ec.europa.eu/eurostat/web/gisco/geodata/reference-data/administrative-units-statistical-units/nuts#nuts16.

Faessler, Bernhard, Michael Schuler, Markus Preißinger, and Peter Kepplinger. 2017. "Battery storage systems as grid-balancing measure in low-voltage distribution grids with distributed generation." *Energies* 10 (12): 2161. https://doi.org/

10.3390/en10122161.

Fares, Robert L., and Michael E. Webber. 2017. "The impacts of storing solar energy in the home to reduce reliance on the utility." *Nature Energy* 2 (2): 1-10. https://doi.org/10.1038/nenergy.2017.1.

Figgener, Jan, David Haberschusz, Kai-Philipp Kairies, Oliver Wessels, Benedikt Tepe, and Dirk U. Sauer. 2018. *Wissenschaftliches Mess- und Evaluierungsprogramm Solarstromspeicher 2.0 - Jahresbericht 2018.* Institut für Stromrichtertechnik und Elektrische Antriebe der RWTH Aachen (Aachen, Germany). Accessed 11 November 2019. http://www.speichermonitoring.de/fileadmin/user_upload/Speichermonitoring_Jahresbericht_2018_ISEA_RWTH_Aachen.pdf.

Flato, Gregory, Jochem Marotzke, Babatunde Abiodun, Pascale Braconnot, Sin C. Chou, William J. Collins, Peter Cox, Fatima Driouech, Seita Emori, and Veronika Eyring. 2013. "Evaluation of Climate Models." In *Climate Change 2013: The Physical Science Basis. Contribution of Working Group I to the Fifth Assessment Report of the Intergovernmental Panel on Climate* edited by T.F. Stocker, D. Qin, G.-K. Plattner, M. Tignor, S.K. Allen, J. Boschung, A. Nauels, Y. Xia, V. Bex and P.M. Midgle, 741-866. Cambridge, United Kingdom and New York, NY, USA: Cambridge University Press.

Frankfurt School-UNEP Centre/BNEF. 2019. *Global Trends in Renewable Energy Investment.* (Frankfurt am Main, Germany). Accessed 09 June 2020. http://www.fs-unep-centre.org.

Fraunhofer ISE. 2019a. *Aktuelle Fakten zur Photovoltaik in Deutschland.* Fraunhofer-Institut für Solare Energiesysteme ISE (Freiburg, Germany). Accessed 23 May 2019. www.pv-fakten.de.

Fraunhofer ISE. 2019b. *Recent Facts about Photovoltaics in Germany.* Fraunhofer-Institut für Solare Energiesysteme ISE (Freiburg, Germany). Accessed 21 January 2020. www.pv-fakten.de.

Gemeindewerke Holzkirchen. 2017. *Feed-in data.* Unpublished dataset. (Holzkirchen, Germany).

Gemeindewerke Peißenberg. 2017. *Feed-in data.* Unpublished dataset. (Peißenberg, Germany).

Giddings, J. Calvin, and Edward LaChapelle. 1961. "Diffusion theory applied to radiant energy distribution and albedo of snow." *Journal of Geophysical Research* 66 (1): 181-189. https://doi.org/10.1029/JZ066i001p00181.

Gomez-Gonzalez, Manuel, Jesus C. Hernandez, David Vera, and Francisco Jurado. 2020. "Optimal sizing and power schedule in PV household-prosumers for improving PV self-consumption and providing frequency containment reserve." *Energy* 191: 116554. https://doi.org/10.1016/j.energy.2019.116554.

Gosens, Jorrit, Tomas Kåberger, and Yufei Wang. 2017. "China's next renewable energy revolution: Goals and mechanisms in the 13th Five Year Plan for energy." *Energy Science & Engineering* 5 (3): 141-155. https://doi.org/10.1002/ese3.161.

Green, Martin A. 2002. "Photovoltaic principles." *Physica E: Low-dimensional Systems and Nanostructures* 14 (1): 11-17. https://doi.org/10.1016/S1386-9477(02)00354-5.

Gür, Turgut M. 2018. "Review of electrical energy storage technologies, materials and systems: challenges and prospects for large-scale grid storage." *Energy & Environmental Science* 11 (10): 2696-2767. https://doi.org/10.1039/C8EE01419A.

Haque, Md Mejbaul, and Peter Wolfs. 2016. "A review of high PV penetrations in LV distribution networks: Present status, impacts and mitigation measures." *Renewable Sustainable Energy Reviews* 62: 1195-1208. https://doi.org/10.1016/j.rser.2016.04.025.

Hempel, Sabrina, Katja Frieler, Lila Warszawski, Jacob Schewe, and Franziska Piontek. 2013a. *Bias corrected GCM input data for ISIMIP Fast Track, GFZ Data Services.* GFZ Data Services. http://doi.org/10.5880/PIK.2016.001.

Hempel, Sabrina, Katja Frieler, Lila Warszawski, Jacob Schewe, and Franziska Piontek. 2013b. "A trend-preserving bias correction–the ISI-MIP approach." *Earth System Dynamics Discussions* 4. https://doi.org/10.5194/esdd-4-49-2013

Hersch, Paul, and Kenneth Zweibel. 1982. *Basic photovoltaic principles and methods.* Solar Energy Research Institute (Golden, CO, USA).

Hesse, Holger C., Rodrigo Martins, Petr Musilek, Maik Naumann, Cong Nam Truong, and Andreas Jossen. 2017. "Economic optimization of component sizing for residential battery storage systems." *Energies* 10 (7): 835. https://doi.org/10.3390/en10070835.

Hong, Taehoon, Minhyun Lee, Choongwan Koo, Kwangbok Jeong, and Jimin Kim. 2017. "Development of a method for estimating the rooftop solar photovoltaic (PV) potential by analyzing the available rooftop area using hillshade analysis." *Applied Energy* 194: 320-332. https://doi.org/10.1016/j.apenergy.2016.07.001.

Huber, Isabelle, Luca Bugliaro, Michael Ponater, Hella Garny, Claudia Emde, and Bernhard Mayer. 2016. "Do climate models project changes in solar resources?" *Solar Energy* 129: 65-84. https://doi.org/10.1016/j.solener.2015.12.016.

Huber, Nica, Rico Hergert, Bronwyn Price, Christian Zäch, Anna M. Hersperger, Marco Pütz, Felix Kienast, and Janine Bolliger. 2017. "Renewable energy sources: Conflicts and opportunities in a changing landscape." *Regional Environmental Change* 17 (4): 1241-1255. https://doi.org/10.1007/s10113-016-1098-9.

IEA. 2019a. "Data and statistics." International Energy Agency. Accessed March 13, 2020. https://www.iea.org/data-and-statistics.

IEA. 2019b. *Energy Efficiency 2019.* International Energy Agency (Paris, France). Accessed 09 June 2020. https://www.iea.org/reports/energy-efficiency-2019.

IEA. 2019c. *Renewables 2019.* International Energy Agency (Paris, France). Accessed 04 June 2020. https://www.iea.org/reports/renewables-2019.

IEA. 2020. *Introduction to System Integration of Renewables.* International Energy Agency (Paris, France). Accessed 29 May 2020. https://www.iea.org/reports/introduction-to-system-integration-of-renewables.

IEA PVPS. 2019. *T1:36 2019. Trends in Photovoltaic Applications. Task 1. Strategic PV Anlaysis and Outreach.* International Energy Agency. Photovoltaic Power Systems Programme. Accessed 08 May 2020. https://iea-pvps.org/trends_reports/2019-edition/.

IEC. 2020. "World Plugs. Plugs and Sockets." International Electrotechnical Commission. Accessed 28 June 2020. https://www.iec.ch/worldplugs/list_byfrequency.htm.

Institut für Demoskopie. 2015. *Energie- und Klimapolitik im Spiegel der öffentlichen Meinung.* Berichte für das Bundespresseamt (Allensbach, Germany). Accessed 25 June 2018. http://nbn-resolving.de/urn:nbn:de:0168-ssoar-458780.

IPPC. 2014. *Climate Change 2014: Synthesis Report. Contribution of Working Groups I, II and III to the Fifth Assessment Report of the Intergovernmental Panel on Climate Change*. Edited by Core Writing Team, Rajendra K. Pachauri and Leo Meyer. Geneva, Switzerland: IPCC.

IRENA. 2017a. *Cost and Competitiveness Indicators: Rooftop Solar PV.* International Renewable Energy Agency (Abu Dhabi). Accessed 25 June 2020. https://www.irena.org/publications/2017/Dec/IRENA-cost-and-competitiveness-indicators-Rooftop-solar-PV.

IRENA. 2017b. *Electricity Storage and Renewables: Costs and Markets to 2030.* International Renewable Energy Agency (Abu Dhabi). Accessed 25 June 2020. https://www.irena.org/publications/2017/Oct/Electricity-storage-and-renewables-costs-and-markets.

IRENA. 2019. *Future of Solar Photovoltaic: Deployment, investment, technology, grid integration and socio-economic aspects (A Global Energy Transformation: paper).* International Renewable Energy Agency (Abu Dhabi). Accessed 25 June 2020. https://www.irena.org/publications/2019/Nov/Future-of-Solar-Photovoltaic.

IRENA. 2020. *Electricity Storage Valuation Framework: Assessing system value and ensuring project viability.* International Renewable Energy Agency (Abu Dhabi). Accessed 25 June 2020. https://irena.org/publications/2020/Mar/Electricity-Storage-Valuation-Framework-2020.

Jerez, Sonia, Isabelle Tobin, Robert Vautard, Juan P. Montávez, Jose M. López-Romero, Françoise Thais, Blanka Bartok, Ole B. Christensen, Augustin Colette, Michel Déqué, Grigory Nikulin, Sven Kotlarski, Erik van Meijgaard, Claas Teichmann, and Martin Wild. 2015. "The impact of climate change on photovoltaic power generation in Europe." *Nature Communications* 6: 10014. https://doi.org/10.1038/ncomms10014.

Klingler, Anna-Lena. 2017. "Self-consumption with PV+Battery systems: A market diffusion model considering individual consumer behaviour and preferences." *Applied Energy* 205: 1560-1570.

https://doi.org/10.1016/j.apenergy.2017.08.159.

Koskela, Juha, Antti Rautiainen, and Pertti Järventausta. 2019. "Using electrical energy storage in residential buildings – Sizing of battery and photovoltaic panels based on electricity cost optimization." *Applied Energy* 239: 1175-1189. https://doi.org/10.1016/j.apenergy.2019.02.021.

Layton, Bradley E. 2008. "A comparison of energy densities of prevalent energy sources in units of Joules per cubic meter." *International Journal of Green Energy* 5 (6): 438-455. https://doi.org/10.1080/15435070802498036.

Lechwerke. 2017. *Feed-in data.* Unpublished dataset. (Augsburg, Germany).

Lee, Minhyun, Taehoon Hong, Kwangbok Jeong, and Jimin Kim. 2018. "A bottom-up approach for estimating the economic potential of the rooftop solar photovoltaic system considering the spatial and temporal diversity." *Applied Energy* 232: 640-656. https://doi.org/10.1016/j.apenergy.2018.09.176.

Li, Jiaming. 2019. "Optimal sizing of grid-connected photovoltaic battery systems for residential houses in Australia." *Renewable Energy* 136: 1245-1254. https://doi.org/10.1016/j.renene.2018.09.099.

Lin, Jeremy, and Fernando H. Magnago. 2017. *Electricity Markets: Theories and Applications*. John Wiley & Sons.

Linden, David. 1995. "Handbook of batteries." *Fuel and Energy Abstracts* 36 (4): 265.

Litjens, Gert B. M. A., Bala B. Kausika, Ernst Worrell, and Wilfried G. J. H. M. van Sark. 2018. "A spatio-temporal city-scale assessment of residential photovoltaic power integration scenarios." *Solar Energy* 174: 1185-1197. https://doi.org/10.1016/j.solener.2018.09.055.

Locherer, Veronika. 2018. *Technical Release No. 1: INOLA Software Documentation. The Solar Energy Component. Solar Power and Solar Heat Modules.* Department of Geography at LMU Munich (Munich, Germany). Accessed 20 May 2020. https://doi.org/10.5282/ubm/epub.69611.

Lödl, Martin, Rolf Witzmann, and Michael Metzger. 2011. "Operation strategies of energy storages with forecast methods in low-voltage grids with a high degree of decentralized generation." Electrical Power and Energy Conference (EPEC), 2011.

Lowitzsch, Jens, and Florian Hanke. 2019. "Renewable Energy Cooperatives." In *Energy Transition*, 139-162. Springer.

Lucon, Oswaldo, Diana Ürge-Vorsatz, Azni Zain Ahmed, Hashem Akbari, Paolo Bertoldi, Luisa F. Cabeza, Nicholas Eyre, Ashok Gadgil, L. D. Danny Harvey, Yi Jiang, Enoch Liphoto, Sevastianos Mirasgedis, Shuzo Murakami, Jyoti Parikh, Christopher Pyke, and Maria V. Vilariño. 2014. "Buildings." In *Climate Change 2014: Mitigation of Climate Change. Contribution of Working Group III to the Fifth Assessment Report of the Intergovernmental Panel on Climate Change*, edited by Ottmar Edenhofer, Ramón Pichs-Madruga, Youba Sokona, Ellie Farahani, Susanne Kadner, Kristin

Seyboth, Anna Adler, Ina Baum, Steffen Brunner, Patrick Eickemeier, Benjamin Kriemann, Jussi Savolainen, Steffen Schlömer, Christoph von Stechow, Timm Zwickel and Jan C. Minx. Cambridge, United Kingdom and New York, NY, USA: Cambridge University Press.

Luque, Antonio, and Gerardo L. Araujo. 1989. *Solar cells and optics for photovoltaic concentration*. A. Hilger.

Luthander, Rasmus, Joakim Widén, Joakim Munkhammar, and David Lingfors. 2016. "Self-consumption enhancement and peak shaving of residential photovoltaics using storage and curtailment." *Energy* 112: 221-231. https://doi.org/10.1016/j.energy.2016.06.039.

Luthander, Rasmus, Joakim Widén, Daniel Nilsson, and Jenny Palm. 2015. "Photovoltaic self-consumption in buildings: A review." *Applied Energy* 142: 80-94. https://doi.org/10.1016/j.apenergy.2014.12.028.

Malhotra, Abhishek, Benedikt Battke, Martin Beuse, Annegret Stephan, and Tobias Schmidt. 2016. "Use cases for stationary battery technologies: A review of the literature and existing projects." *Renewable Sustainable Energy Reviews* 56: 705-721. https://doi.org/10.1016/j.rser.2015.11.085.

Mauser, Wolfram. 2016. "The Statistical Climate Generator." In *Regional Assessment of Global Climate Change Impacts. The Project GLOWA-Danube*, edited by Wolfram Mauser and Monika Prasch. Cham: Springer.

Mauser, Wolfram, and Heike Bach. 2009. "PROMET - Large scale distributed hydrological modelling to study the impact of climate change on the water flows of mountain watersheds." *Journal of Hydrology* 376 (3): 362-377. https://doi.org/10.1016/j.jhydrol.2009.07.046.

Mauser, Wolfram, Heike Bach, Toni Frank, Tobias Hank, Franziska Koch, Thomas Marke, Markus Muerth, Monika Prasch, Ulrich Strasser, and Florian Zabel. 2015. *PROMET – Processes of Mass and Energy Transfer. An Integrated Land Surface Processes and Human Impacts Simulator for the Quantitative Exploration of Human-Environment Relations. Part 1: Algorithms Theoretical Baseline Document. Version 5.8.* (Munich, Germany). Accessed 11 September 2019. https://www.geographie.uni-muenchen.de/department/fiona/forschung/projekte/promet_handbook/promethandbook1.pdf.

McClatchey, Robert A., Robert W. Fenn, John E. A. Selby, Frederic E. Volz, and Jyneza S. Garing. 1972. *Optical Properties of the Atmosphere, third ed.* Air-Force Cambridge Research Laboratories, (AFCRL-72-0497, Environmental Research Paper No. 411) (L. G. Hanscom Field, Bedford, Massachusetts).

Möser, Werner, and Erhard Raschke. 1983. "Mapping of global radiation and cloudiness from METEOSAT image data." *Meteorologische Rundschau* 36 (2): 33-37.

Moshövel, Janina, Kai-Philipp Kairies, Dirk Magnor, Matthias Leuthold, Mark Bost, Swantje Gährs, Eva Szczechowicz, Moritz Cramer, and Dirk U. Sauer. 2015. "Analysis of the maximal possible grid relief from PV-peak-power impacts by using storage

systems for increased self-consumption." *Applied Energy* 137: 567-575. https://doi.org/10.1016/j.apenergy.2014.07.021.

Müller, Johannes, Doris Folini, Martin Wild, and Stefan Pfenninger. 2019. "CMIP-5 models project photovoltaics are a no-regrets investment in Europe irrespective of climate change." *Energy* 171: 135-148. https://doi.org/10.1016/j.energy.2018.12.139.

Nejat, Payam, Fatemeh Jomehzadeh, Mohammad M. Taheri, Mohammad Gohari, and Muhd Z. Abd. Majid. 2015. "A global review of energy consumption, CO_2 emissions and policy in the residential sector (with an overview of the top ten CO_2 emitting countries)." *Renewable and Sustainable Energy Reviews* 43: 843-862. https://doi.org/10.1016/j.rser.2014.11.066.

Nyholm, Emil, Joel Goop, Mikael Odenberger, and Filip Johnsson. 2016. "Solar photovoltaic-battery systems in Swedish households - Self-consumption and self-sufficiency." *Applied Energy* 183: 148-159. https://doi.org/10.1016/j.apenergy.2016.08.172.

Olaszi, Balint D., and Jozsef Ladanyi. 2017. "Comparison of different discharge strategies of grid-connected residential PV systems with energy storage in perspective of optimal battery energy storage system sizing." *Renewable Sustainable Energy Reviews* 75: 710-718. https://doi.org/10.1016/j.rser.2016.11.046.

Opiyo, Nicholas. 2016. "Energy storage systems for PV-based communal grids." *Journal of Energy Storage* 7: 1-12. https://doi.org/10.1016/j.est.2016.05.001.

Parida, Bhubaneswari, Selvarasan Iniyan, and Ranko Goic. 2011. "A review of solar photovoltaic technologies." *Renewable and Sustainable Energy Reviews* 15 (3): 1625-1636. https://doi.org/10.1016/j.apenergy.2018.06.118.

Pistoia, Gianfranco. 2013. *Lithium-ion batteries: advances and applications*. Newnes.

Prasch, Monika, and Andrea Reimuth. 2018. *Technical Release No. 5: INOLA Software Documentation. The Energy Consumption Component.* Department of Geography at LMU Munich (Munich, Germany). Accessed 20 May 2020. https://doi.org/10.5282/ubm/epub.69617.

Prognos AG, EWI, and GWS. 2014. *Entwicklung der Energiemärkte - Energiereferenzprognose. Projekt Nr. 57/12. Studie im Auftrag des Bundesministeriums für Wirtschaft und Technologie.* (Basel/Köln/Osnabrück, Germany). Accessed 23 May 2019. https://www.bmwi.de/Redaktion/DE/Publikationen/Studien/entwicklung-der-energiemaerkte-energiereferenzprognose-endbericht.pdf?__blob=publicationFile&v=7.

Quaschning, Volker. 2013. *Regenerative Energiesysteme. Technlogie - Berechnung - Simulation*. München: Carl Hanser Verlag.

Ramirez Camargo, Luis, Felix Nitsch, Katharina Gruber, and Wolfgang Dorner. 2018. "Electricity self-sufficiency of single-family houses in Germany and the Czech Republic." *Applied Energy* 228: 902-915. https://doi.org/10.1016/j.apenergy.2018.06.118.

Ramirez Camargo, Luis, Roland Zink, Wolfgang Dorner, and Gernot Stoeglehner. 2015. "Spatio-temporal modeling of roof-top photovoltaic panels for improved technical potential assessment and electricity peak load offsetting at the municipal scale." *Computers, Environment and Urban Systems* 52: 58-69. https://doi.org/10.1016/j.compenvurbsys.2015.03.002.

Reimuth, Andrea. 2017a. *Technical Release No. 6: INOLA Software Documentation. The Energy Storage Component.* Department of Geography at LMU Munich (Munich, Germany). Accessed 20 May 2020. https://doi.org/10.5282/ubm/epub.69618.

Reimuth, Andrea. 2017b. *Technical Release No. 7: INOLA Software Documentation. The Energy Management Component.* Department of Geography at LMU Munich (Munich, Germany). Accessed 19 November 2019. https://doi.org/10.5282/ubm/epub.69619.

Reimuth, Andrea, Monika Prasch, Veronika Locherer, Martin Danner, and Wolfram Mauser. 2019. "Influence of different battery charging strategies on residual grid power flows and self-consumption rates at regional scale." *Applied Energy* 238: 572-581. https://doi.org/10.1016/j.apenergy.2019.01.112.

Resch, Matthias, Bagus Ramadhani, Jochen Bühler, and Andreas Sumper. 2015. "Comparison of control strategies of residential PV storage systems." 9th International Renewable Energy Storage Conference and Exhibition (IRES 2015), March 9-11, 2015, Düsseldorf.

Rogelj, Joeri, Drew Shindell, Kejun Jiang, Solomone Fifita, Piers Forster, Veronika Ginzburg, Collins Handa, Haroon Kheshgi, Shigeki Kobayashi, Elmar Kriegler, Luis Mundaca, Roland Séférian, and Maria V. Vilariño. 2018. *Mitigation Pathways Compatible with 1.5°C in the Context of Sustainable Development*. Global Warming of 1.5°C. An IPCC Special Report on the impacts of global warming of 1.5°C above pre-industrial levels and related global greenhouse gas emission pathways, in the context of strengthening the global response to the threat of climate change, sustainable development, and efforts to eradicate poverty ed., edited by Valérie Masson-Delmotte, Panmao Zhai, Hans-Otto Pörtner, Debora Roberts, Jim Skea, Priyadarshi R. Shukla, Anna Pirani, Wilfran Moufouma-Okia, Clotilde Péan, Roz Pidcock, Ssrah Connors, J. B. Robin Matthews, Yang Chen, Xiao Zhou, Melissa I. Gomis, Elisabeth Lonnoy, Tom Maycock, Melinda Tignor and Waterfield Tim. In Press.

Rogner, Hans-Holger, Roberto F. Aguilera, Christina Archer, Ruggero Bertani, Subhes C. Bhattacharya, Maurice B. Dusseault, Luc Gagnon, Helmut Haberl, Monique Hoogwijk, Arthur Johnson, Mathis Leung Rogner, Horst Wagner, and Vladimir Yakushev. 2012. "Chapter 7 - Energy Resources and Potentials." In *Global Energy Assessment - Toward a Sustainable Future*, 423-512. Cambridge University Press, Cambridge, UK and New York, NY, USA and the International Institute for Applied Systems Analysis, Laxenburg, Austria.

Rubel, Franz, and Markus Kottek. 2010. "Observed and projected climate shifts 1901–2100 depicted by world maps of the Köppen-Geiger climate classification." *Meteorologische Zeitschrift* 19 (2): 135-141. https://doi.org/10.1127/0941-2948/2010/0430.

Sani Hassan, Abubakar, Liana Cipcigan, and Nick Jenkins. 2017. "Optimal battery storage operation for PV systems with tariff incentives." *Applied Energy* 203: 422-441. https://doi.org/10.1016/j.apenergy.2017.06.043.

Schoop, Edgar. 2013. *Stationäre Batterieanlagen. Auslegung, Installation und Wartung*. 1 ed.: HUSS-Medien Berlin.

Schopfer, Sandro, Verena Tiefenbeck, and Thorsten Staake. 2018. "Economic assessment of photovoltaic battery systems based on household load profiles." *Applied Energy* 223: 229-248. https://doi.org/10.1016/j.apenergy.2018.03.185.

Schram, Wouter L., Ioannis Lampropoulos, and Wilfried G. J. H. M. van Sark. 2018. "Photovoltaic systems coupled with batteries that are optimally sized for household self-consumption: Assessment of peak shaving potential." *Applied Energy* 223: 69-81. https://doi.org/10.1016/j.apenergy.2018.04.023.

Schram, Wouter L., Atse Louwen, Ioannis Lampropoulos, and Wilfried G. J. H. M. Van Sark. 2019. "Comparison of the greenhouse gas emission reduction potential of energy communities." *Energies* 12 (23): 4440. https://doi.org/10.3390/en12234440.

Schumacher, Kira, Felix H. Krones, Russell McKenna, and Frank Schultmann. 2019. "Public acceptance of renewable energies and energy autonomy: A comparative study in the French, German and Swiss Upper Rhine region." *Energy Policy* 126: 315-332. https://doi.org/10.1016/j.enpol.2018.11.032.

Shafiee, Shahriar, and Erkan Topal. 2009. "When will fossil fuel reserves be diminished?" *Energy Policy* 37 (1): 181-189. https://doi.org/10.1016/j.enpol.2008.08.016.

Sharma, Vanika, Mohammed H. Haque, and Syed M. Aziz. 2019. "Energy cost minimization for net zero energy homes through optimal sizing of battery storage system." *Renewable Energy* 141: 278-286. https://doi.org/10.1016/j.renene.2019.03.144.

Sims, Ralph, Pedro Mercado, Wolfram Krewitt, Gouri Bhuyan, Damian Flynn, Hannele Holttinen, Gilberto Jannuzzi, Smail Khennas, Yongqian Liu, Lars J. Nilsson, Joan Ogden, Kazuhiko Ogimoto, Mark O'Malley, Hugh Outhred, Øystein Ulleberg, and Frans van Hulle. 2011. "Integration of Renewable Energy into Present and Future Energy Systems." In *IPCC Special Report on Renewable Energy Sources and Climate Change Mitigation*, edited by Ottmar Edenhofer, Ramón Pichs-Madruga, Youba Sokona, Kristin Seyboth, Patrick Matschoss, Susanne Kadner, Timm Zwickel, Patrick Eickemeier, Gerrit Hansen, Steffen Schlömer and Christoph von Stechow. Cambridge, United Kingdom and New York, NY, USA: Cambridge University Press.

Smil, Vaclav. 2010. *Energy transitions: history, requirements, prospects*. ABC-CLIO.

Soares, Pedro M. M., Miguel C. Brito, and João A. M. Careto. 2019. "Persistence of the high solar potential in Africa in a changing climate." *Environmental Research Letters* 14 (12): 124036. https://doi.org/10.1088/1748-9326/ab51a1.

SolarPower Europe. 2019. *Global Market Outlook For Solar Power 2019–2023.* Solar Power Europe (Brussels, Belgium). Accessed 20 June 2020. https://www.solarpowereurope.org/wp-content/uploads/2019/07/SolarPower-Europe_Global-Market-Outlo

ok-2019-2023.pdf.

Stadtwerke Bad Tölz. 2017. *Feed-in data.* Unpublished dataset. (Bad Tölz, Germany).

Stadtwerke Bad Tölz. 2019. *Feed-in data of Bad Tölz.* Unpublished dataset. (Bad Tölz, Germany).

Stadtwerke Unna. 2015. *VDEW Lastprofile. Version October 10, 2015.* Verband der Elektrizitätswirtschaft VDEW. Accessed 20 December 2019. http://www.gips projekt.de/featureGips/Gips;jsessionid=36DBE8EAF15E68329A3F6493121749 DB?Session-Man-dant=sw_unna&Anwendung=EnWGKnotenAnzeigen&PrimaryI d=133029&Mandantkuerzel=sw_unna&Navigation=J.

Statistische Ämter des Bundes und der Länder. 2014. "Gebäude mit Wohnraum nach Baujahr (Jahrzwanzigste) und Art des Gebäudes. Auszählungsergebnis aus der Gebäude- und Wohnungszählung. Stadt Bad Tölz. Zensus Mai 2011." Accessed 05 November 2019. https://ergebnisse.zensus2011.de/#StaticContent:091730112 112,GWZ_1_2_1,m,table.

Statistisches Bundesamt (DESTATIS). 2016. *Kreisfreie Städte und Landkreise nach Fläche, Bevölkerung und Bevölkerungsdichte am 31.12.2015. Erscheinungsmonat: Dezember 2016.* Accessed 16 October 2017. https://www.destatis.de/DE/ ZahlenFakten/LaenderRegionen/Regionales/Gemeindeverzeichnis/Administrati v/Aktuell/04Kreise.html.

Statistisches Bundesamt (DESTATIS). 2019. *Material- und Energieflüsse. Stromverbrauch der privaten Haushalte nach Haushaltsgrößenklassen.* Statistisches Bundesamt. Accessed 04 November 2019. https://www.destatis.de/DE/Themen/Gesellschaf t-Umwelt/Umwelt/Materialfluesse-Energiefluesse/Tabellen/stromverbrauch-ha ushalte.html.

Sütterlin, Bernadette, and Michael Siegrist. 2017. "Public acceptance of renewable energy technologies from an abstract versus concrete perspective and the positive imagery of solar power." *Energy Policy* 106: 356-366. https://doi.org/10.1016/ j.enpol.2017.03.061.

Talent, Orlando, and Haiping Du. 2018. "Optimal sizing and energy scheduling of photovoltaic-battery systems under different tariff structures." *Renewable Energy* 129: 513-526. https://doi.org/10.1016/j.renene.2018.06.016.

Tsiropoulos, Ioannis, Dalius Tarvydas, and Natalia Lebedeva. 2018. *Li-ion batteries for mobility and stationary storage applications Scenarios for costs and market growth.* Publications Office of the European Union (Luxembourg). Accessed 28 June 2020.

van der Schoor, Tineke, and Bert Scholtens. 2015. "Power to the people: Local community initiatives and the transition to sustainable energy." *Renewable and Sustainable Energy Reviews* 43: 666-675. https://doi.org/10.1016/j.rser.2014.10.089.

van Vuuren, Detlef P., Jae Edmonds, Mikiko Kainuma, Keywan Riahi, Allison Thomson, Kathy Hibbard, George C. Hurtt, Tom Kram, Volker Krey, Jean-Francois Lamarque, Toshihiko Masui, Malte Meinshausen, Nebojsa Nakicenovic, Steven J. Smith, and

Steven K. Rose. 2011. "The representative concentration pathways: an overview." *Climatic Change* 109 (1): 5. https://doi.org/10.1007/s10584-011-0148-z.

VDEW. 1999. *Repräsentative VDEW-Lastprofile. VDEW-Materialien M-32/99.* (Frankfurt, Germany). Accessed 20 December 2019. https://www.bdew.de/media/documents/1999_Repraesentative-VDEW-Lastprofile.pdf.

VDI. 2013. *VDI Guideline 3807. Characteristic consumption values for buildings. June 2013*. Berlin, Germany: Beuth-Verlag.

von Appen, Jan, Thomas Stetz, Martin Braun, and Armin Schmiegel. 2014. "Local voltage control strategies for PV storage systems in distribution grids." *IEEE Transactions on Smart Grid* 5 (2): 1002-1009. https://doi.org/10.1109/TSG.2013.2291116.

Warszawski, Lila, Katja Frieler, Veronika Huber, Franziska Piontek, Olivia Serdeczny, and Jacob Schewe. 2014. "The inter-sectoral impact model intercomparison project (ISI–MIP): project framework." *Proceedings of the National Academy of Sciences* 111 (9): 3228-3232. https://doi.org/10.1073/pnas.1312330110

Weniger, Johannes, Tjarko Tjaden, and Volker Quaschning. 2014. "Sizing of residential PV battery systems." *Energy Procedia* 46: 78-87. https://doi.org/10.1016/j.egypro.2014.01.160.

Wild, Martin, Doris Folini, Florian Henschel, Natalie Fischer, and Björn Müller. 2015. "Projections of long-term changes in solar radiation based on CMIP5 climate models and their influence on energy yields of photovoltaic systems." *Solar Energy* 116: 12-24. https://doi.org/10.1016/j.solener.2015.03.039.

Young, Sharon, Anna Bruce, and Iain MacGill. 2019. "Potential impacts of residential PV and battery storage on Australia's electricity networks under different tariffs." *Energy Policy* 128: 616-627. https://doi.org/10.1016/j.enpol.2019.01.005.

Zahedi, Ahmad. 2011. "Maximizing solar PV energy penetration using energy storage technology." *Renewable and Sustainable Energy Reviews* 15 (1): 866-870. https://doi.org/10.1016/j.rser.2010.09.011.